DEOXYRIBONUCLEIC ACID AS A MODEL FOR THE DESIGN OF FUNCTIONAL, DEGRADABLE POLYMERS

A Dissertation

by

YI-YUN TSAO

Submitted to the Office of Graduate and Professional Studies of
Texas A&M University
in partial fulfillment of the requirements for the degree of

DOCTOR OF PHILOSOPHY

Chair of Committee,	Karen L. Wooley
Committee Members,	David E. Bergbreiter
	Lei Fang
	Melissa A. Grunlan
Head of Department,	Simon W. North

December 2018

Major Subject: Chemistry

ABSTRACT

A grand challenge that crosses synthetic chemistry and biology is the scalable production of functional analogues of biomacromolecules. This dissertation has focused on the use of deoxynucleoside building blocks bearing non-natural bases to develop a synthetic methodology that allows for the construction of high molar mass deoxynucleotide polymers. Two thymidine-derived bicyclic monomers, (*R*)- and (*S*)-3′,5′-bicyclic 3-(3-butenyl) thymidine ethylphosphate, were synthesized in two steps directly from thymidine, *via* butenylation and diastereoselective cyclization promoted by *N*,*N*-dimethyl-4-aminopyridine. Poly(3′,5′-bicyclic 3-(3-butenyl) thymidine ethylphosphate)s with low dispersities ($Đ < 1.10$) were obtained from ring-opening polymerizations of the more thermodynamically unstable (*R*)-monomer, catalyzed by 1,5,7-triazabicyclo[4.4.0]dec-5-ene at ambient temperature. These studies established a reliable synthetic pathway to thymidine-derived polydeoxyribonucleotide analogues from a six-membered bicyclic phosphoester.

Regioregularity is a crucial property in the synthesis of DNA analogues, as natural DNA is synthesized exclusively in 5′-to-3′ direction. From the ^{31}P resonance frequency assignments of synthesized model compounds of 3′,3′-, 3′,5′-, and 5′,5′-linkages, ^{31}P NMR spectra revealed the major connectivity in the polymer backbone to be 3′,5′-linkages, with ≤30% of other isomeric forms. Model reactions employing a series of alcohol initiators imparting various degrees of steric hindrance, to mimic the increased steric hindrance of the propagating alcohol relative to the initiator, were then

conducted to afford the corresponding ring-opened unimer adducts. ^{1}H–^{31}P heteronuclear multiple-bond correlation spectroscopy showed ethanol and 4-methoxybenzyl alcohol initiation to yield only the P–O5′ bond cleavage product, whereas attack by isopropyl alcohol afforded both P–O3′ and P–O5′ bond cleavage products, supporting our hypothesis that the increased steric hindrance of the propagating species dictates the regioselectivity of the P–O bond cleavage. Further model reactions suggested that the P–O5′ bond cleavage products can be detected upon the formation of dimers during the ring-opening polymerization.

Overall, this advanced design combines the merits of natural product-derived materials and functional, degradable polymers to provide a new platform for functional, synthetically derived polydeoxyribonucleotide-analogue materials. Furthermore, this dissertation provides a fundamental understanding of the polymerization behavior of six-membered cyclic phosphoesters, and broadens the scope of DNA analogues from the ring-opening polymerization of 3′,5′-bicyclic phosphoesters.

DEDICATION

To my family and educators for providing the foundation to complete this work.

ACKNOWLEDGEMENTS

I would first like to thank my advisor, Professor Karen L. Wooley. She is kind, supportive, passionate, diligent, and considerate. Her encouragement and support have allowed me to pursue my passion, my curiosity, and the science that I have found most interesting over these last five years. Karen has shown me that, besides her tremendous knowledge of science, what makes her a successful scientist is to be meticulous about all the experimental details, to ask questions to herself all the time, and most importantly, to be constantly curious. Although I have always been worrying about my experiments being non-productive — especially in the first three years of failures — she never stopped providing me with freedom, support and suggestions to explore the fields that I deem interesting and exciting. Karen's persistence in science provides huge impact on me: never "hope" in scientific matters, although she might not remember it was me that used a lot of "hope" in the group meeting presentation to bring this tradition into the group. With these limited words, I cannot express all my gratitude of having her as my supervisor.

Secondly, I would like to thank my dissertation committee members, Professors David E. Bergbreiter, Lei Fang, and Melissa A. Grunlan for their technical expertise, valuable advice and simulating discussions, which led to improved research toward the completion of this dissertation.

Within the Wooley group, I am also extremely thankful for my friend Dr. Kevin T. Wacker for numerous valuable discussions on both science and trials of graduate

school. I want to acknowledge my mentee, Travis H. Smith, for his great help in my research. I would also like to thank other past and present members of the Wooley group, Ryan Allen, Dr. Yannick Borguet, Dr. Yingchao Chen, Dr. Sangho Cho, Ben Demor, Mei Dong, Dr. Mahmoud F. A. El Sabahy, Simcha E. Felder, Dr. Jeniree A. Flores Delgado, Dr. Marco Giles, Amelia Gonzalez, Alexis Gooch, Dr. Tiffany P. Gustafson, Jessica H. Huang, Dr. Ashlee A. Jahnke, Nari Kang, Christopher H. Komatsu, Dr. Gyu Seong Heo, Dr. Amandine Noel, Dr. Samantha L. Kristufek, Eric E. Leonhardt, Dr. Rachel A. Letteri, Dr. Young Lim, Yen-Nan Lin, Dr. Lauren Link, Dr. Alexander Lonnecker, Mahsa Minaeian, Shota Osumi, Dr. Adriana Pavia-Sanders, Stephanie F. Pollack, Randinu Pulukkody, Dr. Kellie Seetho, Yue Song, Dr. Lu Su, David K. Tran, Eric Vavra, Mariela Vazquez, Brooke A. Versaw, Hai Wang, Sarah Ward, Dr. Xiang Zhu, and Dr. Jennifer S. Zigmond, who created a friendly and safe work environment and supported my research. Finally, I would like to thank the Wooley staff and managers (Sherry Melton, Andy Moutray, Dr. Jeff E. Raymond, and Justin A. Smolen) for all their help not just in teaching but in keeping the Wooley lab going. It has been fulfilling to work with these talented researchers on problems we have found mutually interesting and I am thankful for their help, direction, and patience in teaching me.

Additionally, I would be remiss to not acknowledge all of the Administrative and Support Staff in the Chemistry Department, particularly the Graduate Office (Sandy Horton, Valerie A. McLaughlin, Dr. Joanna Goodey-Pellois, and Dr. Simon W. North), Business Operations (Ron G. Carter, Curtis Lee, Angie T. Stickley, Judy R. Ludwig,

Julie A. Zercher, Angie T. Medina, and Melvin C. William), NMR facilities (Drs. Greg P. Wylie, Vladimir Bakhmoutov, and Douglas W. Elliott), Mass Spectrometry (Drs. Bo Wang, Doyong Kim, Yohannes Rezenom, and Vanessa Santiago), Laboratory for Molecular Simulation (Dr. Lisa M. Pérez), Electronics (Tim P. Pehl), Glass Blowing (Bill C. Merka), Machine Shops (Bill T. Seward), and IT (Steve Tran and Mike D. Green) — I am thankful for all that you have done, especially the work that often goes unnoticed by the students but keeps the Department of Chemistry at Texas A&M running.

I would like to thank my Taiwanese friends, better known as the "Taiwanese Mafia" in the Department of Chemistry. Because of them, the loneliness brought by studying abroad was taken away from my graduate experience.

Lastly, I would like to thank my mom for her continued support for in life and throughout my education. She has given me a lot of care and love, without which I could not have such an awesome life.

CONTRIBUTORS AND FUNDING SOURCES

Contributors

This work was supervised by a dissertation committee consisting of Professor Karen L. Wooley (advisor) of the Departments of Chemistry, Chemical Engineering, and Materials Science and Engineering; Prof. David E. Bergbreiter (committee member) of the Department of Chemistry; Prof. Lei Fang (committee member) of the Departments of Chemistry, and Materials Science and Engineering; and Prof. Melissa A. Grunlan (committee member) of the Departments of Biomedical Engineering, and Materials Science and Engineering, and Chemistry.

In Chapter II, the ^{1}H–^{31}P Heteronuclear Multiple Bond Correlation experiments were performed by Mr. Steven D. Sorey at The University of Texas at Austin. Drs. Bo Wang and Doyong Kim of the Laboratory for Biological Mass Spectrometry obtained mass spectra.

In Chapter III, the syntheses of model reactions were performed with the help by Mr. Travis H. Smith.

All other experiments were carried out independently by the student.

Funding Sources

The work in Chapter II was made possible by the National Heart Lung and Blood Institute of the National Institutes of Health as a Program of Excellence in Nanotechnology (HHSN268201000046C), the National Science Foundation (CHE-

1410272, CHE-1610311 and CHE-0541587) and the Welch Foundation through the W. T. Doherty-Welch Chair in Chemistry (A-0001).

The work in Chapter III and IV was made possible by financial support from the National Science Foundation (CHE-1610311 and CHE-0541587) and the Welch Foundation through the W. T. Doherty-Welch Chair in Chemistry (A-0001).

These contents are solely the responsibility of the authors and do not necessarily represent the official views of the National Science Foundation, National Institutes of Health, and the Welch Foundation.

NOMENCLATURE

ATRP	Atom transfer radical polymerization
Boc	*tert*-Butyloxycarbonyl
cAMP	Cyclic adenosine monophosphate
cGMP	Cyclic guanosine monophosphate
CTMA	Cetyltrimethylammonium
$Đ$	Dispersity
DBU	1,8-Diazabicyclo[5.4.0]undec-7-ene
DFT	Density functional theory
DIPEA	*N*,*N*-Diisopropylethylamine
DMAP	4-Dimethylaminopyridine
DMF	*N*,*N*-Dimethylformamide
DNA	Deoxyribonucleic acid
DSC	Differential scanning calorimetry
ESI–MS	Electrospray ionization mass spectrometry
FTIR	Fourier-transform infrared
HMBC	Heteronuclear multiple bond correlation
HPLC	High-performance liquid chromatography
M_n	Number-average molar mass
NMR	Nuclear magnetic resonance
NOESY	Nuclear Overhauser spectroscopy

PCBT	Poly(3′,5′-bicyclic 3-(3-butenyl) thymidine ethylphosphate)
RAFT	Reversible addition-fragmentation chain transfer
RNA	Ribonucleic acid
ROP	Ring-opening polymerization
SEC	Size exclusion chromatography
SM	Starting material
STQN	Synchronous transit-guided quasi-Newton
T_g	Glass transition temperature
T_m	Melting temperature
TS	Transition state
TBD	1,5,7-Triazabicyclo[4.4.0]dec-5-ene
TGA	Thermogravimetric analysis
THF	Tetrahydrofuran

TABLE OF CONTENTS

Page

LIST OF FIGURES

Page

LIST OF TABLES

Page

CHAPTER I

INTRODUCTION

1.1 Development of Novel, Non-toxic, Functionalizable and Degradable Materials Based on Deoxyribonucleic Acid

In the design of functional polymeric nanomedical devices, it is important to consider the full life cycle of the components to reduce patient risk. At the end of the life cycle, these polymeric nanomedical devices should degrade during a specified time frame into harmless end products. Therefore, biodegradable synthetic polymers have received considerable attention due to their potential for environmental and biological clearance.[1,2]

In addition to several well-known, degradable polymer classes such as polyesters[3], polycarbonates[4], and polylactic acid[5] designed for biomedical applications, polyphosphoesters have exhibited accelerated biodegradability through hydrolytic and enzymatic cleavage of the phosphoester bonds in the backbone under physiological conditions.[1] Polyphosphoesters have also proven biocompatible and have inherent structural similarity to biomacromolecules such as nucleic and teichoic acids, leading to extensive investigation toward the construction of diverse functional nanostructures.[6-36] From a chemical perspective, polyphosphoesters are impressively versatile due to the pentavalent phosphorus center that allows for functionalization of both the main backbones and side chains of the polymers. This unique property of phosphorus allows

the introduction of bioactive molecules and extensive modulation of the physical and chemical properties of the polyphosphoesters.

Stemming from the synthetic control available, controllability of the macromolecular structure of polyphosphoesters is also important for the design of advanced materials. A variety of approaches for the synthesis of polyphosphoesters based on non-controlled polymerization such as polycondensation[37,38] and transesterification[39,40] were extensively studied in the 1990s and early 2000s. Recent advances have enabled the molar mass control of polyphosphoesters using controlled polymerization reactions,[31] including enzymatic polymerization[41] and ring-opening polymerization (ROP).[13,16,18-21,25-28,42] Notably, organocatalytic ROP can afford polyphosphoesters with molar masses up to 70 kDa with dispersities ($Đ$) as low as 1.05.[17]

The Wooley lab has performed extensive studies on the synthesis and assembly of polyphosphoesters in biomedical applications.[16,18-21,25-28] These early works utilized a post-polymerization modification strategy, including click chemistries (copper catalyzed azide–alkyne cycloaddition, thiol–ene, and thiol–yne reactions) and reversible silver–alkyne interaction, to introduce functionalities useful for drug delivery to the pendant triester side chains. Although facile synthetic methods for ROP of phospholanes (five-membered cyclic phosphotriesters) have been developed for the preparation of functionalizable polyphosphoesters, it has also been recognized that the types of polyphosphoesters that have been central in the Wooley lab undergo hydrolysis into ethylene glycol, among other products. As the toxicity of ethylene glycol presents

potential safety concerns for human use, this dissertation describes the design, synthesis, and characterization of polyphosphoesters derived from DNA that will not degrade into ethylene glycol and will more closely resemble nucleic acid- and teichoic acid-based natural polyphosphoester systems.

In Nature, nucleic acid (DNA/RNA) represents one of the most powerful biomolecules, by performing gene transcription and translation as genetic material by hybridization with complementary strands. In materials science, nucleic acids also allow for selective hybridization, unique geometry, ability to form nanoscale building blocks, directional self-assembly, and flexible programmability.[43,44] As a result, polymer chemists have made various attempts, enzymatically or non-enzymatically, and particularly with controlled polymerization techniques, to synthesize DNA-mimicking polymers.[45]

Among various controlled polymerization techniques yielding polymers with narrow molar mass distributions and well-defined architectures, ROP of cyclic esters, amides, carbonates, and phosphoesters is especially valuable in the context of developing degradable polymers. Toward DNA-derived polyphosphoesters from ROP, the ability to undergo initiation and propagation of six-membered cyclic phosphoesters represents a significant challenge (Figure 1.1). Studies on the ROP of the six-membered cyclic phosphorinane monomer, 2-hydro-2-oxo-1,3,2-dioxaphosphorinane, have been reported by Penczek and co-workers.[46-48] To side step the direct polymerization of phosphorus(V), this system polymerizes *via* tautomerization of the phosphorinane center to generate the active phosphorus(III) species *in situ*[49] that provide a less sterically-

hindered environment at the electrophilic phosphorus center (Figure 1.2). However, the only report on the ROP of a non-tautomerizable six-membered cyclic phosphoester, 2-methoxy-2-oxo-1,3,2-dioxaphosphorinane, led to oligomers (degree of polymerization ≤ 10) under harsh conditions (neat, 135 °C), due to extensive chain transfer originating from the low ring strain energy.[50] Therefore, our strategy to introduce ring strain energy into the six-membered cyclic system, and thereby achieve higher molar mass polyphosphoester, is presented and discussed in Chapter II.

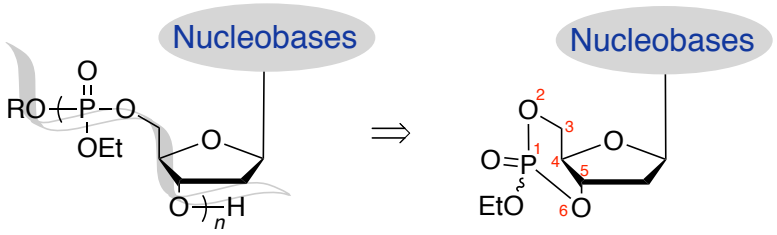

Figure 1.1. Retrosynthetic analysis of DNA-derived polyphosphoesters from ROP of six-membered cyclic monomers.

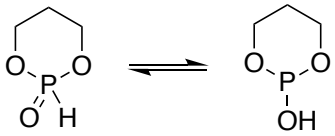

Figure 1.2. Tautomerization of the phosphorinane center of 2-hydro-2-oxo-1,3,2-dioxaphosphorinane to generate the active phosphorus(III) species for ROP.

1.2 Regioisomeric Preference in the Organocatalytic ROP of Six-membered Cyclic Phosphoesters into DNA Analogues

Regioregularity is a crucial property in the synthesis of DNA analogues, as natural DNA is synthesized exclusively in the 5′-to-3′ direction. Therefore, in Chapter III, the investigation of regioisomeric preference in the organocatalytic ROP of six-membered cyclic phosphoesters into DNA analogues will be discussed in order to provide fundamental understanding of the polymerization behavior.

Several types of cyclic monomers, such as carbonates, epoxides, phosphazenes, phosphoesters, *H*-phosphonates, phosphonites, phosphorothioates, siloxanes, and thiocarbonates, undergo ROP from opening of cyclic monomers from either side of the ring. If such monomers are asymmetrical, there are formally two ways the monomer ring can be opened, *i.e.*, the regioisomeric ROP can yield polymers with head-to-head, head-to-tail, and tail-to-tail configurations (Figure 1.3). Although not trivial, careful microstructural analysis by model reactions and nuclear magnetic resonance (NMR) spectroscopy can determine the preferred reaction route. Vandenberg,[51] Penczek,[52] and Wurm[53] performed microstructural analyses of cyclic phosphorothioates, *H*-phosphonates, and phosphoesters to understand the regioselectivity of these phosphorus-containing monomers for ROP from the spectroscopic characteristics of these isomers. Although early work was constrained due to limited NMR capabilities, these studies concluded that head-to-tail configuration was the dominant connectivity when steric effects from both ring-opening directions were different, *e.g.*, primary and secondary

alcohols formed from the ring-opening reactions. Our ultimate goal is to develop a synthetic strategy, by careful monomer design and proper catalyst choice, to gain control of the polymerization direction that leads to regioregular DNA/RNA polymers provided in enzymatic syntheses.

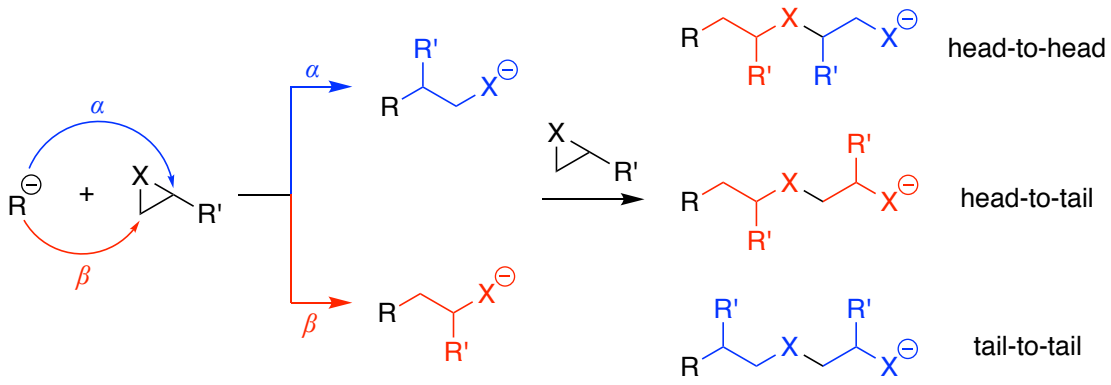

Figure 1.3. Nucleophilic ROP of asymmetrical hetereocycles.

This dissertation focuses on the synthesis, characterization, and development of polymeric materials from thymidine, one of the four natural nucleosides. Compared to the other nucleosides, thymidine is the most amenable toward selective functionalization, due to the pK_a difference between its N–H and O–H. Several guidelines have encompassed the synthetic thymidine-derived monomers and polymers, including the use of simple, scalable and translatable chemistries. The monomers and polymers are designed such that the resulting material properties are easily manipulated by further functionalization and fine tuning with click chemistries. To our knowledge,

this work is the first instance[45] that well-defined DNA-derived polyphosphoesters with 3′,5′-linkages in the backbones have been prepared *via* ROP. As such, it was an aim of this work to effectively introduce nucleosides into the field of polymer science and lay a foundation from which new chemistries, as well as engineering and biomedical applications may be explored with synthetic nucleoside-based polymers.

CHAPTER II

SYNTHETIC, FUNCTIONAL THYMIDINE-DERIVED POLYDEOXYRIBONUCLEOTIDE ANALOGUES FROM A SIX-MEMBERED CYCLIC PHOSPHOESTER*

2.1 Introduction

Nucleosides play important roles in Nature.[54] The incorporation of non-natural nucleosides into DNA and RNA allows for significant investigations, including fundamental research on structure and function,[55-61] and development of synthetic materials for clinical applications,[62-64] yet there are only few routes that allow access to well-defined synthetic DNA and RNA derivatives. Enzymatic processes that integrate non-natural nucleosides into DNA and RNA are limited by the activity of the mediating polymerase, which often restricts the extent of incorporation and reaction conditions.[65-68] On the other hand, synthetic methods offer exquisite sequence control, but have focused mainly on stepwise condensation reactions of nucleoside repeat units with electrophiles, such as 3′-phosphoryl chloride,[69] phosphotriester,[70,71] and phosphoramidites[72] (*e.g.*, *via* solid-phase DNA synthesis). Synthetic methods have not yet advanced for the construction of nucleic acid-based polymers having 3′,5′-linkages through controlled

---

* Reprinted (adapted) with permission from "Synthetic, Functional Thymidine-Derived Polydeoxyribonucleotide Analogues from a Six-Membered Cyclic Phosphoester" by Tsao, Y.-Y. T.; Wooley, K. L., *J. Am. Chem. Soc.* **2017**, *139*, 5467–5473. Copyright 2017 American Chemical Society.

chain-growth addition polymerization, which offers rapid and convenient polymer chain growth. Currently, syntheses of DNA-derived polymers[73] by chain-growth chemistries remain limited to non-3′,5′-backbones through uncontrolled radical polymerization,[74,75] atom transfer radical polymerization (ATRP),[76-78] and reversible addition–fragmentation chain transfer (RAFT) polymerization[79] techniques that yield polymers with pendant nucleosides. For 3′,5′-DNA-derived materials, polymerization with predetermined molar mass, and control over end groups and sequence is a feasible, yet unrealized, aim.

Besides several well-known polymer classes used in biological research, such as polyesters and polycarbonates, polyphosphoesters, particularly nucleoside phosphoesters,[80] are attractive due to their biocompatibility, biodegradability through spontaneous and/or enzymatic hydrolysis, as well as their structural similarity to nucleic and teichoic acids.[13] ROP is a versatile synthetic method for generating well-defined macromolecules from carbocyclic or heterocyclic monomers,[81,82] and organocatalytic ROP[14,16,17,21,23,83-85] of five-membered cyclic phosphoesters has been demonstrated to produce well-defined polyphosphoesters.[13,16,18] However, polymerization of six-membered cyclic phosphorus-containing monomers, a potential precursor for well-defined DNA analogues with 3′,5′-backbones, has received less attention. Studies on the ROP of a six-membered phosphorinane monomer, 2-hydro-2-oxo-1,3,2-dioxaphosphorinane, have been reported by Penczek and co-workers.[46-48] Polymerization was possible due to tautomerization of the monomer to generate phosphorus(III) intermediates *in situ*[49] that provide a less sterically-hindered environment at the electrophilic phosphorus center. Such ROPs have not yet been fully

expanded to non-tautomerizable six-membered cyclic phosphoesters, such as cyclic adenosine monophosphate (cAMP) and its guanosine counterpart (cGMP), which play critical metabolic and regulatory roles. The only report on the ROP of a non-tautomerizable six-membered phosphorinane, 2-methoxy-2-oxo-1,3,2-dioxaphosphorinane, led to oligomers (degree of polymerization $\leq$ 10) under harsh conditions (neat, 135 °C), due to extensive chain transfer originating from the low ring strain energy.[50] Hence, in order to achieve higher molar mass polyphosphoesters from six-membered cyclic phosphoesters, introducing ring strain energy into the cyclic system is critical.

Higher ring strain energy is also generally accepted to be the key factor that facilitates the polymerization of five-membered cyclic phosphoesters. The hydrolysis rates of five-membered cyclic phosphoesters increase by an order of 10^5 compared to the acyclic species, which were attributed to enthalpy of activation,[86] $\Delta H^{\ddagger}$, rather than to the entropy of activation,[87] $\Delta S^{\ddagger}$, according to Eyring plots. Ring strain and its relief are enthalpic phenomena and, hence, we reasoned that, if relief of ring strain in the transition state of the rate-determining step is crucial to the acceleration of hydrolysis in the cyclic phosphoesters, analysis of those ring strain energies could guide monomer design.

Herein, we report a synthetic strategy that includes organocatalytic ROP of a six-membered cyclic phosphoester monomer at ambient temperature to afford a new type of thymidine-derived 3′,5′-linked polyphosphoester with a butenyl group located on each repeat unit and number-average molar masses (M_n) up to 11 kDa. The monomer was prepared in two steps, and the polymerization proceeded in a controlled fashion to afford

polymers with low *Đ*. This article focuses on the synthesis of the novel monomers and polymers that comprise a thymidine DNA derivative with a polyphosphoester backbone. To the best of our knowledge, no well-defined DNA-derived polyphosphoesters with 3′,5′-linkages in the backbones from ROP have been reported to date.

2.2 Results and Discussions

The ring strain energies of monocyclic five-membered, monocyclic six-membered, and 3′,5′-bicyclic phosphoesters were calculated using density functional theory (DFT). The theoretical estimation of ring strain energies serves as computational insight into direct the rational design of 3′,5′-bicyclic phosphoesters in nucleosides as a skeleton for ROP of six-membered cyclic phosphoesters. Ring strain energy is a relative quantity, and is defined as the excess energy between a cyclic molecule and an appropriately selected strain-free, linear counterpart. Theoretical estimates of ring strain energy can be obtained by using group equivalents to convert DFT energies into reasonably accurate heats of formation. To investigate the feasibility of ROP of 3′,5′-bicyclic phosphoesters, ring strain energies of different cyclic phosphoesters (Figure 2.1a) were calculated with DFT using an approach similar to a previous report by the Lim group[88] at the B3LYP/6-31+G*, B97-D/6-31+G*, and M06-2X/6-31+G* levels of theory to include adjustments for medium-range electron and dispersion corrections (Table 2.1). With the six-membered cyclic phosphoester **1** assumed to be unstrained, the

validity of DFT calculations was verified by comparing the calculated ring strain energies of **2** to experimental values.[89] While a systematic study on the ring strain energy of the 3′,5′-bicyclic system was not reported, enthalpies of hydrolysis of cAMP and diethyl phosphate, 11.49 ± 0.35 and 2.50 ± 0.45 kcal/mol, respectively,[90] suggest a large ring strain energy for the 3′,5′-bicyclic system and are in agreement with the calculation results. Therefore, it was expected that the higher ring strain energy of the designed 3′,5′-bicyclic phosphoester **3** would allow for ROP on a six-membered cyclic phosphoester under mild conditions. Moreover, the diastereomer **(*R*)-3** was found to be more strained, due to the anomeric effect in **(*S*)-3**.[91-95]

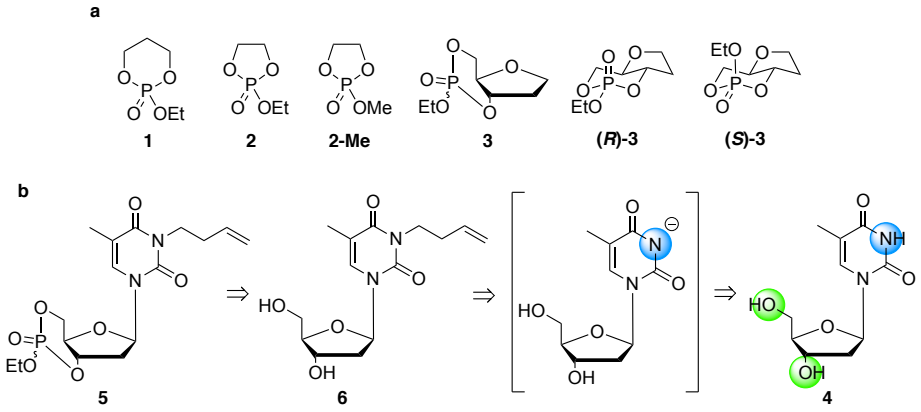

Figure 2.1. Design and retrosynthesis of thymidine-derived DNA analogues. (a) Different cyclic phosphoesters for DFT calculation of ring strain energies. (b) Retrosynthetic analysis of the cyclic monomer **4** from thymidine **6**. Reprinted with permission from "Synthetic, Functional Thymidine-Derived Polydeoxyribonucleotide Analogues from a Six-Membered Cyclic Phosphoester" by Tsao, Y.-Y. T.; Wooley, K. L., *J. Am. Chem. Soc.* **2017**, *139*, 5467–5473. Copyright 2017 American Chemical Society.

Table 2.1. Experimental and DFT calculation of the ring strain energies (kcal/mol) of six-membered cyclic phosphoester (**1**), five-membered cyclic phosphoester (**2**), and 3′,5′-bicyclic phosphoester (**3**). Reprinted with permission from "Synthetic, Functional Thymidine-Derived Polydeoxyribonucleotide Analogues from a Six-Membered Cyclic Phosphoester" by Tsao, Y.-Y. T.; Wooley, K. L., *J. Am. Chem. Soc.* **2017**, *139*, 5467–5473. Copyright 2017 American Chemical Society.

Method	**1**	**2**	**(*R*)-3**	**(*S*)-3**
Experimental	–	5.9 ± 0.3[a]	–	–
B3LYP/6-31+G*	0	4.1	6.3	5.9
M06-2X/6-31+G*	0	5.0	7.2	5.4
B97-D/6-31+G*	0	4.2	7.0	5.8

[a]Experimental value of **2-Me** was reported.[89]

In order to construct a 3′,5′-bicyclic system similar to **3**, thymidine (**4**) was chosen of the four natural deoxyribonucleosides, due to the potential for selective functionalization at the 3′-OH, 5′-OH and N^3-positions. Selective functionalization at the N^3-position can be achieved with weak bases, such as potassium carbonate, given the pK_a differences between alcohols (pK_a ≈ 16–17) and the N^3-proton (pK_a ≈ 9.5).[73] In contrast, strong bases, such as sodium hydride, have the capability to deprotonate the 3′-OH, 5′-OH, and N^3-protons, with functionalization occurring preferentially at the 3′-OH and 5′-OH positions, due to the increased nucleophilicity of alkoxides over imide anions. The standard retrosynthetic analysis for the target monomer, **5**, a strained 3′,5′-bicyclic structure, is given in Figure 2.1b. The synthesis was realized through a two-step procedure that involved selective butenylation at the N^3-position in the presence of weak base, followed by cyclization of 3′-OH and 5′-OH.

Installation of a butenyl group at N^3 was conducted to coincidentally protect the imide, enhance organic solubility, and install a functionality that would allow for later

chemical modification. Due to the two electron-withdrawing carbonyl groups at the 2- and 4-positions of the thymine unit, chemical modification *via* nucleophilic substitution to afford N^3-substituted thymidine typically requires several days for completion. Choice of solvents is also limited, due to the solubility of the thymidine starting material, **4**. Butenylation at the N^3-position was found to be possible in *N*,*N*-dimethylformamide (DMF) at 60 °C to give **6** as a white hygroscopic solid with high yields (> 90%) within 48 h, while reaction in methanol under the same conditions required longer reaction times (at least 96 h).

A key challenge in the second step of the synthetic approach is to favor cyclization over oligomerization. Cyclization of **6** was expected to be both kinetically and thermodynamically difficult, given the large ring strain barrier as well as slow kinetics of cyclizing a trans-diol, which is in agreement with results from the Buchard group.[96,97] A linear oligomer was obtained upon reaction with ethyl dichlorophosphate (**7**), in the presence of triethylamine in tetrahydrofuran (THF) under dilute conditions. Sufficient time for the conformational change from the intermediate (**8**) was hypothesized to be important, in order to bring the second alcohol and phosphorus into proximity to close the ring, *vs.* bimolecular reactions that could lead to oligomerization. Additionally, it was considered that weaker leaving groups might slow the condensation reaction, and 4-nitrophenol has been shown to be a moderate leaving group for phosphoester cleavage in the presence of an activator.[98] Jain and Kalman have reported the use of 4-nitrophenol and 1,8-diazabicyclo[5.4.0]undec-7-ene (DBU) as leaving group and activator, respectively, to cyclize 5-fluoro-2′-deoxyuridine.[99] However, attempts at

ring closure by reaction of **6** with ethyl bis(4-nitrophenyl)phosphate encountered the challenge of incomplete separation of the monomer from the by-product 4-nitrophenol, which could be a deactivator of the organocatalyst for ROP. Cyclization conditions were then screened with the aim of optimizing the cyclization reaction using ethyl dichlorophosphate (Table 2.2).

Table 2.2. Condition screening for cyclization of **6** with **7** using various solvents and bases at –78 °C. Reprinted with permission from "Synthetic, Functional Thymidine-Derived Polydeoxyribonucleotide Analogues from a Six-Membered Cyclic Phosphoester" by Tsao, Y.-Y. T.; Wooley, K. L., *J. Am. Chem. Soc.* **2017**, *139*, 5467–5473. Copyright 2017 American Chemical Society.

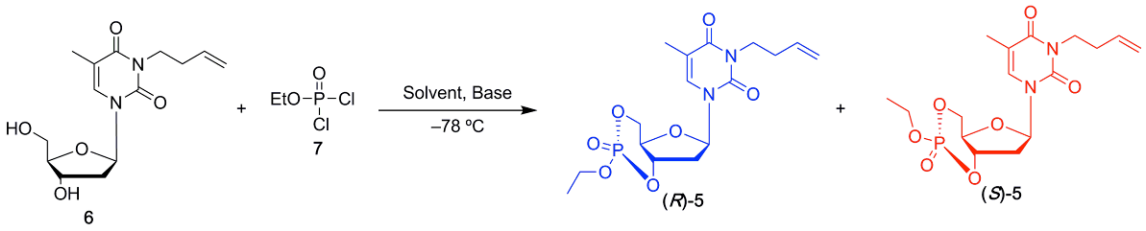

Entry	Solvent	Base	Result	Yield (%)	(*R*)/(*S*)[a]
1	THF	Et_3N	Oligomerization	–	–
2	THF	Pyridine	Oligomerization	–	–
3	THF	DMAP	Oligomerization	–	–
4	THF	DIPEA	Oligomerization	–	–
5	DMF	Et_3N	Oligomerization	–	–
6	DMF	Pyridine	Oligomerization	–	–
7	DMF	DMAP	Oligomerization	–	–
8	DMF	DIPEA	Oligomerization	–	–
9	CH_2Cl_2	Et_3N	No reaction	–	–
10	CH_2Cl_2	Pyridine	No reaction	–	–
11	CH_2Cl_2	DMAP	Cyclization	58	88:12
12	CH_2Cl_2	DIPEA	Cyclization	4	8:92

[a](*R*)/(*S*) ratio was determined by ^{31}P NMR of reaction crude.

Oligomerization occurred when the reactions were conducted in DMF and THF, in the presence of a variety of bases. Polar aprotic solvents, such as DMF and THF, were found to promote oligomerization over cyclization, presumably, by shortening the lifetime of the intermediate (**8**). The bases 4-dimethylaminopyridine (DMAP) and *N*,*N*-diisopropylethylamine (DIPEA) effectively facilitated cyclization in dichloromethane. Interestingly, the diastereoselectivity of these two reactions differed significantly, where DMAP and DIPEA yielded (*R*):(*S*) ratios of 88:12 and 8:92, respectively. This selectivity is attributed to the nucleophilic characteristic of DMAP to activate **7** and yield a more stable transition state that leads to kinetic product **(*R*)-5**, even though **(*S*)-5** is more stable by 1.35 kcal/mol at the B3LYP/6-31+G* level of theory (Figure 2.2 and Figure 2.3). Since several recrystallization conditions failed to obtain a single crystal of **5** for X-ray diffraction measurement, the absolute stereochemistries were then determined by an indirect method with one-dimensional nuclear Overhauser spectroscopy (1D-NOESY). The through-space atomic distances between 4′-H (marked in gray on the structures in Figure 2.4) and the methyl protons of the ethyl phosphoester in the diastereomeric pairs are sufficiently different, 6.6 Å *vs.* 4.2 Å for **(*S*)-5** *vs.* **(*R*)-5**, respectively, that the diastereomer assignments could be made by a positive NOE only for the (*R*)-diastereomer in the 1D-NOESY experiment.

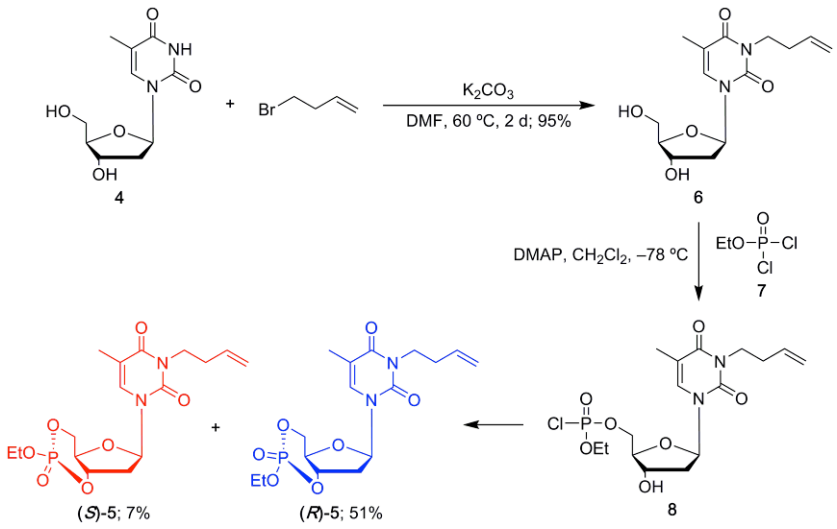

Figure 2.2. Synthetic route from thymidine to monomer **5**. Reprinted with permission from "Synthetic, Functional Thymidine-Derived Polydeoxyribonucleotide Analogues from a Six-Membered Cyclic Phosphoester" by Tsao, Y.-Y. T.; Wooley, K. L., *J. Am. Chem. Soc.* **2017**, *139*, 5467–5473. Copyright 2017 American Chemical Society.

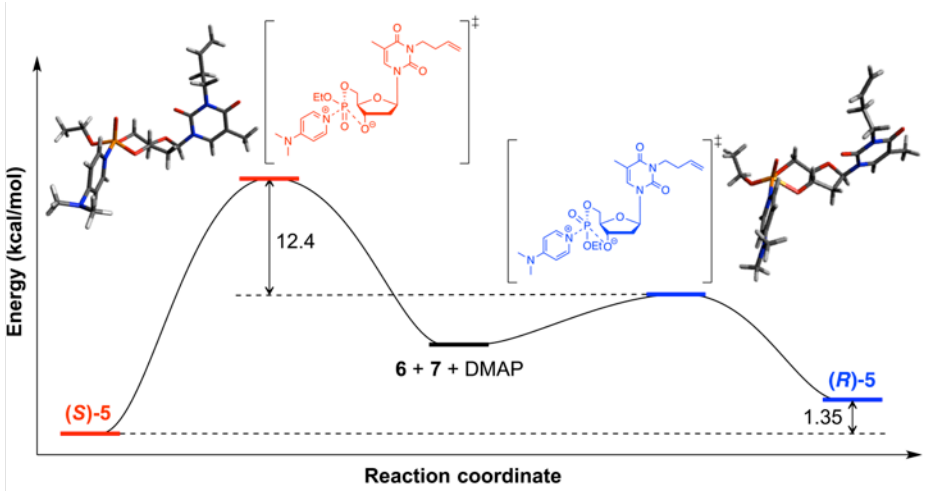

Figure 2.3. Reaction coordinate diagram of using DMAP as activator to promote cyclization of **6** at the B3LYP/6-31+G* level of theory. Reprinted with permission from "Synthetic, Functional Thymidine-Derived Polydeoxyribonucleotide Analogues from a Six-Membered Cyclic Phosphoester" by Tsao, Y.-Y. T.; Wooley, K. L., *J. Am. Chem. Soc.* **2017**, *139*, 5467–5473. Copyright 2017 American Chemical Society.

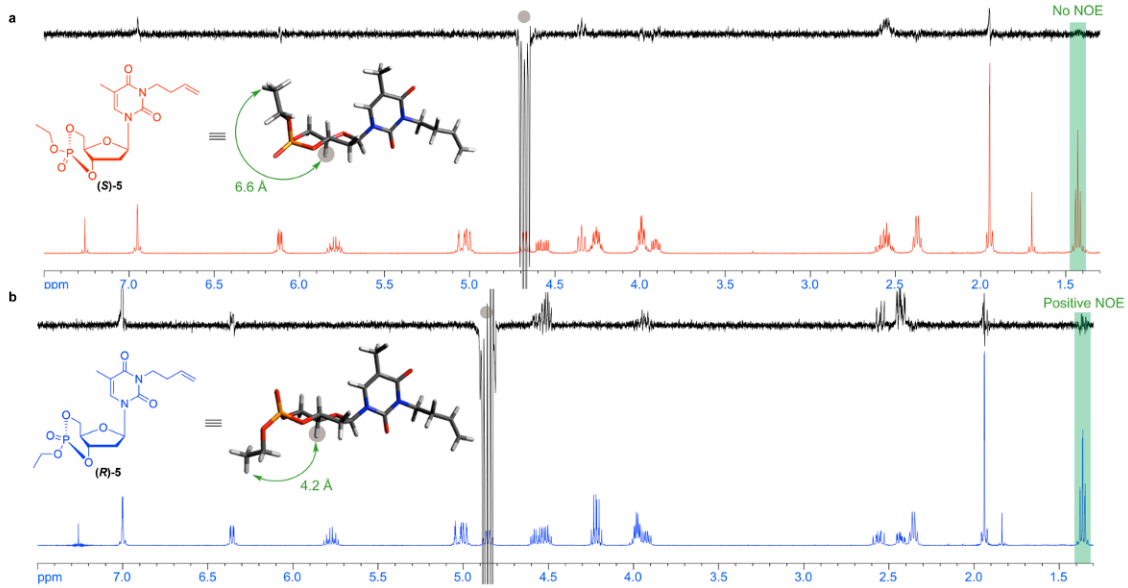

Figure 2.4. Use of 1D-NOESY to identify the diastereomer (a) **(*S*)-5** and (b) **(*R*)-5**, with atomic distance of 6.6 Å and 4.2 Å, respectively, calculated from DFT geometric optimization at the B3LYP/6-31+G* level of theory. Reprinted with permission from "Synthetic, Functional Thymidine-Derived Polydeoxyribonucleotide Analogues from a Six-Membered Cyclic Phosphoester" by Tsao, Y.-Y. T.; Wooley, K. L., *J. Am. Chem. Soc.* **2017**, *139*, 5467–5473. Copyright 2017 American Chemical Society.

ROP of **5** was conducted using 1,5,7-triazabicyclo[4.4.0]dec-5-ene (TBD) as the catalyst, and 4-methoxybenzyl alcohol — a natural chemical found in anise, honey, and vanilla — as the initiator to enable straightforward end-group analysis by NMR and to minimize potential toxicity following hydrolytic degradation (Figure 2.5). ROP of **(*R*)-5** initiated at the onset of TBD addition, according to thin-layer chromatography. In contrast, the diastereomer **(*S*)-5** showed no reaction under the same conditions after 96 h — this lower reactivity is in agreement with the lower ring strain energy calculated for the (*S*)-configuration (Table 2.1). Attempts to polymerize **(*S*)-5** at lower temperatures (0 °C and –78 °C), in order to suppress the entropic penalty, were unsuccessful. The

conversion of **(*R*)-5** monomer to afford poly(3′,5′-bicyclic 3-(3-butenyl) thymidine ethylphosphate) (**PCBT**, **9**) reached over 95% at ambient temperature, with good control of the polymerization being retained, as suggested by low $Đ$ and excellent linear agreement between the M_n and percent monomer conversion (Figure 2.6, Figure 2.7, and Table 2.3). Copolymerization of an 88:12 diastereomeric mixture of **(*R*)-5**:**(*S*)-5** monomers led to incomplete copolymerization, without apparent incorporation of **(*S*)-5**, as indicated by the proportion of polymer to remaining **(*R*)-5** and **(*S*)-5** unreacted monomers being 86:2:12, according to the crude ^{31}P NMR spectrum (Figure 2.8). ^{13}C and ^{31}P NMR spectra of $\mathbf{PCBT_{10}}$, $\mathbf{PCBT_{21}}$ and $\mathbf{PCBT_{32}}$ contained signals resonating at multiple frequencies, which may have resulted from diastereomers and, potentially, combinations of head-to-head, head-to-tail, and tail-to-tail regioisomers. Regioisomeric differences are possible from cleavage of the P-O5′ *vs.* P-O3′ bond during the initial ring opening following attack by an initiator, and also during subsequent ring openings during propagation of the ROP. A model reaction employing excess ethanol as initiator and solvent was conducted to prevent the formation of diastereomeric products and allow for evaluation of the monomeric product(s) from an initial ring-opening reaction. Characterization by ^{1}H, ^{13}C and ^{31}P NMR spectroscopies confirmed the ring opening had occurred and identified a single phosphorus environment (Figure 2.9). ^{1}H–^{31}P HMBC analysis on the product isolated from unreacted **(*R*)-5**, indicated that only unimer **10a** had formed (Figure 2.10), suggesting that the initial ring-opening reaction was more favorable at the P-O5′-position. Further investigations on the regioselectivity during subsequent propagation steps during the ROP are ongoing.

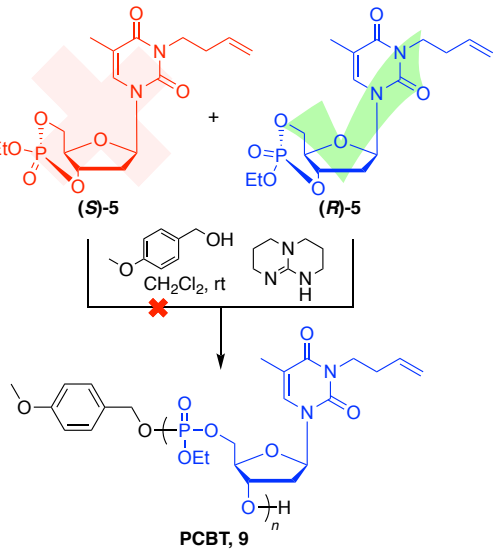

Figure 2.5. Polymerization of **5** with 4-methoxybenzyl alcohol as the initiator and TBD as the catalyst. Although the polymer is illustrated with only one regiochemistry and no stereochemistry, ^{31}P NMR spectra suggested that the polymers contained regioisomeric and diastereoisomeric repeat units. Reprinted with permission from "Synthetic, Functional Thymidine-Derived Polydeoxyribonucleotide Analogues from a Six-Membered Cyclic Phosphoester" by Tsao, Y.-Y. T.; Wooley, K. L., *J. Am. Chem. Soc.* **2017**, *139*, 5467–5473. Copyright 2017 American Chemical Society.

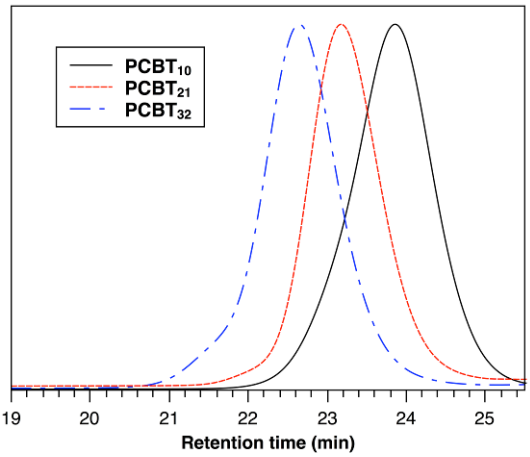

Figure 2.6. SEC traces of **PCBT$_{10}$**, **PCBT$_{21}$**, and **PCBT$_{32}$**. Reprinted with permission from "Synthetic, Functional Thymidine-Derived Polydeoxyribonucleotide Analogues from a Six-Membered Cyclic Phosphoester" by Tsao, Y.-Y. T.; Wooley, K. L., *J. Am. Chem. Soc.* **2017**, *139*, 5467–5473. Copyright 2017 American Chemical Society.

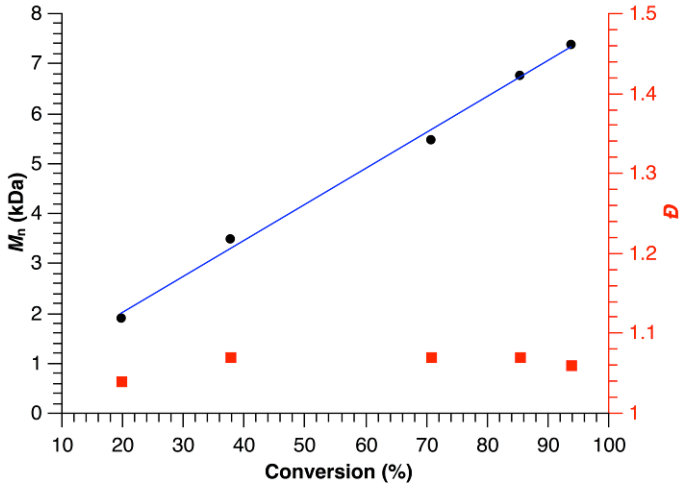

Figure 2.7. Plot of M_n and $Đ$ *vs.* monomer conversion for the polymerization of **(*R*)-5** using TBD as the catalyst and 4-methoxybenzyl alcohol as the initiator, obtained from SEC analyses from one of three runs; monomer/initiator/TBD ratio was 20:1:2. Reprinted with permission from "Synthetic, Functional Thymidine-Derived Polydeoxyribonucleotide Analogues from a Six-Membered Cyclic Phosphoester" by Tsao, Y.-Y. T.; Wooley, K. L., *J. Am. Chem. Soc.* **2017**, *139*, 5467–5473. Copyright 2017 American Chemical Society.

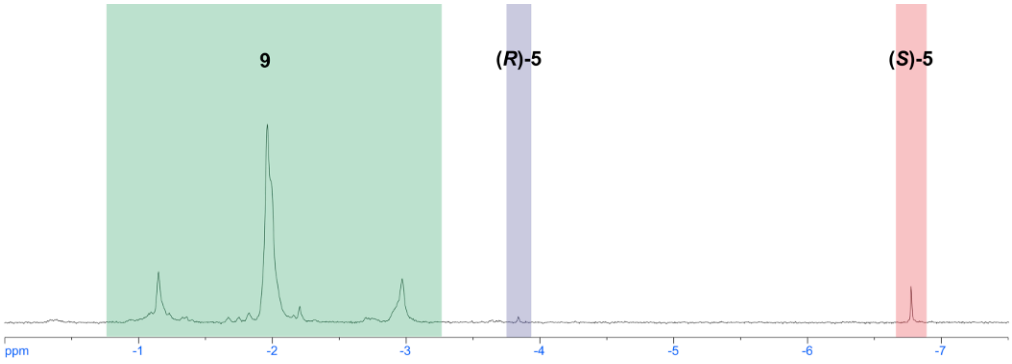

Figure 2.8. Crude ^{31}P NMR (202 MHz; $CDCl_3$) spectrum of the copolymerization of an 88:12 diastereomeric mixture of **5**. Reprinted with permission from "Synthetic, Functional Thymidine-Derived Polydeoxyribonucleotide Analogues from a Six-Membered Cyclic Phosphoester" by Tsao, Y.-Y. T.; Wooley, K. L., *J. Am. Chem. Soc.* **2017**, *139*, 5467–5473. Copyright 2017 American Chemical Society.

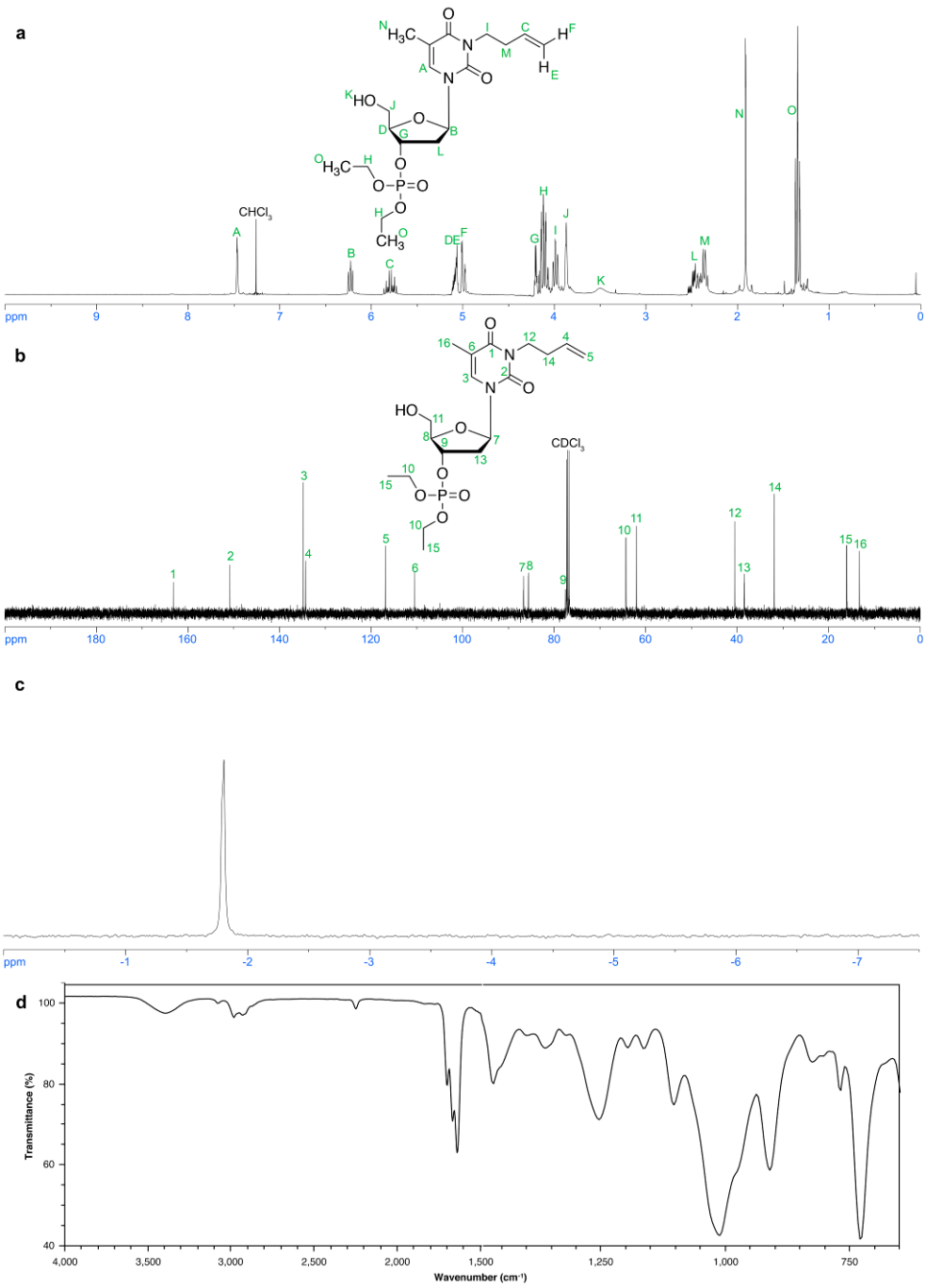

Figure 2.9. Spectroscopic characterization of **10a**. (a) ^{1}H NMR (500 MHz; $CDCl_3$). (b) ^{13}C NMR (125 MHz; $CDCl_3$). (c) ^{31}P NMR (202 MHz; $CDCl_3$). (d) IR spectrum. Reprinted with permission from "Synthetic, Functional Thymidine-Derived Polydeoxyribonucleotide Analogues from a Six-Membered Cyclic Phosphoester" by Tsao, Y.-Y. T.; Wooley, K. L., *J. Am. Chem. Soc.* **2017**, *139*, 5467–5473. Copyright 2017 American Chemical Society.

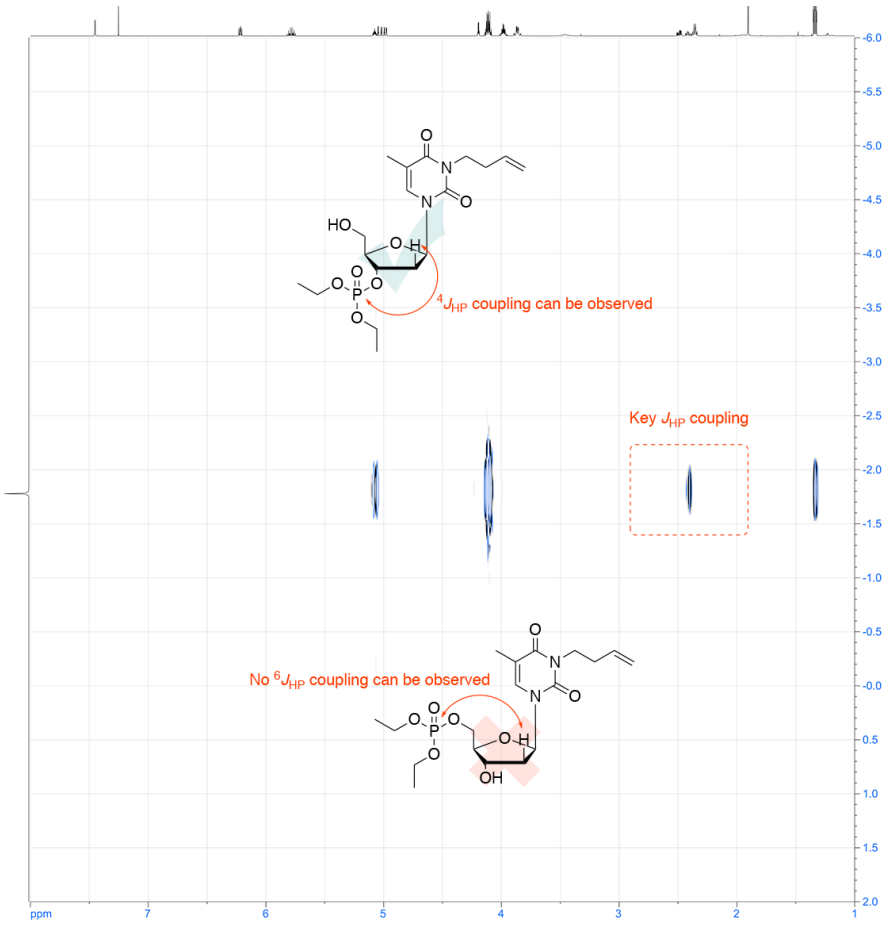

Figure 2.10. ^1H–^{31}P HMBC spectrum of **10**. Reprinted with permission from "Synthetic, Functional Thymidine-Derived Polydeoxyribonucleotide Analogues from a Six-Membered Cyclic Phosphoester" by Tsao, Y.-Y. T.; Wooley, K. L., *J. Am. Chem. Soc.* **2017**, *139*, 5467–5473. Copyright 2017 American Chemical Society.

Table 2.3. Polymerization results of **(*R*)-5** with 4-methoxybenzyl alcohol and TBD at ambient temperature in dichloromethane. Reprinted with permission from "Synthetic, Functional Thymidine-Derived Polydeoxyribonucleotide Analogues from a Six-Membered Cyclic Phosphoester" by Tsao, Y.-Y. T.; Wooley, K. L., *J. Am. Chem. Soc.* **2017**, *139*, 5467–5473. Copyright 2017 American Chemical Society.

Polymer	Catalyst	M:I:catalyst (molar ratio)[a]	Time	Conversion (^{31}P NMR)	M_n, Da (SEC)[b]	Đ (SEC)[b]	M_n, Da (theo)[c]	M_n, Da (^{1}H NMR)[d]
$PCBT_{10}$	TBD	10:1:2	6 h	96%	3,200	1.09	3,800	3,900
$PCBT_{21}$	TBD	20:1:2	8 h	98%	4,800	1.06	7,700	8,200
$PCBT_{32}$	TBD	30:1:4	24 h	95%	6,200	1.09	11,000	12,400

[a]Initial monomer concentration for all entries was 0.25 M in dichloromethane; [b]M_n (SEC) and *Đ* (SEC) were measured by THF SEC calibrated using polystyrene standards; [c]M_n (theo) was calculated from the monomer to initiator ratio and corrected for the conversion; [d]M_n (^{1}H NMR) was calculated by comparing the ^{1}H NMR integration values for the resonance signals of the two aromatic protons *ortho* to the methoxy group of the 4-methoxybenzyl initiated chain terminus (6.89 ppm) with one alkenyl proton of the butylene side chain groups (5.85–5.72 ppm).

The kinetics of ROP of **(*R*)-5** were investigated by conducting three polymerizations simultaneously from stock solutions. In these experiments, **(*R*)-5** and 4-methoxybenzyl alcohol (molar ratio of 20:1) were premixed in anhydrous dichloromethane, and the solution was divided into three portions, to each of which was added solutions of TBD (molar ratio to initiator of 2:1) in anhydrous dichloromethane. After the mixtures were allowed to stir for a pre-determined amount of time, aliquots were quenched by the addition of acetic acid. The monomer conversions were determined by ^{31}P NMR (Figure 2.11), while the molar masses and their distribution values were determined by size exclusion chromatography (SEC) calibrated with linear polystyrene standards using THF as the mobile phase. Attempts to determine absolute molar masses from the light scattering detector SEC traces were unsuccessful due to the

poor signal-to-noise ratio (Figure 2.12). The linearity of M_n *vs.* monomer conversion (Figure 2.7) suggested that the number of macromolecules in the reaction system was constant during polymerization, up to 95% conversion, with $Đ$ less than 1.10 throughout the polymerization. Kinetic plots of $\ln([M]_0/[M])$ *vs.* time showed the ROP of **(*R*)-5** to exhibit pseudo-first order kinetics with a propagation rate constant of $k_p = 9.2 \times 10^{-5}$ s^{-1} (Figure 2.13), suggesting that the rate of initiation was greater than the rate of propagation. Even though **(*R*)-5** was calculated to be more strained, the propagation rate was slower than those observed in the ROPs of five-membered cyclic phosphoesters (calculated as $k_p = 6.3 \times 10^{-3}$ s^{-1} from published data)[16] under the same conditions.

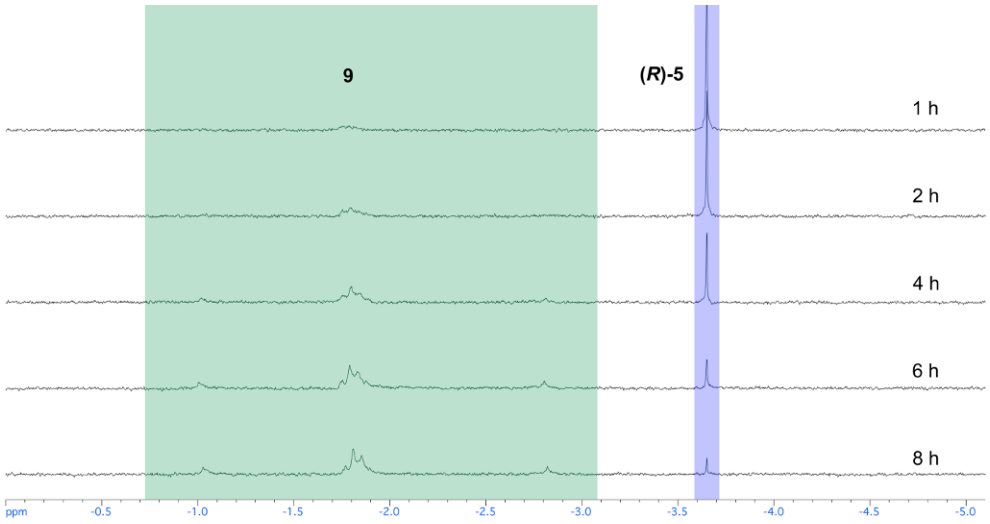

Figure 2.11. ^{31}P NMR (202 MHz; $CDCl_3$) spectra for the calculations of conversions in the kinetic study. Reprinted with permission from "Synthetic, Functional Thymidine-Derived Polydeoxyribonucleotide Analogues from a Six-Membered Cyclic Phosphoester" by Tsao, Y.-Y. T.; Wooley, K. L., *J. Am. Chem. Soc.* **2017**, *139*, 5467–5473. Copyright 2017 American Chemical Society.

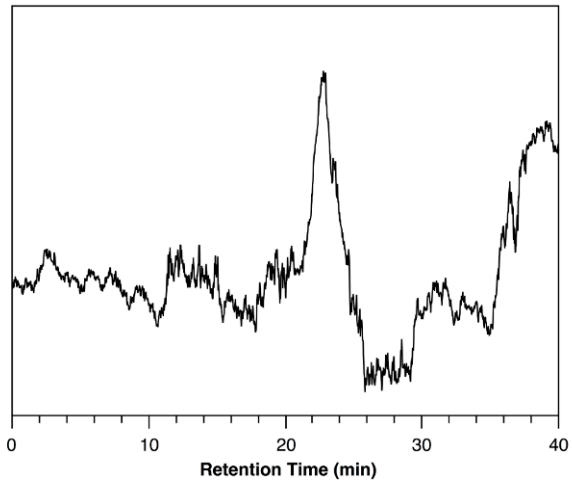

Figure 2.12. Light scattering detector trace (90°) for **PCBT$_{32}$** from THF SEC, demonstrating poor signal-to-noise ratio. Reprinted with permission from "Synthetic, Functional Thymidine-Derived Polydeoxyribonucleotide Analogues from a Six-Membered Cyclic Phosphoester" by Tsao, Y.-Y. T.; Wooley, K. L., *J. Am. Chem. Soc.* **2017**, *139*, 5467–5473. Copyright 2017 American Chemical Society.

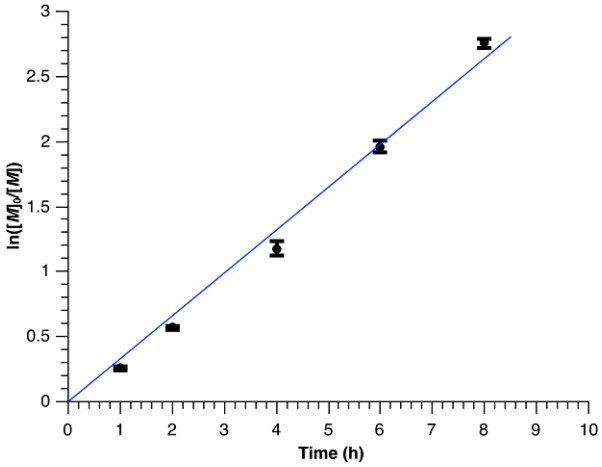

Figure 2.13. Kinetic plot of ln([M]$_0$/[M]) *vs.* time, obtained from ^{31}P NMR data averaged over three runs. Linear regression equation: $y = 0.33\ x$; $R^2 = 0.98$. Reprinted with permission from "Synthetic, Functional Thymidine-Derived Polydeoxyribonucleotide Analogues from a Six-Membered Cyclic Phosphoester" by Tsao, Y.-Y. T.; Wooley, K. L., *J. Am. Chem. Soc.* **2017**, *139*, 5467–5473. Copyright 2017 American Chemical Society.

A series of polymer **9** was synthesized in a variety of molar masses by controlling the monomer to initiator ratio, as summarized in Table 2.3. The Waymouth and Hedrick groups conducted investigations of TBD-catalyzed ROP of cyclic esters,[100] and found the reaction rates decrease with solvent polarity, *i.e.*, THF and DMF were observed to inhibit the catalytic activity of TBD due to hydrogen bond interference. A similar phenomenon was expected in the ROP of **(*R*)-5**, due to the presence of two strong hydrogen bond acceptors on the thymine unit, therefore, higher equivalents of TBD were required to efficiently drive the ROP as the stoichiometric ratio of **(*R*)-5** to initiator increased. The degrees of polymerization calculated from conversions determined by ^{31}P NMR spectroscopy agreed with those calculated from ^{1}H NMR chain end analyses, which compared the integration values for the resonance signals of the two aromatic protons *ortho* to the methoxy group of the 4-methoxybenzyl-initiated chain terminus (6.89 ppm) with one alkenyl proton of the butylene side chain groups (5.85–5.72 ppm). Further analysis of $\mathbf{PCBT_{21}}$ and $\mathbf{PCBT_{32}}$ with electrospray ionization mass spectrometry (ESI–MS) suggested that chain end analyses provided more accurate molar mass results than THF SEC (Figure 2.14).

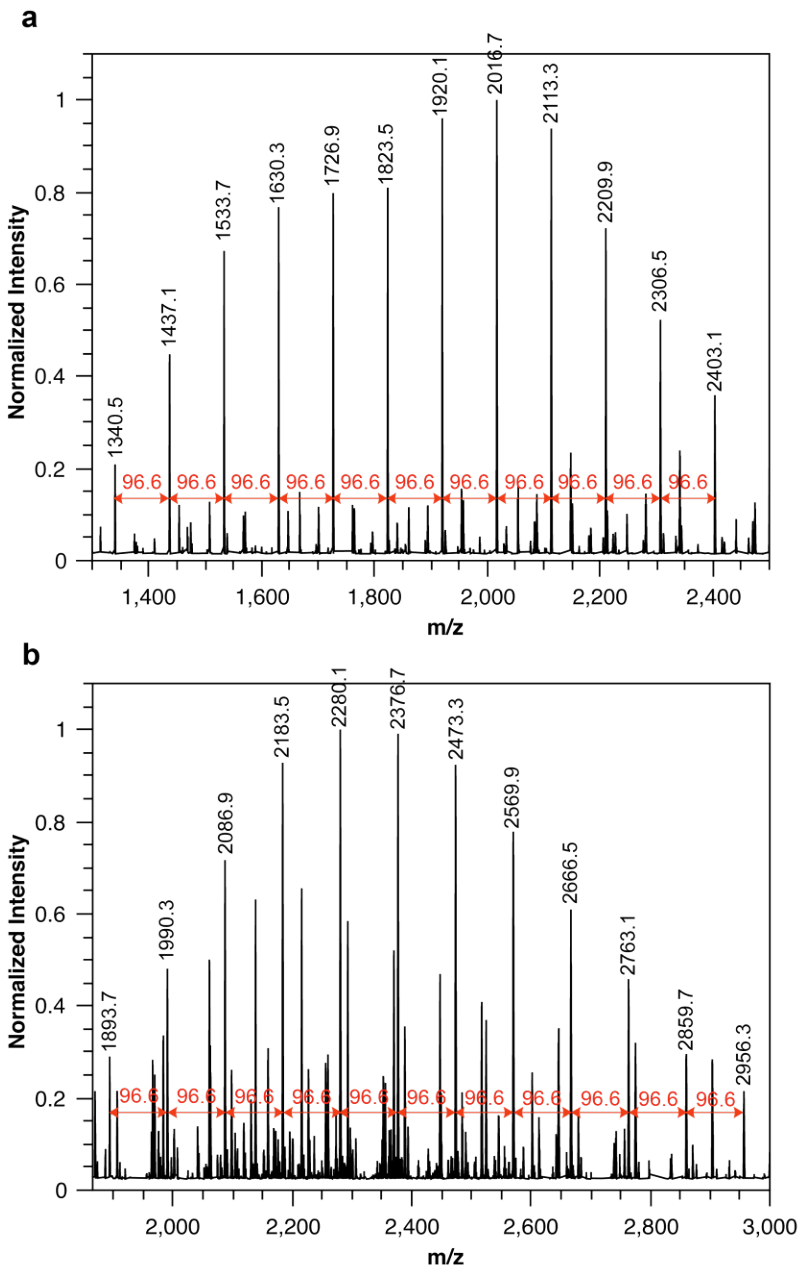

Figure 2.14. ESI-MS analysis for **PCBT$_{21}$** and **PCBT$_{32}$**. (a) **PCBT$_{21}$** (z = 4, repeating unit = 386.1 Da or 96.5 Th). (b) **PCBT$_{32}$** (z = 4, repeating unit = 386.1 Da or 96.5 Th), both indicating that chain end analyses (M_n = 8,200 and 12,400 Da, respectively) provided more accurate molar mass estimations than did THF SEC (M_n = 4,800 and 6,200 Da, respectively). Reprinted with permission from "Synthetic, Functional Thymidine-Derived Polydeoxyribonucleotide Analogues from a Six-Membered Cyclic Phosphoester" by Tsao, Y.-Y. T.; Wooley, K. L., *J. Am. Chem. Soc.* **2017**, *139*, 5467–5473. Copyright 2017 American Chemical Society.

Thymidine-derived **9** displayed thermal and physical properties distinct from previously reported polyphosphoesters as well as DNA. Polyphosphoesters synthesized from five-membered cyclic monomers exhibited low glass transition temperatures (T_g) of *ca.* –50 °C.[16,18] In contrast, higher T_g values were measured for **9** (50–55 °C), likely due to the presence of a more rigid backbone. However, no glass transitions were detected for DNA samples,[101] presumably due to the strong Coulombic repulsion between anionic chains that prevents long range chain entanglement. Following treatment with cetyltrimethylammonium (CTMA) chloride to neutralize phosphates, a T_g of 148 °C was reported for the DNA–CTMA powder. This high T_g value, even though not measured from a pure DNA sample, may be attributed to the strong hydrogen bond interactions between base pairs. The lack of hydrogen bond pairs in **9** not only decreased the T_g values, but also increased the hydrophobicity of the polymeric material in combination with the ester protection of anionic phosphates, making **9** insoluble in water but soluble in a variety of organic solvents (methanol, ethanol, chloroform, dichloromethane, dimethyl sulfoxide, DMF, and THF). The peak at *ca.* 270–280 nm in the circular dichroism spectrum acquired in dichloromethane (Figure 2.15) suggested that the stacking behavior of N^3-butenylthymine bases in **PCBT$_{20}$** might be similar to that of thymine bases in natural polythymidine in aqueous buffer.[102]

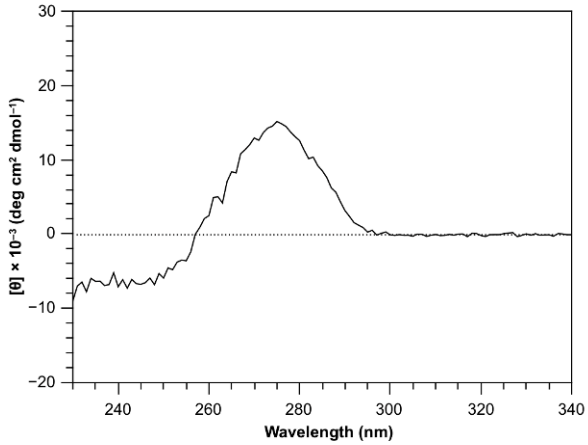

Figure 2.15. Circular dichroism spectrum of **PCBT$_{20}$** (0.01 mg/mL in dichloromethane), demonstrating stacking behavior of N^3-butenylthymine bases. Reprinted with permission from "Synthetic, Functional Thymidine-Derived Polydeoxyribonucleotide Analogues from a Six-Membered Cyclic Phosphoester" by Tsao, Y.-Y. T.; Wooley, K. L., *J. Am. Chem. Soc.* **2017**, *139*, 5467–5473. Copyright 2017 American Chemical Society.

2.3 Experimental Section

2.3.1 Materials

Thymidine, 4-bromo-1-butene, and phosphorus pentoxide were used as received from Chem-Impex International, Inc. (Wood Dale, IL). TBD was used as received from TCI America (Portland, OR). *N*,*N*-Dimethylformamide (DMF, ACS grade), tetrahydrofuran (THF, HPLC grade), hexanes (ACS grade), dichloromethane (ACS grade), and acetone (ACS grade) were used as received from VWR International. Anhydrous solvents were obtained after passage through a drying column of a solvent purification system from JC Meyer Solvent Systems (Laguna Beach, CA). All other

chemicals were purchased from Sigma-Aldrich (St. Louis, MO) and used without further purification unless otherwise noted.

2.3.2 Instrumentation

^{1}H, ^{13}C, and ^{31}P NMR spectra were recorded on a Varian 500 MHz spectrometer interfaced to a Linux computer using VNMR-J software, while ^{1}H–^{31}P HMBC was performed on a Varian 600 MHz spectrometer interfaced to a Linux computer using VNMR-J software with ${}^{n}J_{HP}$ = 8 Hz. Chemical shifts were referenced to the solvent residual signals. All ^{1}H NMR spectra are reported in parts per million (ppm) downfield of tetramethylsilane and were measured relative to the signals for residual $CHCl_3$ (7.26 ppm). All ^{13}C NMR spectra are reported in ppm relative to $CDCl_3$ (77.0 ppm), and were obtained with ^{1}H decoupling. For ^{31}P NMR spectroscopy, phosphoric acid (85 wt% in H_2O) at 0 ppm was used as an external standard. The splitting patterns were reported as s (singlet), d (doublet), t (triplet), q (quartet), quin (quintet), m (multiplet), and br (broad). FTIR spectra were recorded on an IR Prestige 21 system using a diamond ATR lens (Shimadzu Corp., Japan) and analyzed using IRsolution v.1.40 software. The polymer molar mass and molar mass distribution values were determined by size exclusion chromatography (SEC) performed on a Waters 1515 HPLC pump (Waters Chomatography, Inc.) equipped with a 2414 differential refractometer (Waters, Inc.), a PD2020 dual-angle (15° and 90°) light scattering detector (Precision Detectors, Inc.),

and a four-column series of PL gel columns (Polymer Laboratories, Inc.): 5 μm Guard (50 × 7.5 mm), 5 μm Mixed C (300 × 7.5 mm), 5 μm 10^4 Å (300 × 7.5 mm) and 5 μm 500 Å (300 × 7.5 mm). Polymer solutions were prepared at a known concentration and an injection volume of 200 μL was used. The system was equilibrated at 40 °C in THF, which served as the polymer solvent and eluent (flow rate set to 1.00 mL/min). The differential refractometer was calibrated with Polymer Laboratories, Inc. polystyrene standards (300 to 467,000 Da). Data collection and analysis were performed using the Breeze (version 3.30, Waters, Inc.) software. Thermogravimetric analysis (TGA) was performed under argon atmosphere using a Mettler Toledo model TGA/DSC 1 (Mettler Toledo), with a heating rate of 10 °C/min. Measurements were analyzed using Mettler Toledo STAR^e v. 7.01 software. Glass transition temperature (T_g) and melting temperature (T_m) were measured by differential scanning calorimetry (DSC) on a Mettler Toledo DSC822®, with a heating rate of 10 °C/min and a cooling rate of 10 °C/min. Measurements were analyzed using Mettler Toledo STAR^e v. 7.01 software. The T_g values were taken as the midpoint of the inflection tangent upon the third heating scan, and T_m values as the onset temperatures upon the first heating scan.

2.3.3 Synthesis

Synthesis of 3-(3-butenyl) thymidine (**6**). To a 50-mL round-bottom flask equipped with a magnetic stir bar containing 30.0 mL of DMF were added thymidine **4**

(5.5880 g, 23.069 mmol, 1 equiv), 4-bromo-1-butene (5.5865 g, 41.381 mmol, 1.7938 equiv) and potassium carbonate (6.3524 g, 45.965 mmol, 1.9925 equiv). The reaction mixture was allowed to stir at 60 °C for 2 days before it was diluted with 30 mL of water and extracted with dichloromethane (3 × 20 mL). The organic layer was collected, dried over magnesium sulfate, filtered, concentrated, and purified by silica gel column chromatography with acetone/hexanes = 1:1 as eluent followed by lyophilization overnight to give **6** as a white solid with a yield of 95% (6.507 g). ^{1}H NMR (500 MHz; $CDCl_3$) δ 7.36 (d, J = 1.0 Hz, 1H, H^A), 6.86 (t, J = 6.8 Hz, 1H, H^B), 5.79 (ddt, J = 17.1, 10.1, 7.0 Hz, 1H, -CCH^C=CH_2), 5.05 (dd, J = 17.1, 1.0 Hz, 1H, -CCH=CH^DH), 5.00 (dd, J = 10.1, 1.0 Hz, 1H, -CCH=CHH^E), 4.58 (dt, J = 6.6, 3.4 Hz, 1H, H^F), 4.00 (m, 3H, H^G and -NC$H^H{}_2$-), 3.92 (dd, J = 11.8, 3.1 Hz, 1H, $H^I_{pro\text{-}S}$), 3.83 (dd, J = 11.8, 3.1 Hz, 1H, $H^J_{pro\text{-}R}$), 2.49–2.58 (br, -OH), 2.42–2.29 (m, 4H, H^K and -$NCH_2CH^L{}_2$-), 1.91 (d, J = 0.6 Hz, 3H, -CC$H^M{}_3$); ^{13}C NMR (126 MHz; $CDCl_3$) δ 163.4, 150.8 134.7, 134.5, 116.9, 110.1, 86.9, 86.6, 71.2, 62.2, 40.5, 40.1, 31.7, 13.2. FTIR (cm^{-1}): 3518, 3443, 3095–2792, 1666, 1626, 1472, 1402, 1364, 1348, 1294, 1234, 1198, 1097, 989, 920, 770, 631. HR-MS (ESI): calculated $[M + H]^+$ for $C_{14}H_{21}N_2O_5$: 297.1450, found: 297.1481. TGA in Ar: 100–245 °C, 16% mass loss; 245–330 °C, 76% mass loss; 330–500 °C, 4% mass loss; 4% mass remaining above 500 °C. DSC: no melting observed below 170 °C.

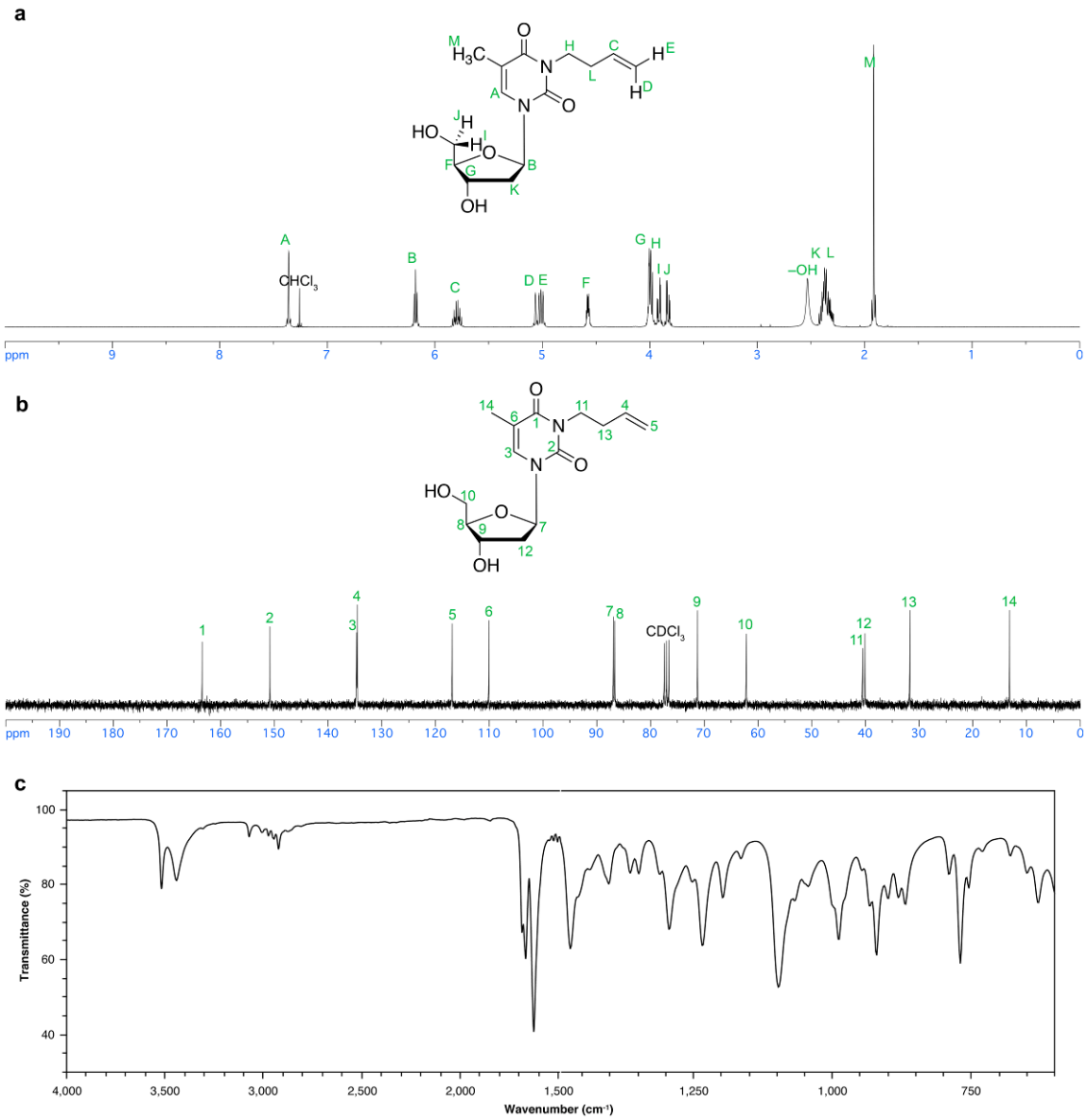

Figure 2.16. Spectroscopic characterization of **6**. (a) ^{1}H NMR (500 MHz; $CDCl_3$). (b) ^{13}C NMR (125 MHz; $CDCl_3$). (c) IR spectrum. Reprinted with permission from "Synthetic, Functional Thymidine-Derived Polydeoxyribonucleotide Analogues from a Six-Membered Cyclic Phosphoester" by Tsao, Y.-Y. T.; Wooley, K. L., *J. Am. Chem. Soc.* **2017**, *139*, 5467–5473. Copyright 2017 American Chemical Society.

Synthesis of 3′,5′-bicyclic 3-(3-butenyl) thymidine ethylphosphate (**5**). In a 250-mL two-neck round-bottom flask equipped with a magnetic stir bar were placed 4-dimethylaminopyridine (807.4 mg, 6.609 mmol, 2.665 equiv) and **6** (735.0 mg, 2.480 mmol, 1 equiv) in 25.0 mL of dichloromethane at –78 °C. A solution of ethyl dichlorophosphate **7** (404.2 mg, 2.481 mmol, 1.000 equiv) in 5.0 mL of dichloromethane was injected *via* syringe in one portion. The reaction mixture was allowed to stir for 1 h while gradually warming up to ambient temperature before it was washed with 5.0 mL of water and purified by silica gel column chromatography with a gradient of hexanes and acetone as eluent to give **(*R*)-5** and **(*S*)-5** with yields of 51% (488.7 mg) and 7% (67.4 mg) as white solids, respectively. **(*R*)-5.** R_f = 0.12 (acetone/hexanes = 2:8); ^{1}H NMR (500 MHz; $CDCl_3$) δ 7.00 (d, *J* = 1.3 Hz, 1H, H^A), 6.36 (dd, *J* = 8.8, 2.6 Hz, 1H, H^B), 5.78 (ddt, *J* = 17.1, 10.1, 7.0 Hz, 1H, -CC*H*^{C}=CH$_2$), 5.04 (dd, *J* = 17.1, 1.7 Hz, 1H, -CCH=C*H*^{D}H), 5.00 (dd, *J* = 10.2, 1.7 Hz, 1H, -CCH=CH*H*^{E}), 4.86 (qd, *J* = 9.3, 0.9 Hz, 1H, H^F), 4.57 (ddd, *J* = 16.6, 9.7, 5.5 Hz, 1H, $H^G_{pro\text{-}S}$), 4.52 (ddd, *J* = 19.7, 8.7, 5.8 Hz, 1H, $H^H_{pro\text{-}R}$), 4.22 (dq, *J* = 8.9, 7.1 Hz, 2H, -OC*H*$^I_2$CH$_3$), 3.98 (td, *J* = 7.4, 3.6 Hz, 2H, -NC*H*$^J_2$-), 3.92 (m, 1H, H^K), 2.56 (ddd, J = 13.6, 10.4, 8.9 Hz, 1H, $H^L_{pro\text{-}S}$), 2.43 (ddd, J = 13.6, 8.2, 2.6 Hz, 1H, $H^M_{pro\text{-}R}$), 2.36 (q, *J* = 7.2 Hz, 2H, -NCH$_2$C*H*$^N_2$-), 1.94 (d, *J* = 1.2 Hz, 3H, -CC*H*$^O_3$), 1.36 (td, *J* = 7.1, 1.1 Hz, 3H, -OCH$_2$C*H*$^P_3$); ^{13}C NMR (126 MHz; $CDCl_3$) *δ* 162.7, 150.5, 134.7, 132.7, 117.0, 111.6, 85.3, 76.9 (d, *J* = 3.9 Hz), 74.0 (d, *J* = 6.2 Hz), 68.9 (d, *J* = 7.3 Hz), 65.9 (d, *J* = 6.3 Hz), 40.7, 35.5 (d, *J* = 8.3 Hz), 31.9, 16.1 (d, *J* = 6.3 Hz), 13.3; ^{31}P NMR (202 MHz; $CDCl_3$) *δ* –3.8. FTIR (cm^{-1}): 3113–2814, 1703, 1666, 1639, 1466, 1448, 1359, 1348, 1273, 1165, 1110, 1009, 926, 891, 820, 768.

HR-MS (ESI): calculated $[M + H]^+$ for $C_{16}H_{24}N_2O_7P$: 387.1321, found: 387.1482. DSC: T_m = 34 °C. **(*S*)-5.** R_f = 0.10 (acetone/hexanes = 2:8); ^{1}H NMR (500 MHz; $CDCl_3$) δ 6.95 (d, J = 1.1 Hz, 1H, H^A), 6.12 (dd, J = 8.5, 3.2 Hz, H^B), 5.79 (ddt, J = 17.1, 10.1, 7.0 Hz, 1H, -CCH^C=CH$_2$), 5.05 (dd, J = 17.1, 1.8 Hz, 1H, -CCH=CH^DH), 5.01 (dd, J = 10.2, 1.8 Hz, 1H, -CCH=CHH^E), 4.68 (q, J = 9.1 Hz, 1H, H^F), 4.57 (ddd, J = 21.3, 9.5, 4.7 Hz, 1H, $H^G_{pro\text{-}S}$), 4.34 (td, J = 10.1, 1.1 Hz, 2H, -OCH^H_2CH$_3$), 4.26 (ddd, J = 9.0, 7.1, 2.9 Hz, 1H, $H^I_{pro\text{-}R}$), 3.99 (td, J = 7.4, 3.0 Hz, 2H, -NCH^J_2-), 3.91 (ddd, J = 10.4, 9.3, 4.6 Hz, 1H, H^K), 2.56 (m, 2H, $H^L_{pro\text{-}S}$ and $H^M_{pro\text{-}R}$), 2.37 (q, J = 7.3 Hz, 2H, -NCH$_2$CH^N_2-), 1.95 (d, J = 1.1 Hz, 3H, -CCH^O_3), 1.43 (td, J = 7.1, 0.7 Hz, 3H, -OCH$_2$CH^P_3); ^{13}C NMR (126 MHz; $CDCl_3$) δ 162.8, 150.3, 134.7, 133.9, 117.0, 111.1, 87.1, 78.0 (d, J = 5.6 Hz), 74.0 (d, J = 6.2 Hz), 69.3(d, J = 9.0 Hz), 64.6 (d, J = 5.7 Hz), 40.6, 35.3 (d, J = 8.3 Hz), 31.9, 16.2 (d, J = 5.9 Hz), 13.3; ^{31}P NMR (202 MHz; $CDCl_3$) δ –6.7. FTIR (cm^{-1}): 3105–2821, 1703, 1666, 1639, 1524, 1466, 1449, 1361, 1348, 1274, 1109, 1011, 928, 891, 818, 767. HR-MS (ESI): calculated $[M + H]^+$ for $C_{16}H_{24}N_2O_7P$: 387.1321, found: 387.1498. DSC: T_m = 33 °C.

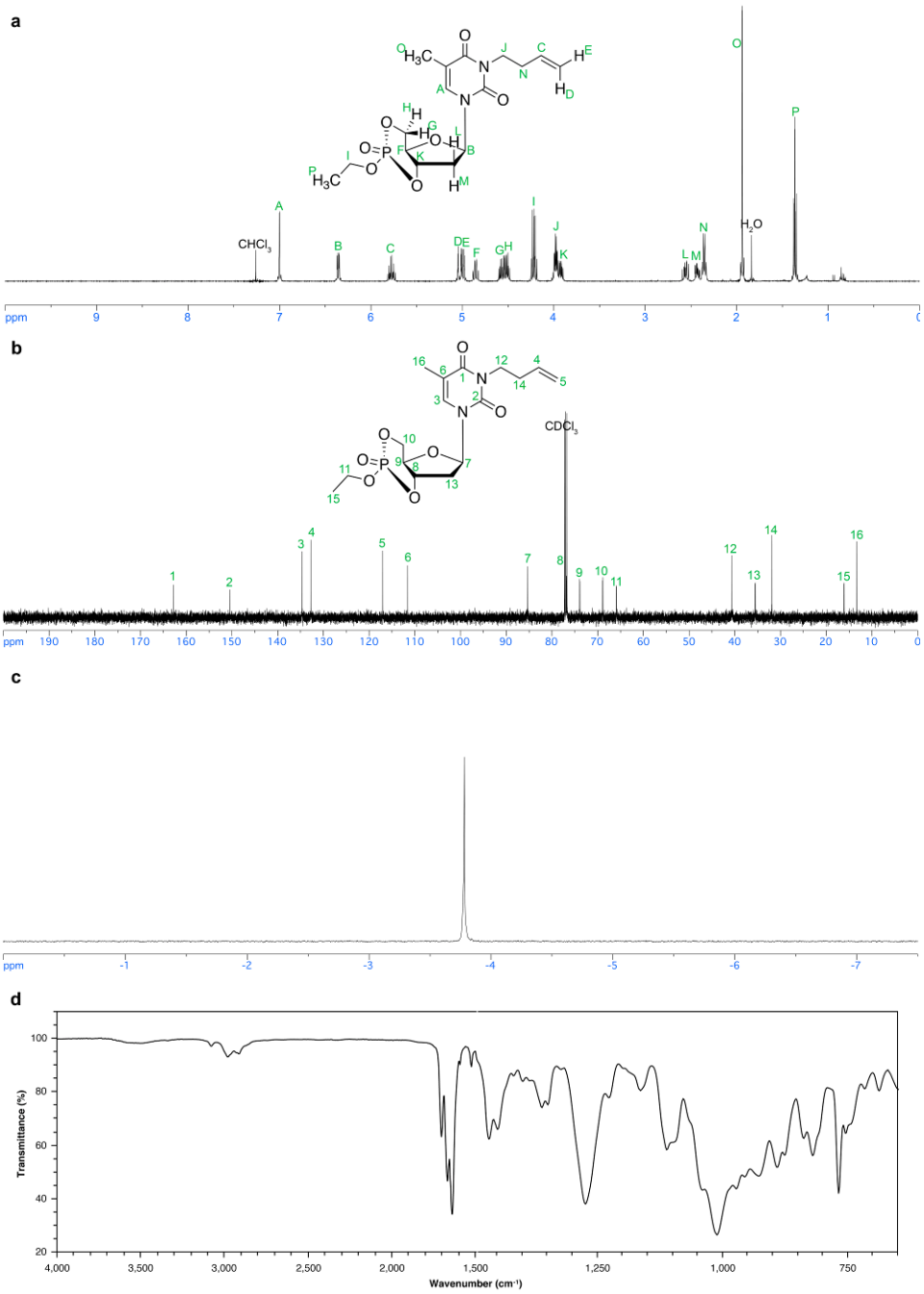

Figure 2.17. Spectroscopic characterization of **(*R*)-5**. (a) ^{1}H NMR (500 MHz; $CDCl_3$). (b) ^{13}C NMR (125 MHz; $CDCl_3$). (c) ^{31}P NMR (202 MHz; $CDCl_3$). (d) IR spectrum. Reprinted with permission from "Synthetic, Functional Thymidine-Derived Polydeoxyribonucleotide Analogues from a Six-Membered Cyclic Phosphoester" by Tsao, Y.-Y. T.; Wooley, K. L., *J. Am. Chem. Soc.* **2017**, *139*, 5467–5473. Copyright 2017 American Chemical Society.

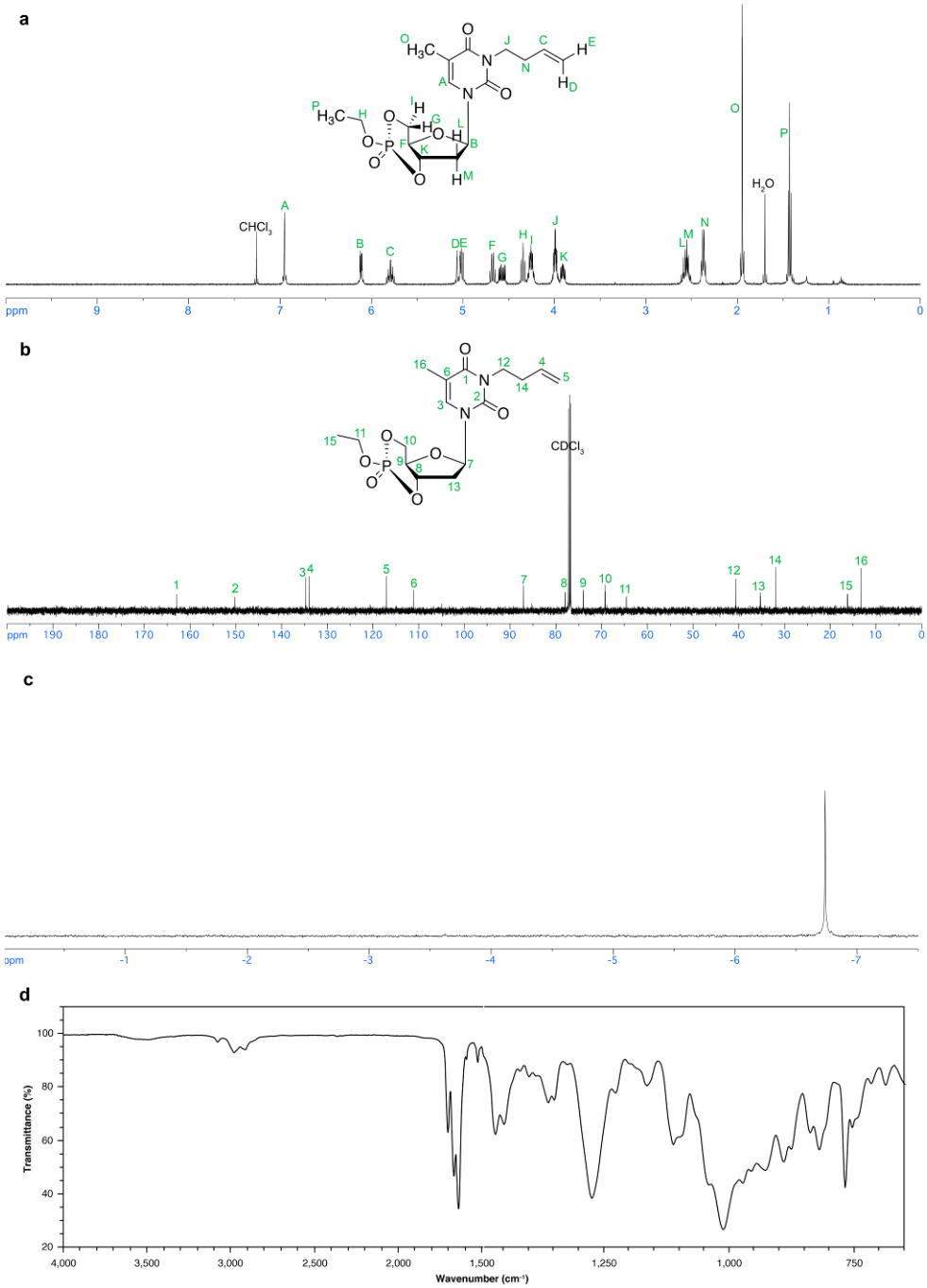

Figure 2.18. Spectroscopic characterization of **(*S*)-5**. (a) ^{1}H NMR (500 MHz; $CDCl_3$). (b) ^{13}C NMR (125 MHz; $CDCl_3$). (c) ^{31}P NMR (202 MHz; $CDCl_3$). (d) IR spectrum. Reprinted with permission from "Synthetic, Functional Thymidine-Derived Polydeoxyribonucleotide Analogues from a Six-Membered Cyclic Phosphoester" by Tsao, Y.-Y. T.; Wooley, K. L., *J. Am. Chem. Soc.* **2017**, *139*, 5467–5473. Copyright 2017 American Chemical Society.

General procedure for polymerization of **5**. A solution of **5** (98.1 mg, 0.254 mmol) and a given amount of 4-methoxybenzyl alcohol (1.2–3.5 mg, 0.00847–0.0254 mmol) in anhydrous dichloromethane (0.90 mL) was transferred into a flame-dried 10-mL Schlenk flask equipped with a magnetic stir bar and a glass stopper on a dual-manifold Schlenk line. A solution of a given amount of TBD (4.7–7.1 mg, 0.0339–0.0508 mmol) in anhydrous dichloromethane (0.10 mL) was injected into the Schlenk flask *via* syringe to initiate the polymerization, while being maintained under a nitrogen gas atmosphere at ambient temperature. After stirring for a predetermined period of time (6 h to 24 h), the reaction was quenched by addition of a solution of acetic acid (excess) in dichloromethane *via* pipette. The poly(3′,5′-bicyclic 3-(3-butenyl) thymidine ethylphosphate) (**PCBT**, **9**) was purified by precipitation from dichloromethane (0.5 mL) into diethyl ether (15 mL, 3 times), and dried *in vacuo* to give an average yield of 50%. δ ^{1}H NMR (500 MHz; $CDCl_3$) δ 7.38–7.30 (br), 6.89 (d, J = 8.6 Hz), 6.40–6.20 (br), 5.85–5.72 (br), 5.15–4.95 (br), 4.40–4.22 (br), 4.21–4.12 (br), 4.01–3.91 (br), 3.90 (s), 2.61–2.48 (br), 2.41–2.32 (br), 1.96–1.90 (br), 1.40–1.32 (br); ^{13}C NMR (126 MHz; $CDCl_3$) δ 163.0, 150.7, 134.8, 133.1, 130.0, 117.0, 114.1, 110.8, 85.6, 83.0, 77.6, 66.9, 65.0, 55.3, 46.8, 40.6, 38.3, 31.9, 20.7, 16.2, 13.2; ^{31}P NMR (202 MHz; $CDCl_3$) δ –1.0, –1.7, –1.8, –2.8. FTIR (cm^{-1}): 3117–2813, 1701, 1666, 1639, 1466, 1450, 1361, 1269, 1195, 1161, 1099, 1011, 910, 833, 768. DSC: T_g = 50 (**PCBT$_{10}$**), 55 (**PCBT$_{21}$**), and 54 °C (**PCBT$_{32}$**). TGA in Ar: 235–285 °C, 50% mass loss; 285–500 °C, 12% mass loss; 38% mass remaining above 500 °C (**PCBT$_{10}$**); 235–285 °C, 50% mass loss; 285–500 °C,

13% mass loss; 37% mass remaining above 500 °C (**PCBT$_{21}$**); 235–272 °C, 60% mass loss; 272–500 °C, 14% mass loss; 26% mass remaining above 500 °C (**PCBT$_{32}$**).

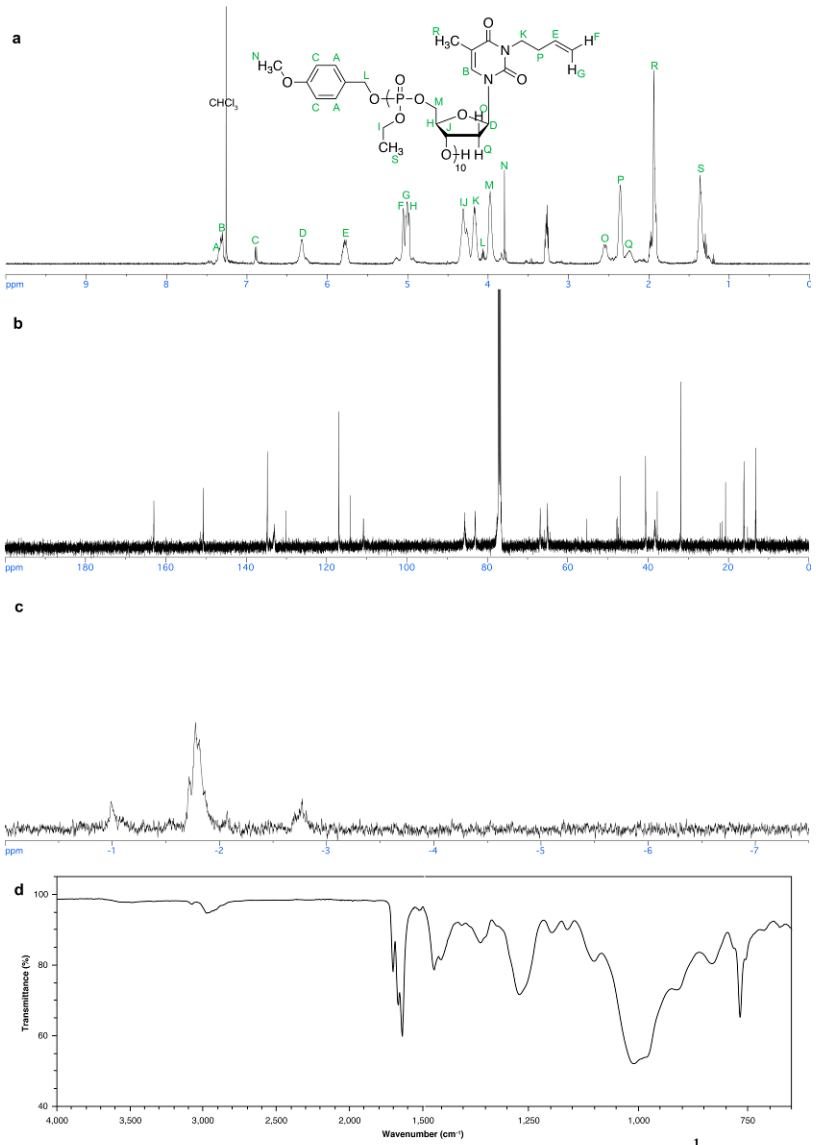

Figure 2.19. Spectroscopic characterization of **PCBT$_{10}$**. (a) ^{1}H NMR (500 MHz; $CDCl_3$). (b) ^{13}C NMR (125 MHz; $CDCl_3$). (c) ^{31}P NMR (202 MHz; $CDCl_3$). (d) IR spectrum. Reprinted with permission from "Synthetic, Functional Thymidine-Derived Polydeoxyribonucleotide Analogues from a Six-Membered Cyclic Phosphoester" by Tsao, Y.-Y. T.; Wooley, K. L., *J. Am. Chem. Soc.* **2017**, *139*, 5467–5473. Copyright 2017 American Chemical Society.

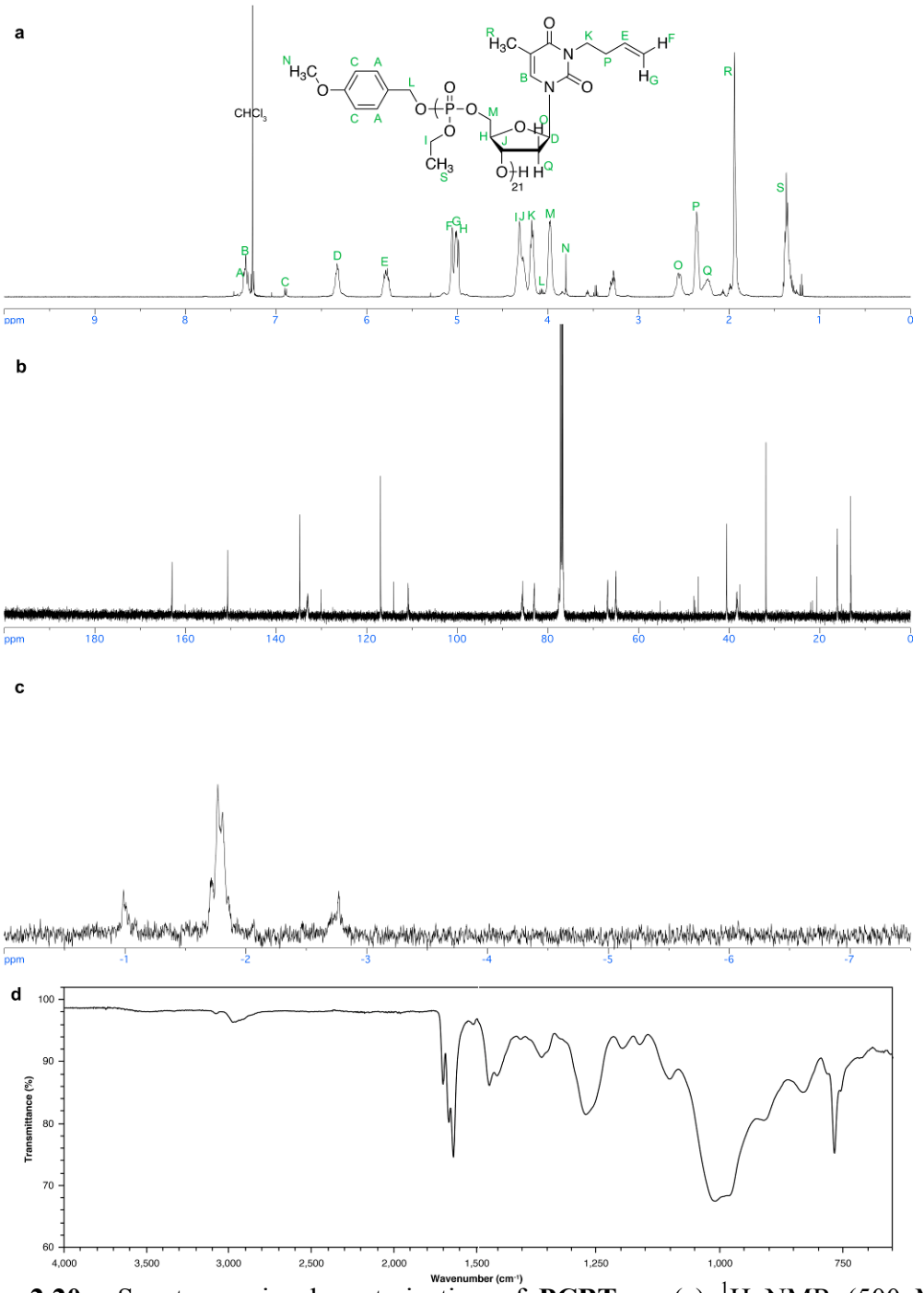

Figure 2.20. Spectroscopic characterization of **PCBT$_{21}$**. (a) ^{1}H NMR (500 MHz; $CDCl_3$). (b) ^{13}C NMR (125 MHz; $CDCl_3$). (c) ^{31}P NMR (202 MHz; $CDCl_3$). (d) IR spectrum. Reprinted with permission from "Synthetic, Functional Thymidine-Derived Polydeoxyribonucleotide Analogues from a Six-Membered Cyclic Phosphoester" by Tsao, Y.-Y. T.; Wooley, K. L., *J. Am. Chem. Soc.* **2017**, *139*, 5467–5473. Copyright 2017 American Chemical Society.

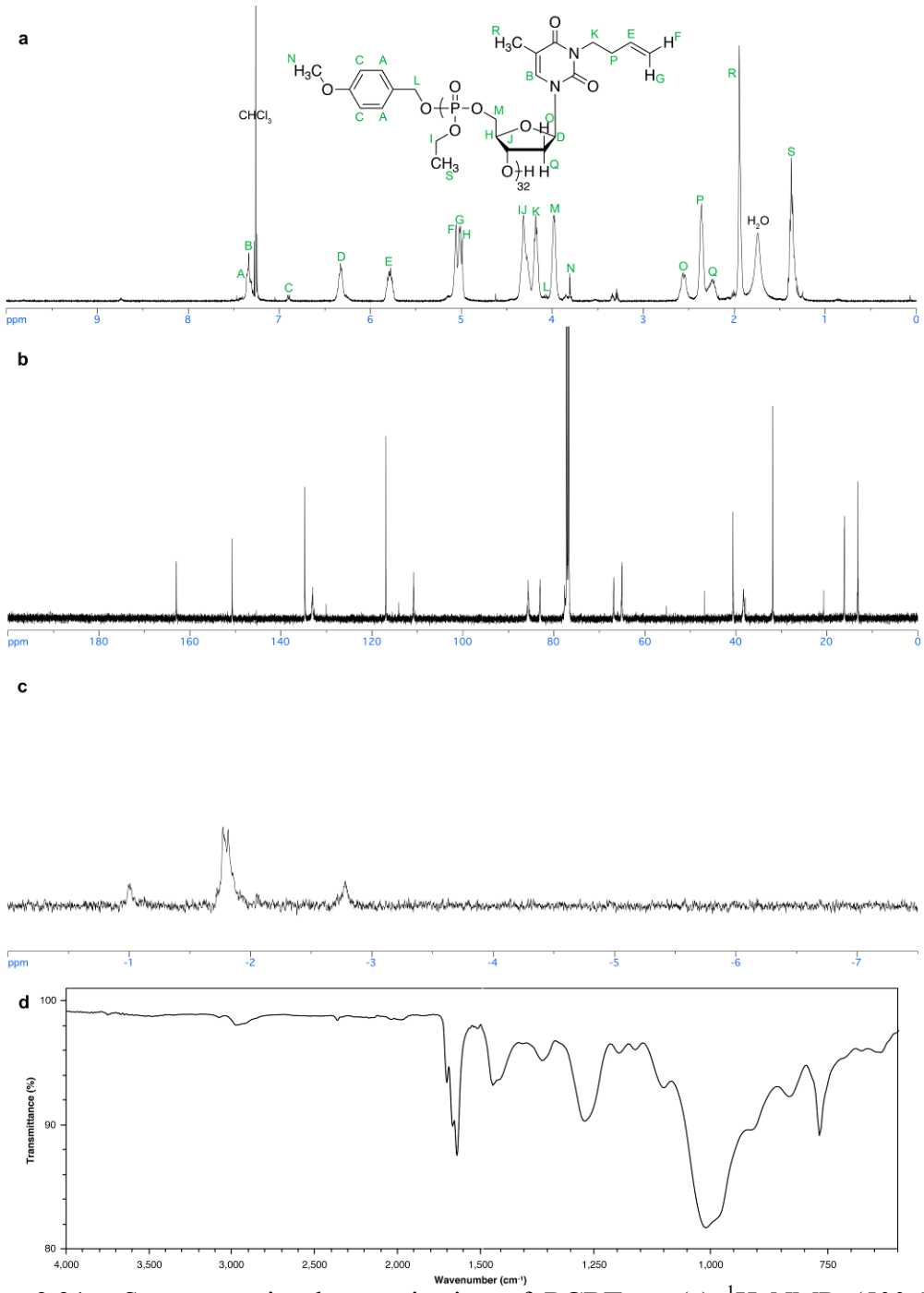

Figure 2.21. Spectroscopic characterization of **PCBT$_{32}$**. (a) ^{1}H NMR (500 MHz; $CDCl_3$). (b) ^{13}C NMR (125 MHz; $CDCl_3$). (c) ^{31}P NMR (202 MHz; $CDCl_3$). (d) IR spectrum. Reprinted with permission from "Synthetic, Functional Thymidine-Derived Polydeoxyribonucleotide Analogues from a Six-Membered Cyclic Phosphoester" by Tsao, Y.-Y. T.; Wooley, K. L., *J. Am. Chem. Soc.* **2017**, *139*, 5467–5473. Copyright 2017 American Chemical Society.

Synthesis of 3′-thymidine monophosphate diethylester (**10a**). A solution of **(*R*)-5** (113.8 mg, 0.295 mmol, 1 equiv) in ethanol (0.50 mL) was transferred into a flame-dried 10-mL Schlenk flask equipped with a magnetic stir bar and a glass stopper on a dual-manifold Schlenk line. A solution of TBD (20.1 mg, 0.144 mmol, 0.0488 equiv) in ethanol (0.50 mL) was injected into the Schlenk flask *via* syringe to initiate the reaction, which was stirred under a nitrogen gas atmosphere at ambient temperature for 1 h. Excess ethanol was removed by rotary evaporation before the reaction mixture was purified by silica gel column chromatography with acetone/hexanes = 3:7 as eluent to give **10a** as a colorless liquid with a yield of 80% (102.4 mg). R_f = 0.20 (acetone/hexanes = 3:7); ^{1}H NMR (500 MHz; $CDCl_3$) δ 7.47 (d, J = 1.2 Hz, 1H, H^A), 6.23 (t, J = 6.9 Hz, 1H, H^B), 5.79 (ddt, J = 17.1, 10.1, 7.0 Hz, 1H, -CCH=CH^CH), 5.09 (m, 2H, H^D and H^E), 4.99 (dd, J = 10.5, 1.5 Hz, 1H, -CCH=CHH^F), 4.20 (q, J = 2.6 Hz, 1H, H^G), 4.12 (qd, J = 7.4, 1.3 Hz, 4H, -OCH^H_2CH$_3$), 3.99 (t, J = 7.5 Hz, 2H, -NCH^I_2-), 3.87 (t, J = 2.4 Hz, 2H, H^J), 3.60–3.40 (br, 1H, -OH^K), 2.54-2.44 (m, 2H, H^L), 2.36 (q, J = 7.2 Hz, 3H, -NCH$_2$CH^M_2-), 1.91 (d, J = 1.1 Hz, 4H, H^N), 1.34 (td, J = 7.1, 0.9 Hz, 6H, H^O); ^{13}C NMR (126 MHz; $CDCl_3$) δ 163.2, 150.8 134.8, 134.3, 116.9, 110.4, 86.7, 85.6 (d, J = 4.92 Hz), 77.5 (d, J = 5.46 Hz), 64.3 (d, J = 6.18 Hz), 62.0, 40.5, 38.5 (d, J = 5.04 Hz), 31.9, 16.1 (d, J = 6.79 Hz), 13.3; ^{31}P NMR (202 MHz; $CDCl_3$) δ –1.81. FTIR (cm^{-1}): 3572–3228, 3109–2777, 2249, 1701, 1666, 1639, 1466, 1362, 1254, 1196, 1161, 1103, 1011, 910, 826, 768, 729. HR-MS (ESI): calculated $[M + Na]^+$ for $C_{18}H_{29}N_2O_8PNa$: 455.1559, found: 455.1545.

2.3.4 Details of Computational Chemistry

All calculations were performed with Gaussian 09. All geometries for ring-strain energies were optimized using the B3LYP/6-31+G*, B97-D/6-31+G*, and M06-2X/6-31+G* levels of theory. These levels of theory have been used in numerous studies based on the emphasis on medium-range electron correlation or dispersion correction. The strain energy of a given cyclic molecule relative to another structurally related cyclic reference compound can be calculated by directly comparing the DFT electronic energies of the two molecules given the energy of the fragment, by which the two species differ from each other, is known. A similar theoretical approach to ring strain energy was previously described by Lim and co-workers[88] with *ab initio* calculations at the HF/6-31+G* and MP2/6-31+G* levels of theory. Relative ring strain energies were obtained from the differences between total electronic energies of the targeted molecule and the reference molecule. The QST2 option implemented in Gaussian 09 with the Synchronous Transit-Guided Quasi-Newton (STQN) method at the B3LYP/6-31+G* level of theory was used to locate the transition state, and the electronic energies were reported to explain the diastereoselective cyclization of **6**.

2.4 Conclusions

In summary, we have developed a novel, well-defined DNA-analogue system with 3′,5′-linkages from a six-membered cyclic phosphoester. Computational modeling was used to inform the rational design of stable alkene-functionalized thymidine-derived polyphosphoesters. DFT calculations indicated that the ring strain energy of a six-membered cyclic phosphotriester of a 5,6-fused bicyclic ring system **(*R*)-3** is *ca.* 6–7 kcal/mol greater than a six-membered monocyclic phosphotriester **1**, suggesting that such a structure could serve as a monomer for which ROP would be enabled. Therefore, thymidine was functionalized in the N^3-position and cyclized through the 3′- and 5′-positions to afford a strained six-membered bicyclic phosphotriester monomer, and its organocatalyzed polymerization kinetics were explored. Interestingly, the DFT-calculated 1.35 kcal/mol higher energy of **(*R*)-5**, relative to its diastereomer **(*S*)-5**, led to its selective ability to undergo ROP, whereas **(*S*)-5** was inert under the polymerization reaction conditions. In order to achieve the synthesis of this thermodynamically less stable diastereomer, **(*R*)-5**, the cyclization reaction was conducted under kinetically-controlled conditions at –78 °C. **(*R*)-5** was found to polymerize in a controlled manner ($Đ < 1.10$) under TBD-catalyzed conditions initiated by 4-methoxybenzyl alcohol, and the chain length obtained during ROP could be pre-determined by stoichiometry of monomer to initiator ratios. The pseudo-first order rate constant was measured to be $k_p = 9.2 \times 10^{-5}$ s^{-1}. Overall, this work presents a novel and reliable synthetic methodology

to obtain functional DNA analogues with unique properties and diverse potential applications.

CHAPTER III

REGIOISOMERIC PREFERENCE IN RING-OPENING POLYMERIZATION OF 3′,5′-BICYCLIC PHOSPHOESTERS OF FUNCTIONAL THYMIDINE DNA ANALOGUES[†]

3.1 Introduction

Natural products have been of interest for the replacement of petrochemical-based monomers to increase functionality, decrease the dependence on fossil fuels, and reduce potential biological and environmental adverse effects.[103-106] Natural oils,[107,108] terpenes,[109-112] carbohydrates,[97,113-119] and the sugar components of DNA (2′-deoxyribonucleosides)[34,96,120-123] are attractive and versatile building blocks for the construction of polymeric materials by ROP. Several types of cyclic monomers, such as carbonates, epoxides, phosphazenes, phosphoesters,[32,124] *H*-phosphonates, phosphonites, phosphorothioates, siloxanes, and thiocarbonates, undergo ROP from opening of cyclic monomers from either side of the ring. If such monomers are asymmetrical, the regioisomeric ROP can yield polymers with head-to-head, head-to-tail, and tail-to-tail configurations. Mikami *et al.* reported the regiorandom nature of glucose-derived polycarbonates from organo-base catalyzed ROP of a six-membered 4,6-bicyclic

---

[†] Reprinted (adapted) with permission from "Regioisomeric Preference in Ring-Opening Polymerization of 3′,5′-Cyclic Phosphoesters of Functional Thymidine DNA Analogues" by Tsao, Y.-Y. T.; Smith, T. H.; Wooley, K. L., *ACS Macro Lett.* **2018**, *7*, 153–158. Copyright 2018 American Chemical Society.

carbonate of glucose with the 1-, 2-, and 3 positions protected by methyl groups, as determined from electrospray ionization tandem mass spectrometric analysis by electron transfer dissociation of the polymer species.[125] In contrast, with larger and base-coordinating ethyl carbonate protecting groups, regioregular head-to-tail ROP was observed.[118] Vandenberg,[51] Penczek,[52] and Wurm[53] performed microstructural analyses of cyclic phosphorothioates, *H*-phosphonates, and phosphoesters to understand whether there was regioselectivity of these phosphorus-containing monomers for ROP from the spectroscopic characteristics of corresponding isomers. These studies concluded that head-to-tail configuration was the dominant connectivity when steric effects from both ring-opening directions were different, *e.g.*, primary and secondary alcohols formed from the ring-opening reactions. This selectivity was driven by differing steric effects within the phosphorus-containing five-membered cyclic monomers.[53]

We recently reported the TBD-catalyzed ROP of thymidine-derived six-membered 3′,5′-bicyclic phosphoester monomer **(*R*)-5** and, herein, advance the fundamental understanding of the ROP regiochemical selectivity. As observed by ^{31}P NMR analysis, three resonance frequencies supported the presence of populations of regioisomers. The possible regioisomeric forms of **PCBT** include 3′,3′-, 3′,5′-, and 5′,5′-linkages, corresponding to head-to-head, head-to-tail, and tail-to-tail configurations, respectively (Figure 3.1). Initial model studies indicated that, in addition to the P substituents within the monomer,[53] the nature of the incoming nucleophile could also influence the directionality of ring opening. Therefore, we undertook extensive experimental and computational studies to better understand the mechanistic details of

ring opening for these six-membered cyclic phosphoesters. Ultimately, as we aim to more closely mimic natural DNA,[73] which is synthesized exclusively in the 5′-to-3′ direction, these studies are expected to inform synthetic approaches toward regioregular DNA analogues by ROP of thymidine-derived cyclic phosphoesters.

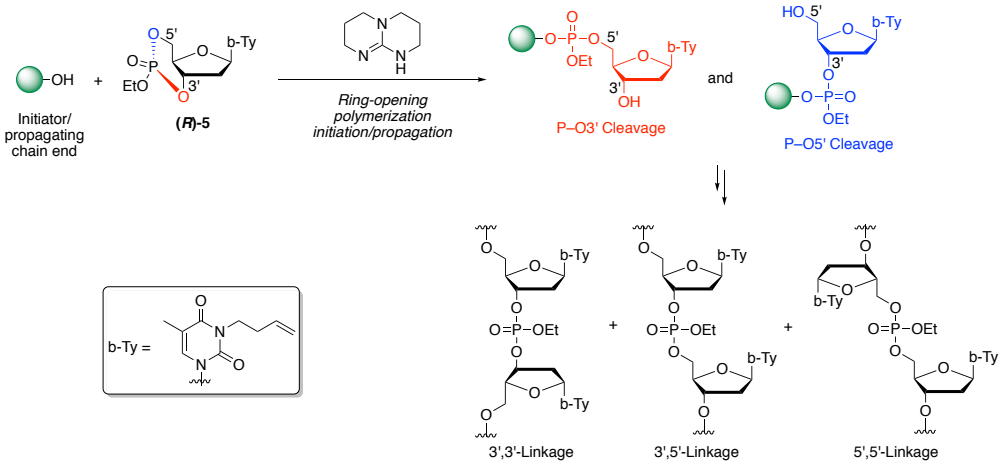

Figure 3.1. Three regioisomeric forms from P–O3′ and P–O5′ cleavages of **(*R*)-5** in TBD-catalyzed ROP. Reprinted with permission from "Regioisomeric Preference in Ring-Opening Polymerization of 3′,5′-Cyclic Phosphoesters of Functional Thymidine DNA Analogues" by Tsao, Y.-Y. T.; Smith, T. H.; Wooley, K. L., *ACS Macro Lett.* **2018**, *7*, 153–158. Copyright 2018 American Chemical Society.

Herein, we report a series of model reactions to investigate the regioisomeric preference in the ROPs of **PCBT**. Alcohols with varying steric effects were used to mimic the differing steric hindrances of the nucleophilic species. With increasing steric hindrance of the nucleophilic alcohol, increasing P–O3′, relative to P–O5′, cleavage products were observed in the product distribution. DFT calculations on the reaction coordinates were employed to rationalize the origin of the selectivity in the ROP

systems. To the best of our knowledge, experimental and computational analyses on regiochemistries has not been extended to the ROP of 3′,5′-bicyclic phosphoester monomers.

3.2 Results and Discussions

To investigate the origin of the ^{31}P NMR signals of **PCBT** and to simplify the complexity of the NMR spectra from nucleobases, 3-hydroxytetrahydrofuran and tetrahydrofurfuryl alcohol were used as models for 3′- and 5′-alcohols, respectively (Figure 3.2a and Figure 3.2b), assuming that the chemical shifts of the phosphorus atoms are influenced exclusively by the nearest environment. By reacting 2 equiv. of these alcohols with 1 equiv. of ethyl dichlorophosphate, **11** and **12** were obtained after purification by column chromatography. By comparing the ^{31}P NMR signals of **11** and **12** to those in the spectrum of **PCBT**, we can conclude that signals from –0.9 to –1.1 ppm and –2.7 to –2.9 ppm arise from 5′,5′- and 3′,3′-linkages, respectively (Figure 3.3). To determine the position of resonances corresponding to 3′,5′-linkages, model compound **13** was synthesized from the reaction of a 1:1 mixture of 3-hydroxytetrahydrofuran and tetrahydrofurfuryl alcohol with ethyl dichlorophosphate (Figure 3.2c). This reaction yielded **11** as the major product, **13** as the minor product, and no evidence of **12**. This result was attributed to the higher reactivity and lower steric hindrance of primary alcohols, as **11** was a product from two primary alcohols, **13** was

from a primary and a secondary alcohol, and **12** was from two secondary alcohols. The ^{31}P NMR spectrum of the 3′,5′-model compound **13** matched that of the **PCBT** signal at –1.7 to –1.9 ppm. Both 3-hydroxytetrahydrofuran and tetrahydrofurfuryl alcohol were racemic mixtures, therefore multiple chemical shifts in ^{31}P NMR spectra could be observed for **11**, **12**, and **13**, due to the combinations of diastereotopic isomers. Therefore, according to the relative integrations of the ^{31}P NMR signals in the spectra of **PCBT**,[34] *ca.* 75% connectivity in the polymer backbone was found to be 3′,5′-linkages, and similar distributions were observed for samples having number-averaged degrees of polymerization of 10, 21, and 32. This observation is consistent with the findings from ROPs of five-membered phosphorus-containing monomers, for which head-to-tail configuration dominated.[51-53]

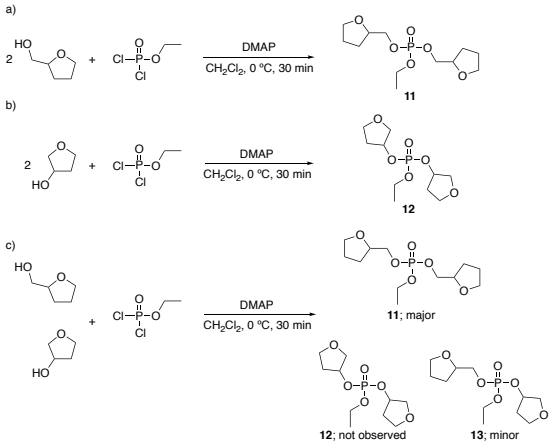

Figure 3.2. Model of (a) 5′,5′-linkage, (b) 3′,3′-linkage, and (c) 3′,5′-linkage from reacting tetrahydrofurfuryl alcohol and 3-hydroxytetrahydrofuran with ethyl dichlorophosphate. Reprinted with permission from "Regioisomeric Preference in Ring-Opening Polymerization of 3′,5′-Cyclic Phosphoesters of Functional Thymidine DNA Analogues" by Tsao, Y.-Y. T.; Smith, T. H.; Wooley, K. L., *ACS Macro Lett.* **2018**, *7*, 153–158. Copyright 2018 American Chemical Society.

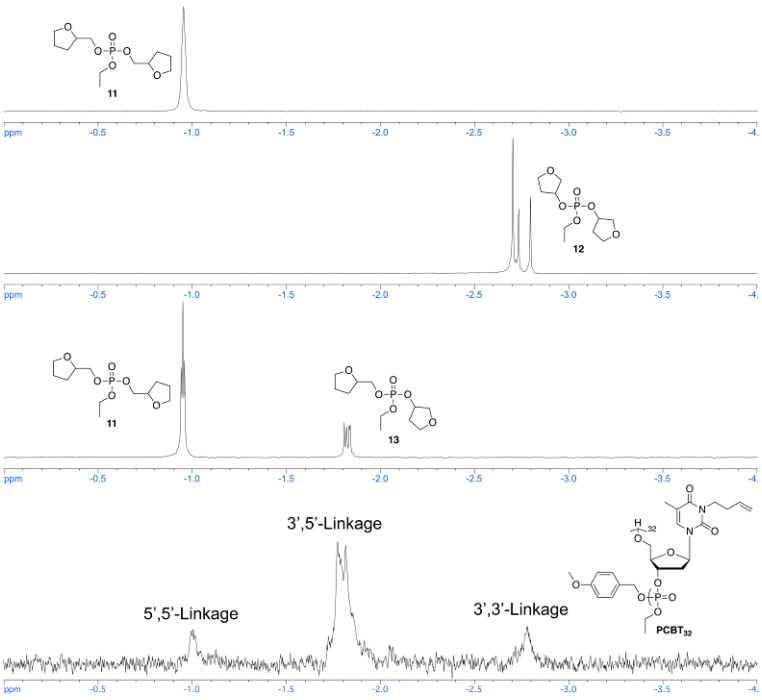

Figure 3.3. ^{31}P NMR spectra (202 MHz; $CDCl_3$) of **11**, **12**, **13**, and **PCBT$_{32}$** suggesting that the three chemical shift regions of **PCBT** correspond to 3′,3′-, 3′,5′-, and 5′,5′-linkages. Reprinted with permission from "Regioisomeric Preference in Ring-Opening Polymerization of 3′,5′-Cyclic Phosphoesters of Functional Thymidine DNA Analogues" by Tsao, Y.-Y. T.; Smith, T. H.; Wooley, K. L., *ACS Macro Lett.* **2018**, *7*, 153–158. Copyright 2018 American Chemical Society.

To understand the preference of ring opening during initiation and propagation of polymerization in more detail, we performed studies on the unimer formed upon reaction with primary, secondary and tertiary alcohols. 3′,5′-Bicyclic monomer **(*R*)-5** was synthesized according to the previously reported procedure.[34] Reaction of 4-methoxybenzyl alcohol, the initiator used in the previous study, with **(*R*)-5** gave the corresponding unimer, allowing for evaluation of the monomeric product(s) from the initial ring-opening reaction. Both unimer and dimer formed when 1 equiv. of 4-methoxybenzyl alcohol was added, and attempts to separate the two products with silica

gel column chromatography were unsuccessful. Excess 4-methoxybenzyl alcohol was then added to suppress dimerization, but removal of the alcohol to obtain **14a** was difficult due to its high boiling point (257–259 °C at 760 Torr)[126] and poor water solubility (not removable by extraction). Due to the separation difficulty of 4-methoxybenzyl alcohol, another model reaction with a primary alcohol was performed. This model reaction utilized excess ethanol as initiator and solvent to ensure the formation of unimer (Table 3.1). The ^{1}H–^{31}P heteronuclear multiple bond correlation (HMBC) analysis indicated that only the product from P–O5′ bond cleavage was formed (Figure 3.4a). This result suggested that the initial ring-opening reaction with 4-methoxybenzyl alcohol was more favorable at the P–O5′ position. However, ^{31}P NMR spectra of **PCBT** suggested both P–O5′ and P–O3′ bond breaking took place during polymerization, which appeared to be contradictory to the ethanol model reaction. To confirm whether ethanol possesses the same ring-opening preference as 4-methoxybenzyl alcohol, a ^{31}P NMR experiment of the crude product using excess 4-methoxybenzyl alcohol was performed, showing a single resonance signal at –1.77 ppm (Figure 3.5). Even though isolation of **14a** from 4-methoxybenzyl alcohol was difficult, the ^{1}H–^{31}P HMBC spectra of crude mixtures revealed that the only product formed was **14a**, due to the presence of $^{4}J_{HP}$ coupling with 2′-H (Figure 3.6). This result indicated that P-O5′ bond cleavage was favored during the initiation by 4-methoxybenzyl alcohol, suggesting that P–O3′ cleavage took place during subsequent propagation steps. Hence, we hypothesized that increased steric hindrance of propagating alcohols, relative to the initiating benzylic alcohol, might alter the regioselectivity during ROP.

Table 3.1. Model reaction of various alcohols with **(*R*)-5** to give unimers. Reprinted with permission from "Regioisomeric Preference in Ring-Opening Polymerization of 3′,5′-Cyclic Phosphoesters of Functional Thymidine DNA Analogues" by Tsao, Y.-Y. T.; Smith, T. H.; Wooley, K. L., *ACS Macro Lett.* **2018**, *7*, 153–158. Copyright 2018 American Chemical Society.

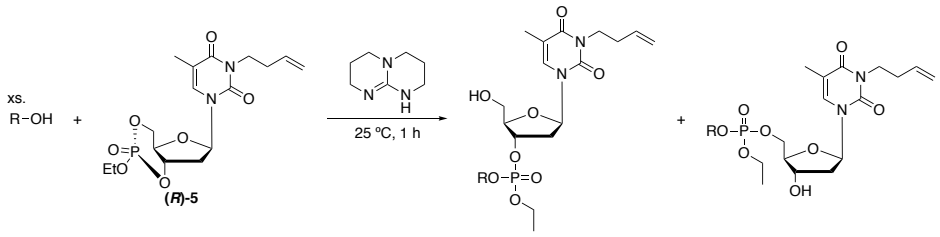

Entry	R	**a**:**b** (molar ratio)
1	Et	100:0
2	4-Methoxybenzyl	100:0[a]
3	iPr	76:24[b]
4	*t*-Bu	NR[c]

[a]Determined by the crude ^{31}P NMR spectrum; [b]determined by the isolated yields; [c]no reaction at both ambient temperature and reflux conditions.

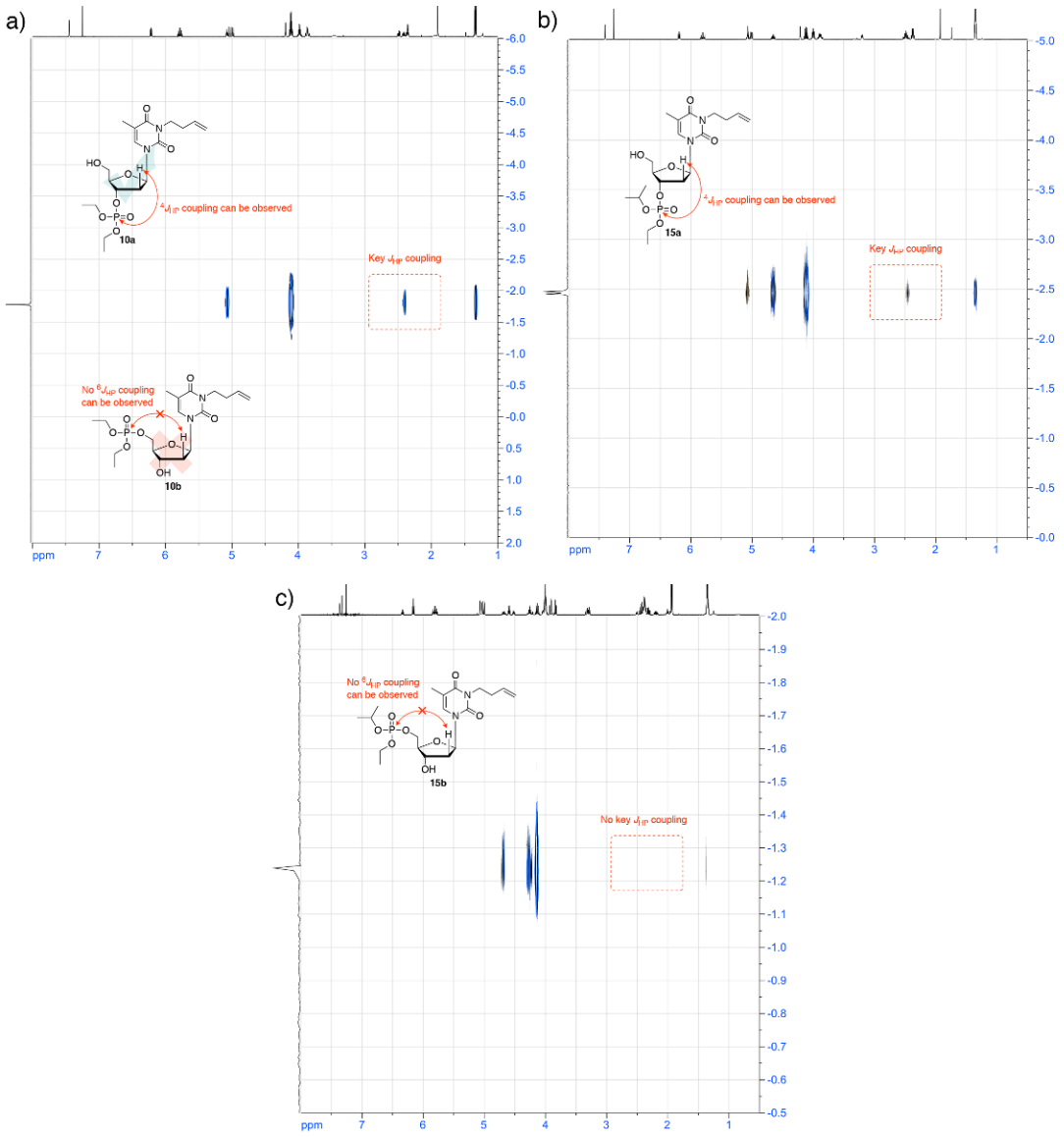

Figure 3.4. ^1H–^{31}P HMBC (500 MHz for ^1H) of (a) **5a**, (b) **7a**, and (c) **7b** in $CDCl_3$, indicating preferential P–O5′ bond breaking during initiation when ethanol was used, but both P–O5′ and P–O3′ cleavages occurred upon reaction of **1** with isopropyl alcohol. Reprinted with permission from "Regioisomeric Preference in Ring-Opening Polymerization of 3′,5′-Cyclic Phosphoesters of Functional Thymidine DNA Analogues" by Tsao, Y.-Y. T.; Smith, T. H.; Wooley, K. L., *ACS Macro Lett.* **2018**, *7*, 153–158. Copyright 2018 American Chemical Society.

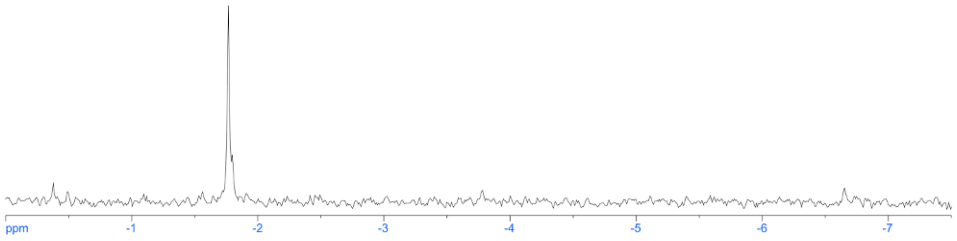

Figure 3.5. ^{31}P NMR (202 MHz; $CDCl_3$) spectrum of crude **14a**. Reprinted with permission from "Regioisomeric Preference in Ring-Opening Polymerization of 3′,5′-Cyclic Phosphoesters of Functional Thymidine DNA Analogues" by Tsao, Y.-Y. T.; Smith, T. H.; Wooley, K. L., *ACS Macro Lett.* **2018**, *7*, 153–158. Copyright 2018 American Chemical Society.

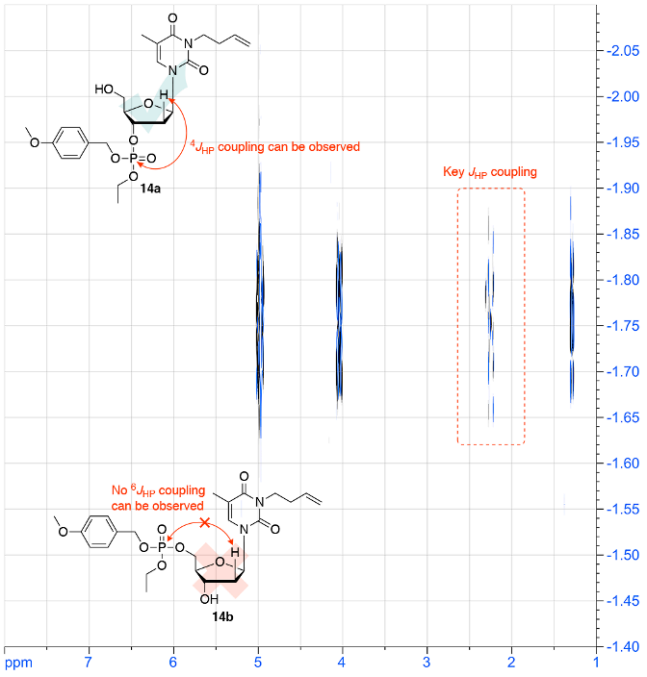

Figure 3.6. ^{1}H–^{31}P HMBC spectrum (500 MHz for ^{1}H; $CDCl_3$) of crude **14a**. Reprinted with permission from "Regioisomeric Preference in Ring-Opening Polymerization of 3′,5′-Cyclic Phosphoesters of Functional Thymidine DNA Analogues" by Tsao, Y.-Y. T.; Smith, T. H.; Wooley, K. L., *ACS Macro Lett.* **2018**, *7*, 153–158. Copyright 2018 American Chemical Society.

To verify our hypothesis of steric hindrance-directed ring-opening preference, excess isopropyl alcohol was used as the nucleophilic solvent to provide increased steric hindrance relative to 4-methoxybenzyl alcohol and ethanol (Table 3.1). Two isomers **15a** and **15b** were formed from the model reaction of **(*R*)-5** with isopropyl alcohol, but the separation was challenging. Even though thin layer chromatography showed complete separation of **15a** and **15b** with 30:70 acetone/hexanes as the eluent (Figure 3.7a), integration from ^{1}H and ^{31}P NMR spectra of **15b** suggested *ca.* 20 mol% of **15a** remained in the **15b** fraction. Use of 25:75 acetone/hexanes eluent did not improve the separation (Figure 3.7b). The low R_f values indicated longer retention time in the silica gel column, and this phenomenon led to mixing of **15a** and **15b** due to longitudinal diffusion (the B-term described in the van Deemter equation).[127] Despite incomplete separation, spectroscopic data of the mixture nevertheless provided evidence for the formation of both **15a** and **15b** upon reaction of **(*R*)-5** with isopropyl alcohol. Due to the slower kinetics of isopropyl alcohol during the initiation step, oligomerization was observed even when excess initiator was used, and the oligomers complicated the analysis of the ^{31}P NMR spectrum of the crude mixture. Thus, the unimers were separated from the oligomers and used to calculate the relative ratio of **15a** and **15b**. These model reactions successfully demonstrated that steric hindrance determines the regioselectivity of ROP of **(*R*)-5**, from preferential P–O5′ cleavage, to mixtures of P–O5′ and P–O3′ bond breaking, giving rise to the 3′,3′- and 5′,5′-linkages in **PCBT**. Further increasing steric hindrance by using *tert*-butyl alcohol as the nucleophile resulted in no reaction at both ambient temperature and upon reflux of the mixture.

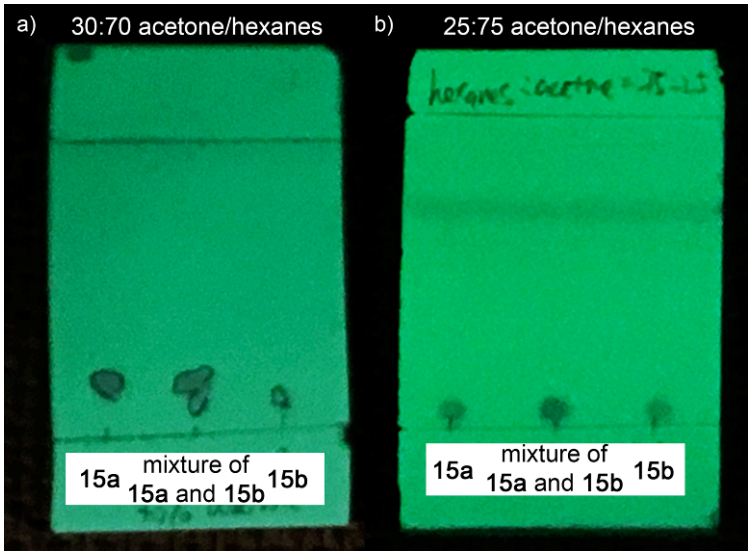

Figure 3.7. Thin layer chromatography showing separation of **7a** and **7b**. (a) 30:70 acetone/hexanes. (b) 25:75 acetone/hexanes as eluent. Reprinted with permission from "Regioisomeric Preference in Ring-Opening Polymerization of 3′,5′-Cyclic Phosphoesters of Functional Thymidine DNA Analogues" by Tsao, Y.-Y. T.; Smith, T. H.; Wooley, K. L., *ACS Macro Lett.* **2018**, *7*, 153–158. Copyright 2018 American Chemical Society.

To further mimic the propagating species present during ROP for the model reaction and explore if the P–O3′ linkages observed in **PCBT** are due to the nature of the propagating alcohol, excess tetrahydrofurfuryl alcohol was used to conduct the TBD-catalyzed ring-opening reaction of **(*R*)-5** in dichloromethane (Table 3.2, entry 1). Only **17a** from P–O5′ cleavage was observed (Figure 3.8), suggesting the steric effect that primarily alters regioselectivity arises from the substituent(s) at the 3′-position (similar to *syn*-pentane interaction). Therefore, the model reaction of **(*R*)-5** with **10a** as the nucleophile was then performed, and the inseparable dimeric mixture of **18a** and **18b** was obtained (Table 3.2, entry 2). The ^{1}H–^{31}P HMBC spectrum (Figure 3.9) revealed peaks around –2.2 ppm and –1.0 ppm in the ^{31}P NMR spectrum, which corresponded to

the **10a** unit and the phosphotriester linkage connecting the dimer, respectively. More interestingly, the ^{31}P NMR spectrum of the mixture not only indicated the presence of the products from P–O3′ and P–O5′ cleavages, but also suggested the occurrence of pseudorotation that yielded diastereomers, and thus, two sets of peaks from **18b** were observed in the ^{31}P NMR spectrum.

Table 3.2. Model reaction of various alcohols with **(*R*)-5** for the propagating step. Reprinted with permission from "Regioisomeric Preference in Ring-Opening Polymerization of 3′,5′-Cyclic Phosphoesters of Functional Thymidine DNA Analogues" by Tsao, Y.-Y. T.; Smith, T. H.; Wooley, K. L., *ACS Macro Lett.* **2018**, *7*, 153–158. Copyright 2018 American Chemical Society.

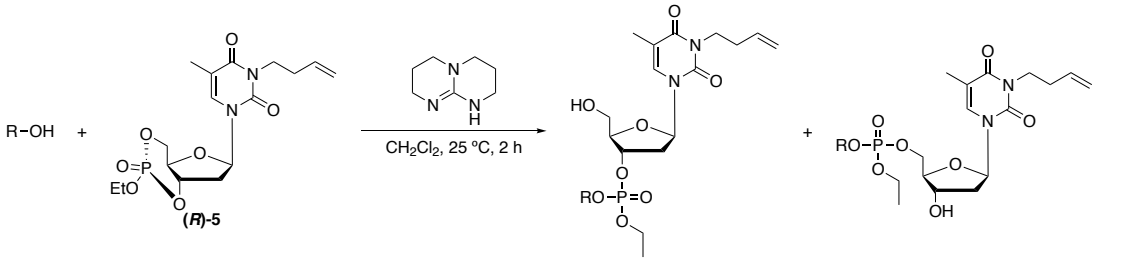

Entry	R	**a**:**b** (molar ratio)
1	Tetrahydrofurfuryl alcohol	100:0
2	**10a**	89:11[a]

[a]Determined by integration values in the ^{1}H NMR spectrum.

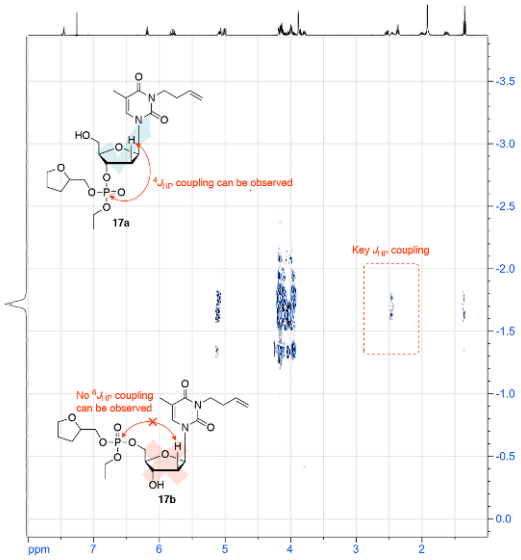

Figure 3.8. ^{1}H–^{31}P HMBC spectrum of **17a**. Reprinted with permission from "Regioisomeric Preference in Ring-Opening Polymerization of 3′,5′-Cyclic Phosphoesters of Functional Thymidine DNA Analogues" by Tsao, Y.-Y. T.; Smith, T. H.; Wooley, K. L., *ACS Macro Lett.* **2018**, *7*, 153–158. Copyright 2018 American Chemical Society.

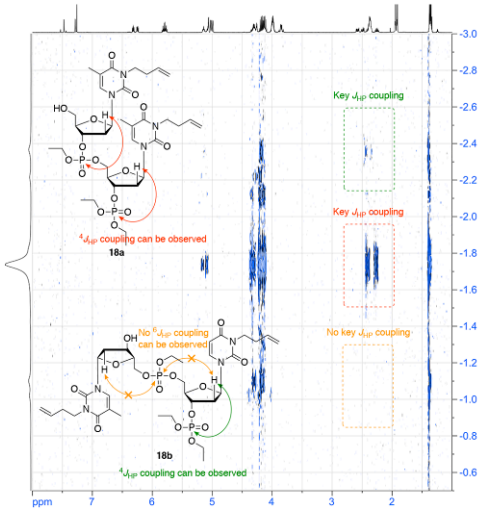

Figure 3.9. ^{1}H–^{31}P HMBC spectrum (500 MHz for ^{1}H) of the mixture of **18a** and **18b**. Reprinted with permission from "Regioisomeric Preference in Ring-Opening Polymerization of 3′,5′-Cyclic Phosphoesters of Functional Thymidine DNA Analogues" by Tsao, Y.-Y. T.; Smith, T. H.; Wooley, K. L., *ACS Macro Lett.* **2018**, *7*, 153–158. Copyright 2018 American Chemical Society.

This steric hindrance-directed selectivity provides new insight into the mechanism of TBD-catalyzed ROP[84] of cyclic phosphoesters and further supports one previously proposed mechanism by Simón and Goodman.[128] Two mechanisms for TBD catalysis including nucleophilic and acid–base catalysis in lactone ROP were investigated by DFT calculations. In the nucleophilic catalytic mechanism, TBD reacted with monomers first to open the ring, and alcohols reacted subsequently. In contrast, the acid–base catalytic mechanism suggested that alcohols, monomers, and TBD reacted *in situ* in the transition state prior to ring-opening of cyclic monomers, *i.e.*, the alcoholic initiators participated in the ring-opening process. In our system, if the TBD-catalyzed ROPs of **(*R*)-5** took place through the nucleophilic catalytic mechanism, steric changes in alcohol should not reflect on the selectivity, because the cyclic monomer would open prior to alcohol involvement. Hence, our finding that the steric hindrance of alcohols dictates ROP regioselectivity is consistent with the acid–base catalytic mechanism for the TBD-catalyzed ROP of **(*R*)-5**.

DFT was used to calculate the energies of the acid–base catalytic mechanism for starting materials (SM), transition states (TS), and final products at the B3LYP/6-31+G* level of theory to rationalize the origin of steric hindrance-directed regioselectivity (Figure 3.10). Products from P–O3′ cleavage (the red route in Figure 3.10) were more thermodynamically stable than from P–O5′ cleavage (the blue route in Figure 3.10) in both model reactions, but a smaller amount, if any, of such product was obtained experimentally. These calculations combined with experimental results suggested that the reaction is kinetically, rather than thermodynamically controlled at ambient

temperature. On the other hand, despite the transition states for P–O3′ cleavage (red route) in both reactions being higher in energy compared to P–O5′ cleavage, the energy difference between the transition states for the two routes resulting from isopropyl alcohol initiation (0.4 kcal/mol) was smaller than that from ethanol initiation (1.2 kcal/mol). This lower differential energy barrier for P–O3′ *vs*. P–O5′ bond cleavage from the transition states following nucleophilic attack by isopropyl alcohol supports the finding of 24% **15b**, the product from P–O3′ cleavage. Together, these DFT calculations applied toward an acid–base catalytic mechanism explained the origin of the regioisomeric ratios being dependent upon the steric hindrance of the attacking nucleophiles. We expect the ROP of **(*R*)-5** might possess different regioselectivity when different catalysts are used, as the reaction mechanism might vary with different catalysts. However, in our trials with TBD, DBU, $Sn(Oct)_2$, $(i\text{-}Bu)_3Al$, and methanesulfonic acid, only TBD successfully initiated the ROP.

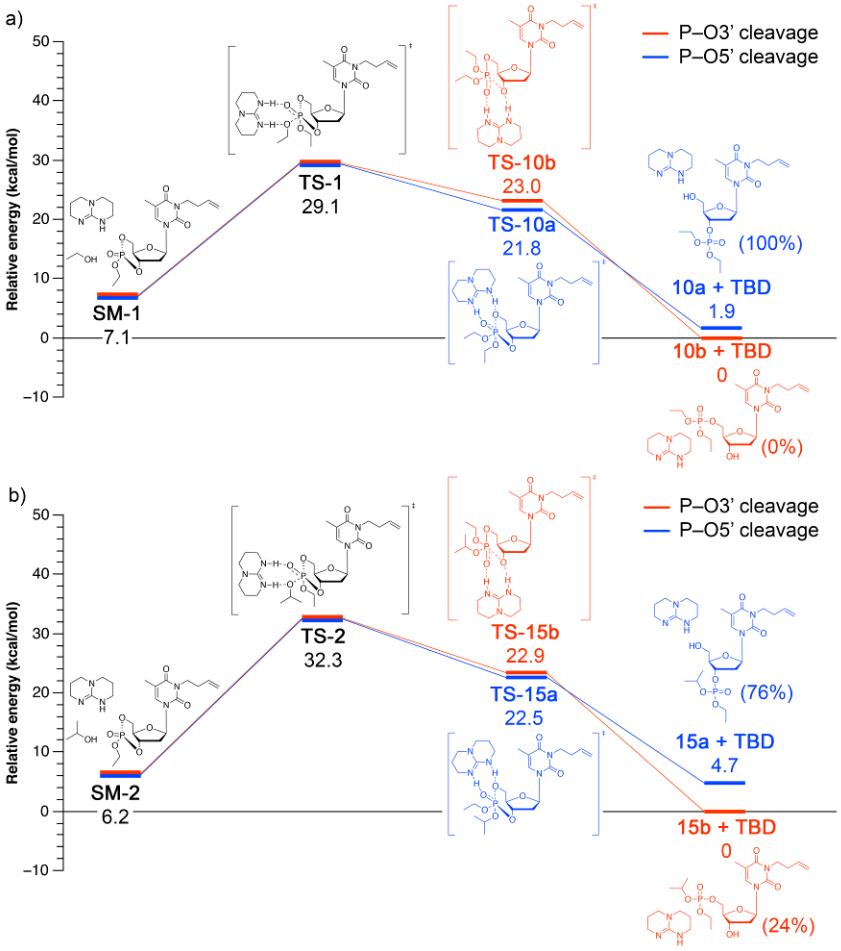

Figure 3.10. DFT calculations on the reaction coordinates of ring-opening reactions (acid–base catalytic mechanism) of **(*R*)-5** with (a) ethanol and (b) isopropyl alcohol. The molar percentages of each product are indicated in parenthesis. Reprinted with permission from "Regioisomeric Preference in Ring-Opening Polymerization of 3′,5′-Cyclic Phosphoesters of Functional Thymidine DNA Analogues" by Tsao, Y.-Y. T.; Smith, T. H.; Wooley, K. L., *ACS Macro Lett.* **2018**, *7*, 153–158. Copyright 2018 American Chemical Society.

3.3 Experimental Section

3.3.1 Materials

Thymidine, 4-bromo-1-butene, and 4-dimethylaminopyridine (DMAP) were used as received from Chem-Impex International, Inc. (Wood Dale, IL). TBD was used as received from TCI America (Portland, OR). Ethyl dichlorophosphate was used as received from Acros Organics (Morris Plains, NJ). *N*,*N*-Dimethylformamide (DMF, ACS grade), hexanes (ACS grade), ethyl acetate (ACS grade), dichloromethane (ACS grade), and acetone (ACS grade) were used as received from VWR International. Anhydrous solvents were obtained after passage through a drying column of a solvent purification system from JC Meyer Solvent Systems (Laguna Beach, CA). All other chemicals were purchased from Sigma-Aldrich (St. Louis, MO) and used without further purification unless otherwise noted.

3.3.2 Instrumentation

^{1}H, ^{13}C, and ^{31}P NMR spectra were recorded on a Varian 500 spectrometer interfaced to a Linux computer using VNMR-J software. ^{1}H–^{31}P HMBC experiments were performed on a Varian 500 spectrometer interfaced to a Linux computer using VNMR-J software with $^{n}J_{HP}$ = 8 Hz. All NMR experiments were performed at ambient

temperature. Chemical shifts were referenced to the solvent residual signals. All ^{1}H NMR spectra are reported in parts per million (ppm) downfield of tetramethylsilane and were measured relative to the signals for residual $CHCl_3$ (7.26 ppm). All ^{13}C NMR spectra are reported in ppm relative to $CDCl_3$ (77.0 ppm), and were obtained with ^{1}H decoupling. For ^{31}P NMR spectroscopy, phosphoric acid (85 wt% in H_2O) at 0 ppm was used as an external standard. The splitting patterns are reported as s (singlet), d (doublet), t (triplet), q (quartet), quin (quintet), m (multiplet), and br (broad). Fourier transform infrared (FTIR) spectra were recorded on an IR Prestige 21 system using a diamond attenuated total reflectance (ATR) lens (Shimadzu Corp., Japan) and analyzed using IRsolution v.1.40 software.

3.3.3 Synthesis

Synthesis of ethyl bis((tetrahydrofuran-2-yl)methyl) phosphate (**11**). To a 50-mL round-bottom flask equipped with a magnetic stir bar containing tetrahydrofurfuryl alcohol (610.5 mg, 5.978 mmol, 1 equiv.) and DMAP (874.4 mg, 7.157 mmol, 1.197 equiv.) in 20.0 mL of dichloromethane was added ethyl dichlorophosphate (573.3 mg, 3.518 mmol, 0.5885 equiv.). The reaction mixture was allowed to stir at 0 °C for 10 min before it was gradually warmed to ambient temperature. The mixture was then washed with water (3 × 20 mL), dried over magnesium sulfate, filtered, concentrated, and purified by silica gel column chromatography with hexanes/ethyl acetate = 1:1 as eluent

(R_f = 0.1) to give **11** as a colorless oil in 47% yield (412.9 mg, as a mixture of diastereomers). ^{1}H NMR (500 MHz; $CDCl_3$) δ 4.12–4.07 (m, 4H, H^A), 4.03–3.93 (m, 4H, H^B and H^C), 3.83 (q, J = 7.1 Hz, 2H, H^D), 3.75 (q, J = 7.1 Hz, 2H, H^E), 1.99–1.91 (m, 2H, H^F), 1.91–1.81 (m, 4H, H^G), 1.69–1.62 (m, 2H, H^H), 1.30 (td, J = 7.1, 0.7 Hz, 3H, H^I); ^{13}C NMR (126 MHz; $CDCl_3$) δ 77.0 (J = 2.1 Hz), 69.1 (J = 1.8 Hz), 68.4, 63.9 (J = 5.9 Hz), 27.6, 25.6, 16.0 (J = 6.8 Hz); ^{31}P NMR (202 MHz; $CDCl_3$) δ –0.9. FTIR (cm^{-1}): 3020–2783, 1652, 1455, 1443, 1394, 1367, 1261, 1189, 1167, 1140, 1077, 1020, 996, 919, 873, 763, 729. HR-MS (ESI): calculated $[M + H]^+$ for $C_{12}H_{24}O_6P$: 295.1311, found: 295.1306.

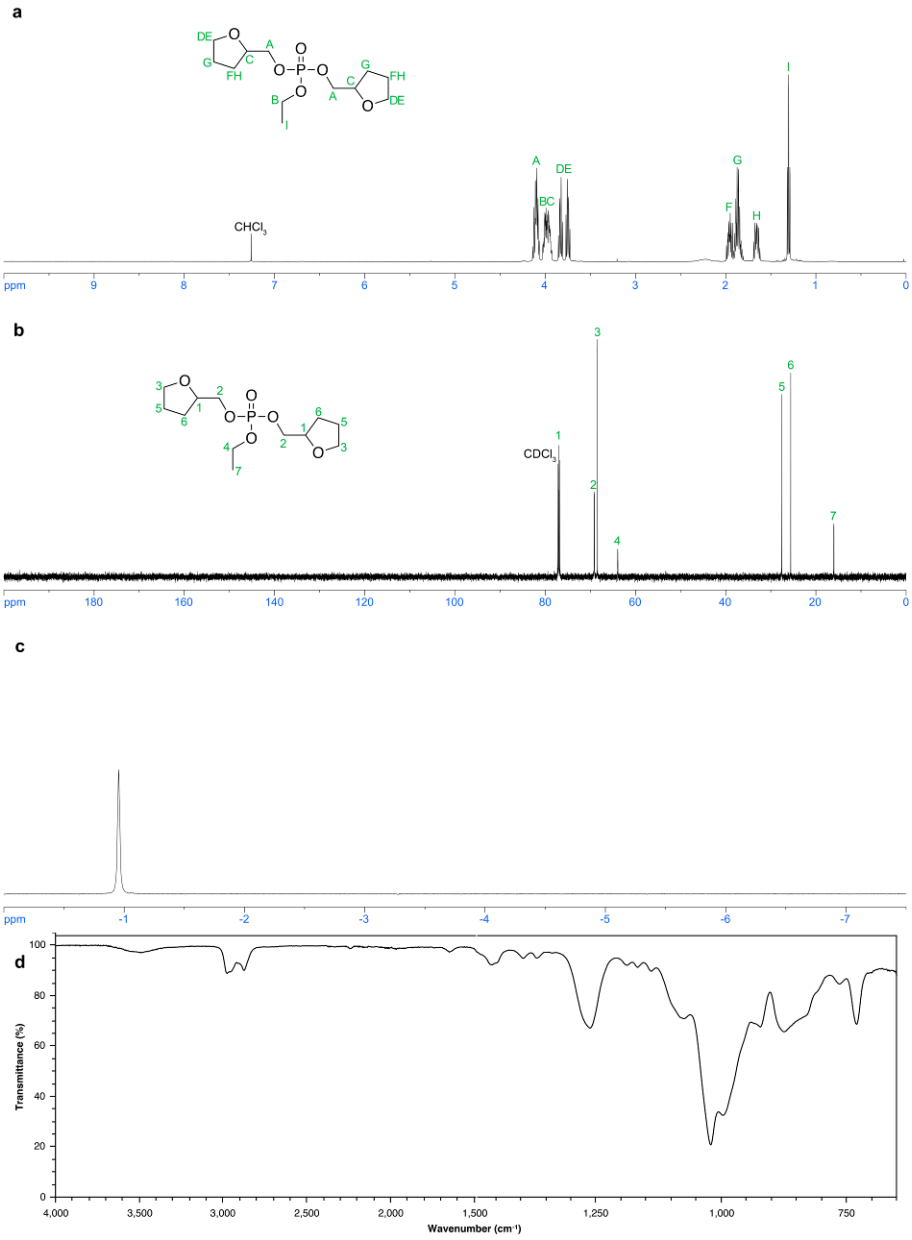

Figure 3.11. Spectroscopic characterization of **11**. (a) ^{1}H NMR (500 MHz; $CDCl_3$). (b) ^{13}C NMR (125 MHz; $CDCl_3$). (c) ^{31}P NMR (202 MHz; $CDCl_3$). (d) IR spectra. Reprinted with permission from "Regioisomeric Preference in Ring-Opening Polymerization of 3′,5′-Cyclic Phosphoesters of Functional Thymidine DNA Analogues" by Tsao, Y.-Y. T.; Smith, T. H.; Wooley, K. L., *ACS Macro Lett.* **2018**, *7*, 153–158. Copyright 2018 American Chemical Society.

Synthesis of ethyl bis(tetrahydrofuran-3-yl) phosphate (**12**). To a 50-mL round-bottom flask equipped with a magnetic stir bar containing 3-hydroxytetrahydrofuran (846.3 mg, 9.605 mmol, 1 equiv.) and DMAP (1409.4 mg, 11.54 mmol, 1.201 equiv.) in 20.0 mL of dichloromethane was added ethyl dichlorophosphate (953.6 mg, 5.852 mmol, 0.6093 equiv.). The reaction mixture was allowed to stir at 0 °C for 10 min before it was gradually warmed to ambient temperature. The mixture was then washed with water (3 × 20 mL), dried over magnesium sulfate, filtered, concentrated, and purified by silica gel column chromatography with hexanes/ethyl acetate = 7:3 as eluent (R_f = 0.3) to give **12** as a colorless oil with a yield of 53% (674.2 mg, as a mixture of diastereomers). ^{1}H NMR (500 MHz; $CDCl_3$) δ 4.93 (tdt, J = 5.7, 3.9, 1.8 Hz, 2H, H^A), 4.01 (td, J = 7.4, 7.4 Hz, 2H, H^B), 3.85–3.80 (m, 4H, H^C), 3.79–3.73 (m, 4H, H^D), 2.09–2.00 (m, 4H, H^E), 1.24 (td, J = 7.1, 0.8 Hz, 3H, H^F); ^{13}C NMR (126 MHz; $CDCl_3$) δ 78.1 (d, J = 5.8 Hz), 73.4 (d, J = 5.4 Hz), 66.5, 63.8 (d, J = 6.0 Hz), 33.7 (d, J = 4.9 Hz), 15.8 (d, J = 6.8 Hz); ^{31}P NMR (202 MHz; $CDCl_3$) δ –2.70, –2.73, –2.80. FTIR (cm^{-1}): 3034–2806, 1648, 1481, 1440, 1394, 1369, 1335, 1262, 1167, 1105, 1079, 1000, 938, 905, 818, 801, 732. HR-MS (ESI): calculated $[M + H]^+$ for $C_{10}H_{20}O_6P$: 267.0997, found: 267.0980.

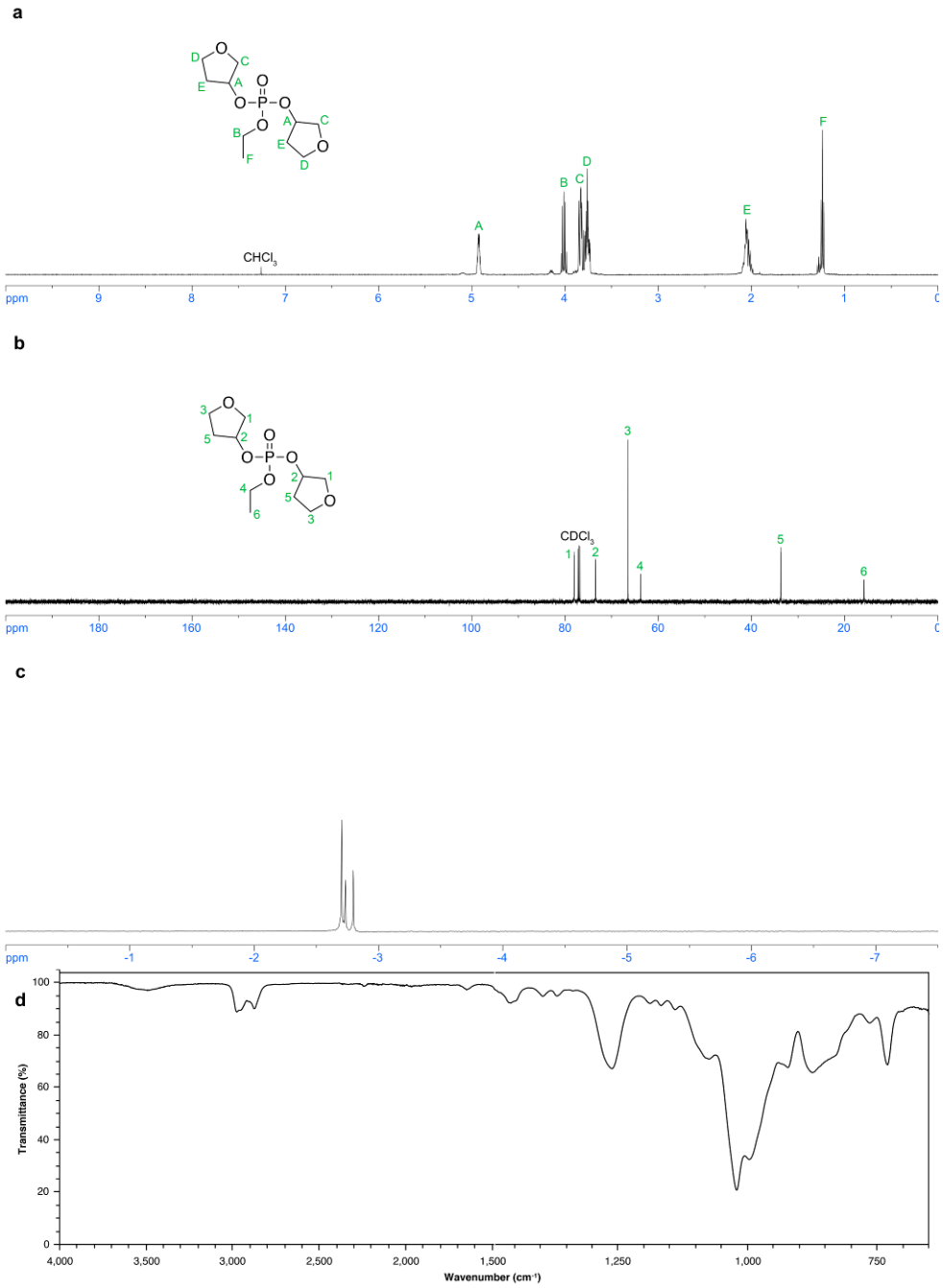

Figure 3.12. Spectroscopic characterization of **12**. (a) ^{1}H NMR (500 MHz; $CDCl_3$). (b) ^{13}C NMR (125 MHz; $CDCl_3$). (c) ^{31}P NMR (202 MHz; $CDCl_3$). (d) IR spectra. Reprinted with permission from "Regioisomeric Preference in Ring-Opening Polymerization of 3′,5′-Cyclic Phosphoesters of Functional Thymidine DNA Analogues" by Tsao, Y.-Y. T.; Smith, T. H.; Wooley, K. L., *ACS Macro Lett.* **2018**, *7*, 153–158. Copyright 2018 American Chemical Society.

Synthesis of 3′-thymidine monophosphate diethylester (**10a**). A solution of **(*R*)-5** (113.8 mg, 0.295 mmol, 1 equiv.) in ethanol (0.50 mL) was transferred into a flame-dried 10-mL Schlenk flask equipped with a magnetic stir bar and a glass stopper on a Schlenk line. A solution of TBD (20.1 mg, 0.144 mmol, 0.0488 equiv.) in ethanol (0.50 mL) was injected into the Schlenk flask *via* syringe to initiate the reaction, which was stirred under a nitrogen gas atmosphere at ambient temperature for 1 h. Excess ethanol was removed by rotary evaporation before the reaction mixture was purified by silica gel column chromatography with acetone/hexanes = 3:7 as eluent to give **10a** as a colorless oil with a yield of 80% (102.4 mg). R_f = 0.20 (acetone/hexanes = 3:7); ^{1}H NMR (500 MHz; $CDCl_3$) δ 7.47 (d, J = 1.2 Hz, 1H, H^A), 6.23 (t, J = 6.9 Hz, 1H, H^B), 5.79 (ddt, J = 17.1, 10.1, 7.0 Hz, 1H, -CCH=CH^CH), 5.09 (m, 2H, H^D and H^E), 4.99 (dd, J = 10.5, 1.5 Hz, 1H, -CCH=CHH^F), 4.20 (q, J = 2.6 Hz, 1H, H^G), 4.12 (qd, J = 7.4, 1.3 Hz, 4H, -OCH^H_2CH$_3$), 3.99 (t, J = 7.5 Hz, 2H, -NCH^I_2-), 3.87 (t, J = 2.4 Hz, 2H, H^J), 3.60–3.40 (br, 1H, -OH^K), 2.54–2.44 (m, 2H, H^L), 2.36 (q, J = 7.2 Hz, 3H, -NCH$_2$CH^M_2-), 1.91 (d, J = 1.1 Hz, 4H, H^N), 1.34 (td, J = 7.1, 0.9 Hz, 6H, H^O); ^{13}C NMR (126 MHz; $CDCl_3$) δ 163.2, 150.8 134.8, 134.3, 116.9, 110.4, 86.7, 85.6 (d, J = 4.9 Hz), 77.5 (d, J = 5.5 Hz), 64.3 (d, J = 6.2 Hz), 62.0, 40.5, 38.5 (d, J = 5.0 Hz), 31.9, 16.1 (d, J = 6.8 Hz), 13.3; ^{31}P NMR (202 MHz; $CDCl_3$) δ –1.81. FTIR (cm^{-1}): 3580–3190, 3105–2793, 2249, 1701, 1666, 1639, 1466, 1362, 1254, 1196, 1161, 1103, 1011, 910, 826, 768, 729. HR-MS (ESI): calculated $[M + Na]^+$ for $C_{18}H_{29}N_2O_8PNa$: 455.1559, found: 455.1545.

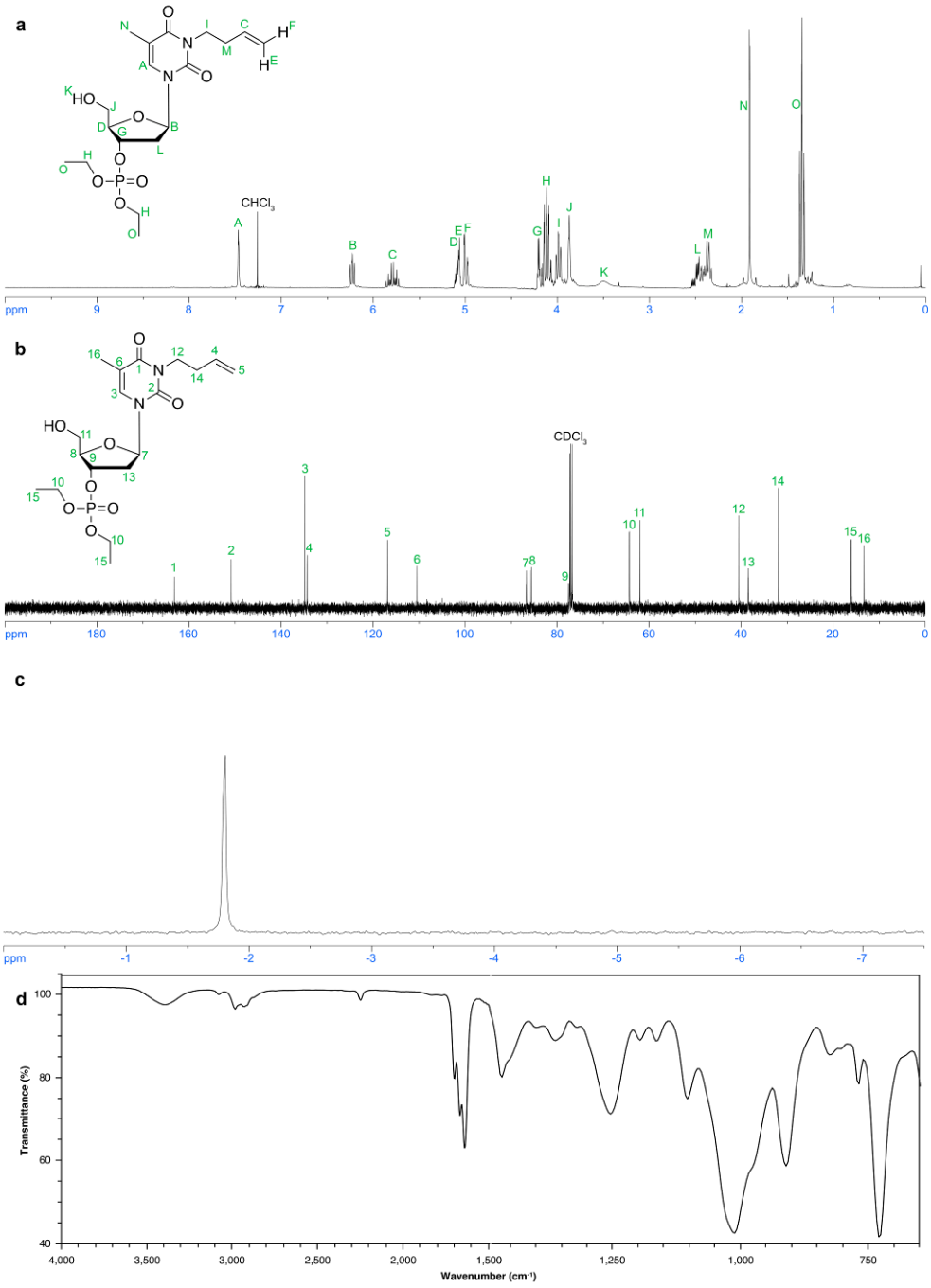

Figure 3.13. Spectroscopic characterization of **10a**. (a) ^{1}H NMR (500 MHz; $CDCl_3$). (b) ^{13}C NMR (125 MHz; $CDCl_3$). (c) ^{31}P NMR (202 MHz; $CDCl_3$). (d) IR spectra. Reprinted with permission from "Regioisomeric Preference in Ring-Opening Polymerization of 3′,5′-Cyclic Phosphoesters of Functional Thymidine DNA Analogues" by Tsao, Y.-Y. T.; Smith, T. H.; Wooley, K. L., *ACS Macro Lett.* **2018**, *7*, 153–158. Copyright 2018 American Chemical Society.

Synthesis of 3′-thymidine monophosphate ethylisopropylester (**15a**) and 5′-thymidine monophosphate ethylisopropylester (**15b**). A solution of **(*R*)-5** (193.4 mg, 0.5007 mmol, 1 equiv.) in isopropyl alcohol (0.50 mL) was transferred into a flame-dried 10-mL Schlenk flask equipped with a magnetic stir bar and a glass stopper on a Schlenk line. A solution of TBD (277.5 mg, 1.994 mmol, 3.982 equiv.) in isopropyl alcohol (0.50 mL) was injected into the Schlenk flask *via* syringe to initiate the reaction, which was stirred under a nitrogen gas atmosphere at ambient temperature for 12 h. Excess isopropyl alcohol was removed by rotary evaporation before the reaction mixture was purified by silica gel column chromatography with acetone/hexanes = 3:7 as eluent to give **15a** and **15b** as colorless oils with yields of 54% (121.4 mg) and 17% (38.2 mg), respectively. **15a.** R_f = 0.18 (acetone/hexanes = 3:7); ^{1}H NMR (500 MHz; $CDCl_3$) δ 7.39 (d, J = 1.1 Hz, 1H, H^A), 6.20 (t, J = 6.9 Hz, 1H, H^B), 5.82 (ddt, J = 17.1, 10.1, 7.0 Hz, 1H, H^C), 5.09–5.03 (m, 2H, H^D and H^E), 5.00 (dd, J = 10.2, 1.8 Hz, 1H, H^F), 4.69–4.63 (m, 1H, H^G), 4.21 (q, J = 2.8 Hz, 1H, H^H), 4.15–4.08 (m, 2H, H^I), 4.00 (td, J = 7.4, 2.9 Hz, 2H, H^J), 3.93–3.85 (m, 2H, H^K), 3.20 (dt, J = 6.5, 3.5 Hz, 1H, H^L), 2.53–2.43 (m, 2H, H^M), 2.38 (q, J = 7.3 Hz, 2H, H^N), 1.93 (d, J = 1.2 Hz, 3H, H^O), 1.37–1.33 (m, 9H, H^P and H^Q); ^{13}C NMR (126 MHz; $CDCl_3$) δ 163.2, 150.8, 134.9, 134.4, 116.9, 110.5, 87.1, 85.6 (d, J = 5.1 Hz), 77.2 (d, J = 5.6 Hz), 73.4 (d, J = 6.0 Hz), 64.1 (d, J = 6.4 Hz), 62.1, 40.6, 38.4 (d, J = 5.1 Hz), 31.9, 23.6, 16.1 (d, J = 6.8 Hz), 13.3; ^{31}P NMR (202 MHz; $CDCl_3$) δ –2.47. FTIR (cm^{-1}): 3657–3179, 3101–2793, 1697, 1643, 1465, 1366, 1250, 1103, 1002, 910, 826, 772, 733. HR-MS (ESI): calculated $[M + H]^+$ for $C_{19}H_{32}O_8P$: 447.1896, found: 447.1899. **15b.** R_f = 0.12 (acetone/hexanes = 3:7); ^{1}H

NMR (500 MHz; $CDCl_3$) δ 7.33 (d, J = 1.2 Hz, 1H, H^A), 6.16 (t, J = 6.8 Hz, 1H, H^B), 5.85–5.77 (m, 1H, H^C), 5.06 (dd, J = 17.1, 1.6 Hz, 2H, H^D), 5.01 (dd, J = 10.2, 1.7 Hz, 2H, H^E), 4.59 (dt, J = 6.7, 3.7 Hz, 1H, H^F), 4.54–4.50 (m, 1H, H^G), 4.26 (td, J = 7.3, 3.2 Hz, 1H, H^H), 4.17–4.11 (m, 2H, H^I), 4.01–3.99 (m, 2H, H^J), 3.92 (dd, J = 11.9, 3.1 Hz, 1H, H^K), 3.83 (dd, J = 11.9, 3.1 Hz, 1H, H^L), 3.35–3.28 (m, 1H, H^M), 2.44–2.36 (m, 4H, H^N and H^O), 1.93 (d, J = 1.2 Hz, 3H, H^P), 1.37–1.34 (m, 9H, H^Q and H^R); ^{13}C NMR (126 MHz; $CDCl_3$) δ 163.2, 150.9, 134.9, 133.3, 116.9, 110.3, 87.6, 84.4 (d, J = 4.1 Hz), 71.3, 70.7 (d, J = 8.4 Hz), 66.0 (d, J = 5.9 Hz), 62.0, 46.9, 40.0, 31.9, 20.7, 16.1 (d, J = 6.9 Hz), 13.3; ^{31}P NMR (202 MHz; $CDCl_3$) δ –1.24. FTIR (cm^{-1}): 3734–3124, 3109–2777, 2353, 1697, 1666, 1636, 1466, 1358, 1258, 1196, 1096, 1011, 918, 772. HR-MS (ESI): calculated $[M + H]^+$ for $C_{19}H_{32}O_8P$: 447.1896, found: 447.1816.

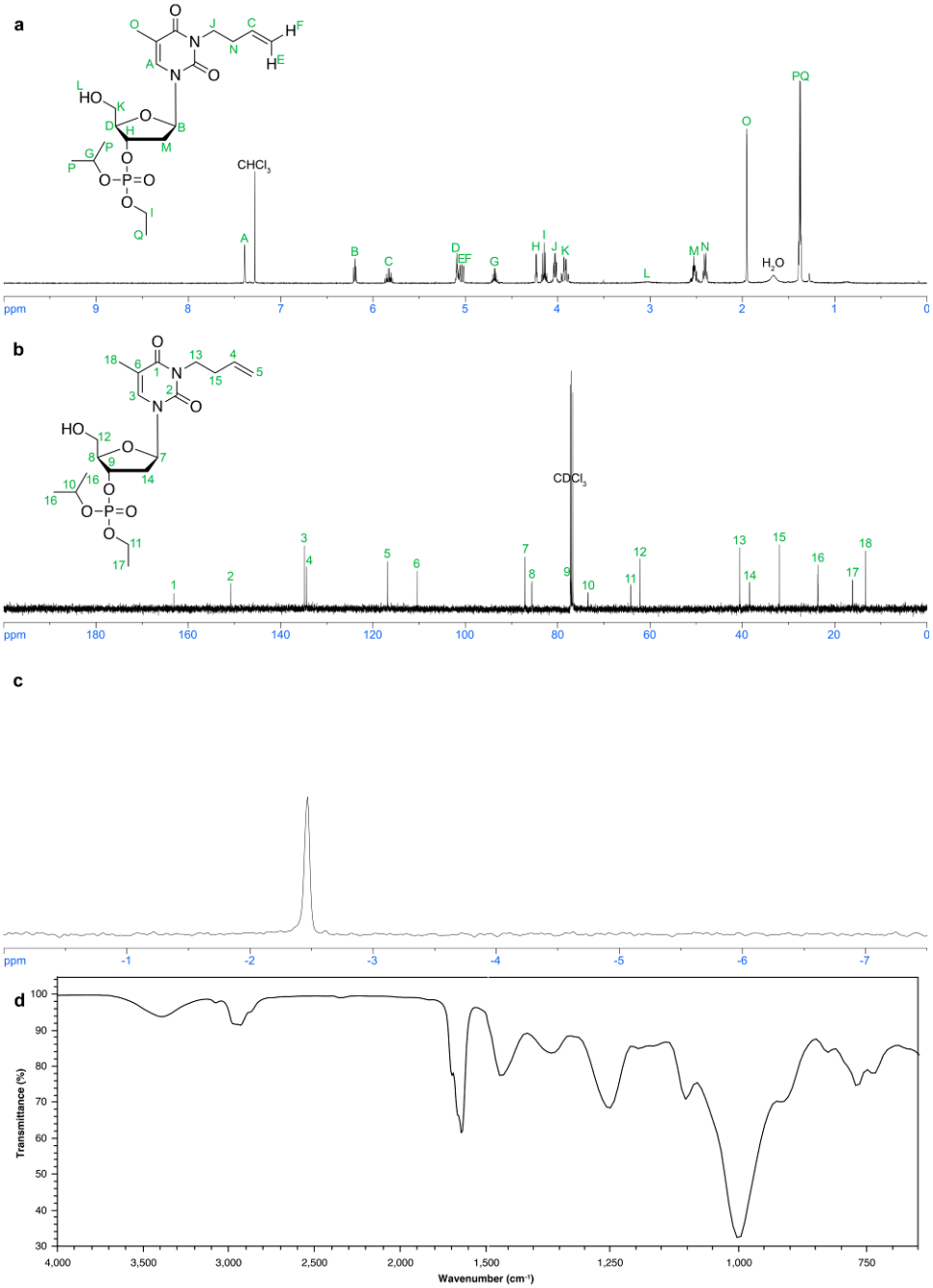

Figure 3.14. Spectroscopic characterization of **15a**. (a) ^{1}H NMR (500 MHz; $CDCl_3$). (b) ^{13}C NMR (125 MHz; $CDCl_3$). (c) ^{31}P NMR (202 MHz; $CDCl_3$). (d) IR spectra. Reprinted with permission from "Regioisomeric Preference in Ring-Opening Polymerization of 3′,5′-Cyclic Phosphoesters of Functional Thymidine DNA Analogues" by Tsao, Y.-Y. T.; Smith, T. H.; Wooley, K. L., *ACS Macro Lett.* **2018**, *7*, 153–158. Copyright 2018 American Chemical Society.

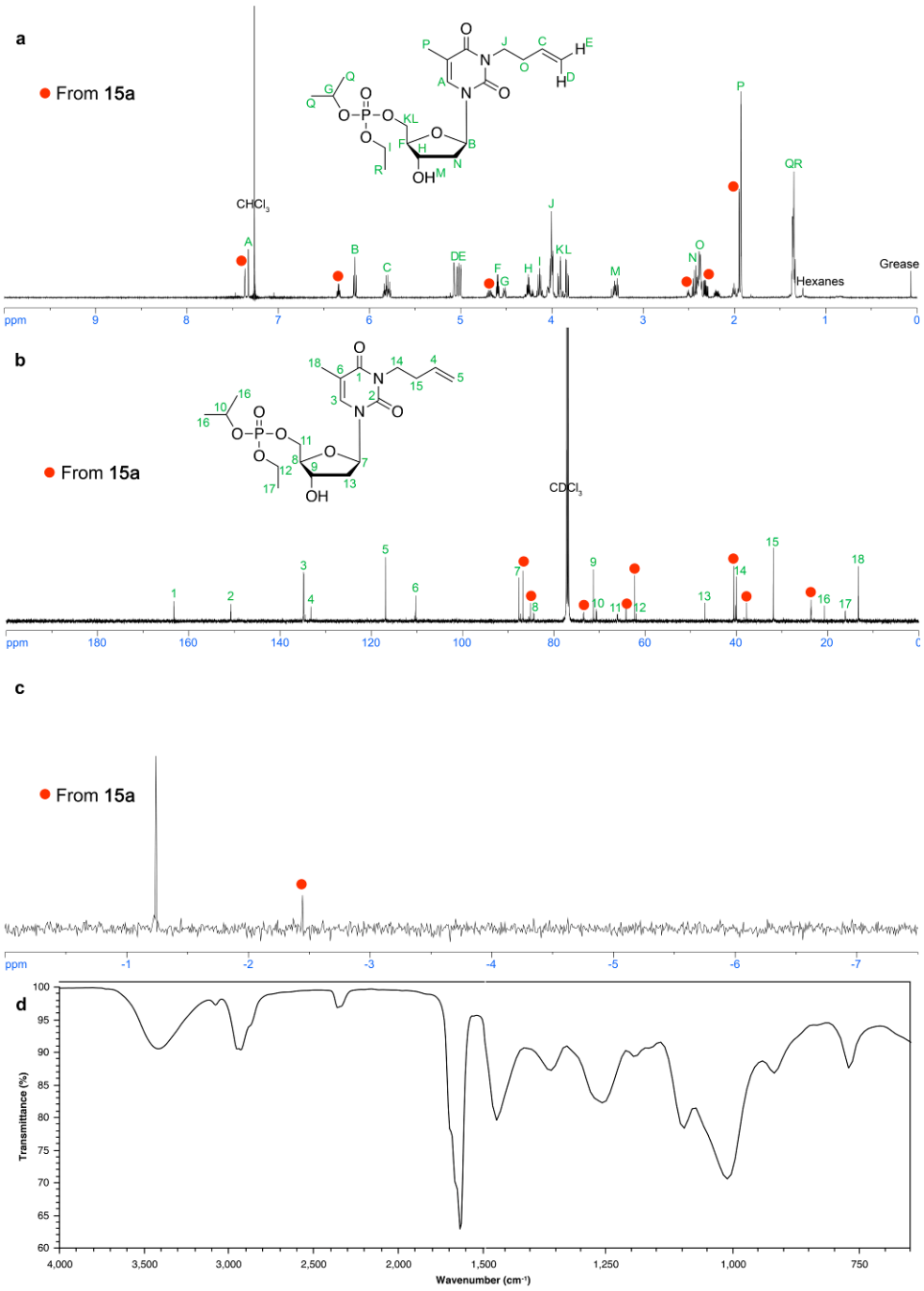

Figure 3.15. Spectroscopic characterization of **15b**. (a) ^{1}H NMR (500 MHz; $CDCl_3$). (b) ^{13}C NMR (125 MHz; $CDCl_3$). (c) ^{31}P NMR (202 MHz; $CDCl_3$). (d) IR spectra. Reprinted with permission from "Regioisomeric Preference in Ring-Opening Polymerization of 3′,5′-Cyclic Phosphoesters of Functional Thymidine DNA Analogues" by Tsao, Y.-Y. T.; Smith, T. H.; Wooley, K. L., *ACS Macro Lett.* **2018**, *7*, 153–158. Copyright 2018 American Chemical Society.

Synthesis of 3′-thymidine monophosphate ethyl tetrahydrofurfuryl ester (**17a**). A solution of **(*R*)-5** (196.1 mg, 0.5077 mmol, 1 equiv.) and tetrahydrofurfuryl alcohol (267.0 mg, 2.614 mmol, 5.149 equiv.) in anhydrous dichloromethane (0.90 mL) was transferred into a flame-dried 10-mL two-neck round-bottom flask equipped with a magnetic stir bar and a rubber septum on a Schlenk line. A solution of TBD (70.7 mg, 0.508 mmol, 1.00 equiv.) in anhydrous dichloromethane (0.10 mL) was injected into the reaction flask *via* syringe to initiate the reaction, which was stirred under a nitrogen gas atmosphere at ambient temperature for 2 h. Excess dichloromethane was removed by rotary evaporation before the reaction mixture was purified by silica gel column chromatography with acetone/hexanes = 3:7 as eluent to give **17a** as a colorless oil with a yield of 62% (154.2 mg). R_f = 0.20 (acetone/hexanes = 3:7); ^{1}H NMR (500 MHz; $CDCl_3$) δ 7.45 (d, J = 1.2 Hz, 1H, H^A), 6.19 (t, J = 6.8 Hz, 1H, H^B), 5.80 (ddt, J = 17.1, 10.2, 7.0 Hz, 1H, H^C), 5.12–5.07 (m, 1H, H^D), 5.05 (dd, J = 17.1, 1.7 Hz, 1H, H^E), 5.00 (dd, J = 10.6, 1.4 Hz, 1H, H^F), 4.19–3.92 (m, 8H, H^G–H^K), 3.89 (d, J = 2.7 Hz, H^L), 3.88–3.84 (m, 1H, H^M), 3.82–3.77 (m, 1H, H^N), 2.54 (m, J = 3.7 Hz, 1H, H^O), 2.48–2.41 (m, 1H, H^P), 2.37 (q, J = 7.4 Hz, 2H, H^Q), 2.04–1.96 (m, 1H, H^R), 1.92 (d, J = 1.1 Hz, 6H, H^S–H^U), 1.67–1.58 (m, 1H, H^V), 1.35 (td, J = 7.1, 1.1 Hz, 3H, H^W); ^{13}C NMR (126 MHz; $CDCl_3$) δ 163.2, 150.8, 134.9, 134.3, 116.9, 110.3 (d, J = 1.8 Hz), 86.6, 85.4 (d, J = 5.3 Hz), 77.19 (d, J = 2.8 Hz), 77.13 (d, J = 2.1 Hz), 69.7 (d, J = 6.7 Hz), 68.5 (d, J = 8.7 Hz), 64.5 (d, J = 5.8 Hz), 61.6 (d, J = 2.5 Hz), 40.5, 38.4, 31.9, 27.4, 25.6 (d, J = 5.7 Hz), 16.1 (d, J = 6.7 Hz), 13.3; ^{31}P NMR (202 MHz; $CDCl_3$) δ –1.72. FTIR (cm^{-1}): 3670–3202, 3113–2791, 2357, 1699, 1666, 1641, 1466, 1452, 1404, 1361, 1259, 1196,

1163, 1101, 1003, 916, 866, 825, 767, 733, 700. HR-MS (ESI): calculated $[M + H]^+$ for $C_{21}H_{34}N_2O_9P$: 489.2002, found: 489.2009.

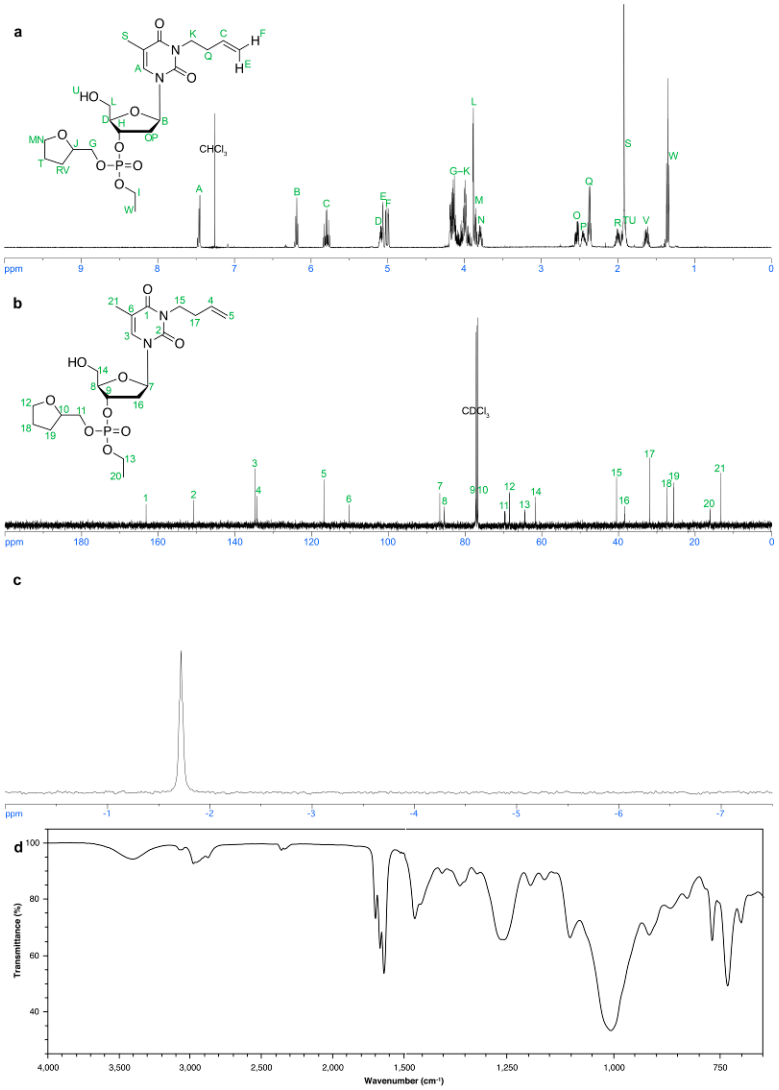

Figure 3.16. Spectroscopic characterization of **17a**. (a) ^{1}H NMR (500 MHz; $CDCl_3$). (b) ^{13}C NMR (125 MHz; $CDCl_3$). (c) ^{31}P NMR (202 MHz; $CDCl_3$). (d) IR spectra. Reprinted with permission from "Regioisomeric Preference in Ring-Opening Polymerization of 3′,5′-Cyclic Phosphoesters of Functional Thymidine DNA Analogues" by Tsao, Y.-Y. T.; Smith, T. H.; Wooley, K. L., *ACS Macro Lett.* **2018**, *7*, 153–158. Copyright 2018 American Chemical Society.

Synthesis of **18a** and **18b**. A solution of **(*R*)-5** (187.3 mg, 0.4849 mmol, 1 equiv.) and **10a** (227.8 mg, 0.5268 mmol, 1.086 equiv.) in anhydrous dichloromethane (0.90 mL) was transferred into a flame-dried 10-mL two-neck round-bottom flask equipped with a magnetic stir bar and a rubber septum on a Schlenk line. A solution of TBD (34.1 mg, 0.245 mmol, 0.505 equiv.) in anhydrous dichloromethane (0.10 mL) was injected into the reaction flask *via* syringe to initiate the reaction, which was stirred under a nitrogen gas atmosphere at ambient temperature for 2 h. Excess dichloromethane was removed by rotary evaporation before the reaction mixture was purified by silica gel column chromatography with ethyl acetate as eluent to give mixture of **18a** and **18b** as a colorless oil with a combined yield of 57% (227.8 mg, **18a**:**18b** = 89:11 according to the integration values). **18a.** R_f = 0.05 (ethyl acetate); ^{1}H NMR (500 MHz; $CDCl_3$) δ 7.47 (d, J = 1.2 Hz, 1H, H^A), 7.28 (d, J = 1.2 Hz, 1H, H^B), 6.32 (dd, J = 7.5, 6.1 Hz, 1H, H^C), 6.25 (dd, J = 8.1, 5.9 Hz, 1H, H^D), 5.84–5.75 (m, 2H, H^E and H^F), 5.16–5.12 (m, 1H, H^G), 5.09 (m, 1H, H^H), 5.04 (dd, J = 17.1, 1.7 Hz, 2H, H^I and H^J), 5.00 (dd, J = 10.2, 1.1 Hz, 2H, H^K and H^L), 4.33–4.25 (m, 4H, H^M), 4.21–4.09 (m, 6H, H^N–H^Q), 3.99 (m, 4H, H^R and H^S), 3.88–3.82 (m, 2H, H^T), 2.58 (ddd, J = 14.1, 6.0, 3.0 Hz, 1H, H^U), 2.49 (ddd, J = 14.1, 5.9, 2.2 Hz, 1H, H^V), 2.42–2.34 (m, 6H, H^W–H^Z), 2.25 (dt, J = 14.2, 6.7 Hz, 1H, H^α), 1.94 (d, J = 1.1 Hz, 3H, H^β), 1.91 (d, J = 1.1 Hz, 3H, H^γ), 1.38–1.34 (m, 9H, H^δ and H^ε); ^{13}C NMR (126 MHz; $CDCl_3$) δ 163.16, 163.01, 150.79, 150.67, 134.81, 134.74, 134.2, 132.8, 116.90, 116.84, 110.7, 110.4, 86.6, 85.8 (d, J = 4.7 Hz), 85.5, 82.8 (d, J = 5.3 Hz), 78.4 (d, J = 5.2 Hz), 76.0 (d, J = 5.1 Hz), 66.1 (d, J = 5.2 Hz), 64.9 (d, J = 5.8 Hz), 64.5 (dd, J = 10.4, 6.0 Hz), 62.0, 40.60, 40.52, 38.51 (d, J = 5.5 Hz), 38.41 (d, J =

4.8 Hz), 31.89, 31.89, 16.15 (d, J = 6.6 Hz), 16.05 (d, J = 6.7 Hz), 13.25, 13.23; ^{31}P NMR (202 MHz; $CDCl_3$) δ –1.74. FTIR (cm^{-1}): 3713–3200, 3105–2793, 2359, 1697, 1666, 1639, 1468, 1450, 1404, 1360, 1258, 1196, 1163, 1101, 1009, 912, 827, 768, 733, 675. HR-MS (ESI): calculated $[M + H]^+$ for $C_{34}H_{53}N_4O_{15}P_2$: 819.2983, found: 819.2998. **18b.** R_f = 0.05 (ethyl acetate). ^{31}P NMR (202 MHz; $CDCl_3$) δ –1.02, –1.10, –2.22, –2.34.

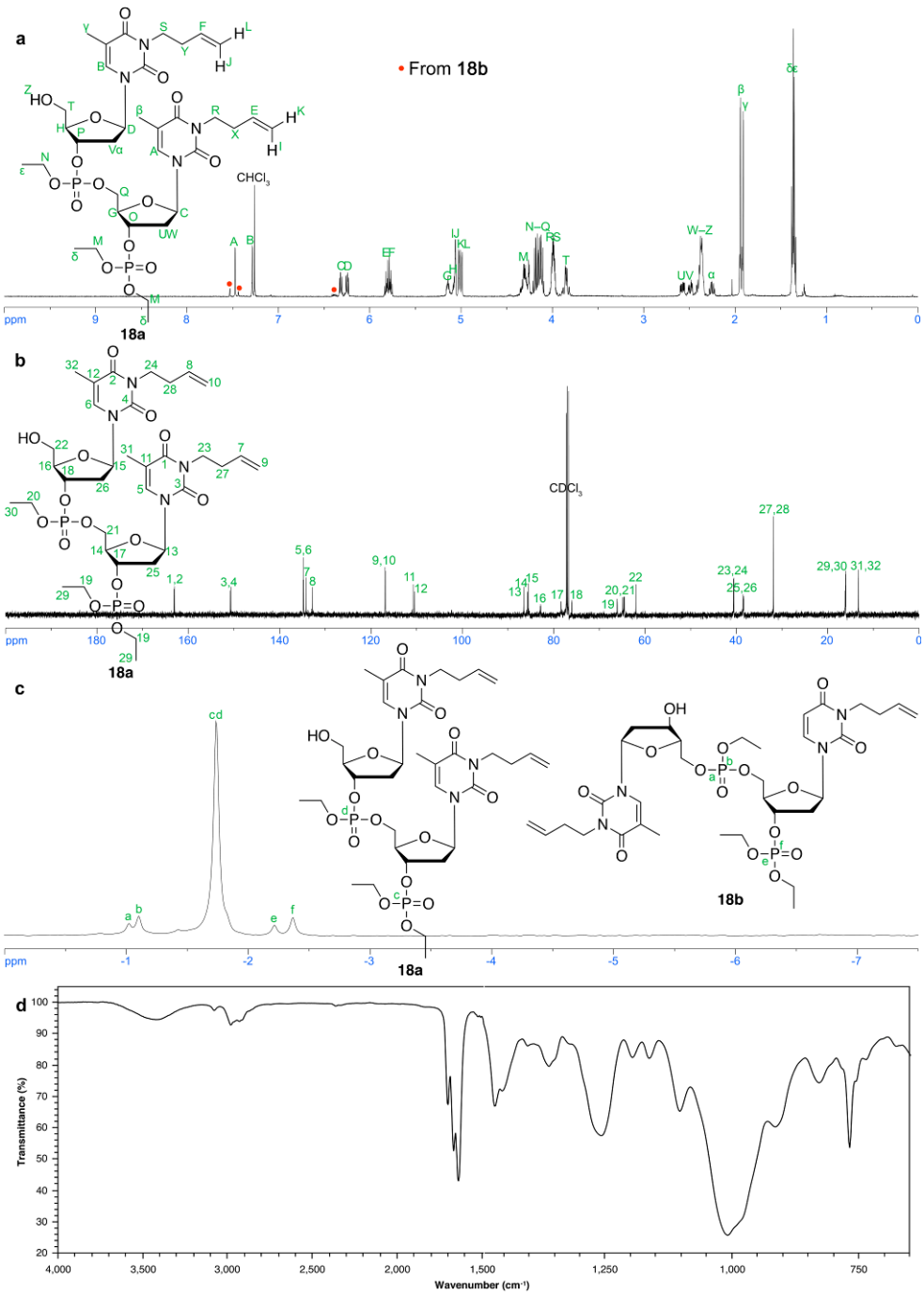

Figure 3.17. Spectroscopic characterization of **18a** and **18b**. (a) ^{1}H NMR (500 MHz; $CDCl_3$). (b) ^{13}C NMR (125 MHz; $CDCl_3$). (c) ^{31}P NMR (202 MHz; $CDCl_3$). (d) IR spectra. Reprinted with permission from "Regioisomeric Preference in Ring-Opening Polymerization of 3′,5′-Cyclic Phosphoesters of Functional Thymidine DNA Analogues" by Tsao, Y.-Y. T.; Smith, T. H.; Wooley, K. L., *ACS Macro Lett.* **2018**, *7*, 153–158. Copyright 2018 American Chemical Society.

3.3.4 Details of Computational Chemistry

All calculations were performed with Gaussian 09. All geometries were optimized using the B3LYP/6-31+G* level of theory. The QST3 option implemented in Gaussian 09 with the Synchronous Transit-Guided Quasi-Newton (STQN) method at the B3LYP/6-31+G* level of theory was used to locate the transition state, and the Gibbs free energies from the frequency calculations are reported to explain the regioselectivity of the ring-opening reaction/polymerization.

3.4 Conclusions

In summary, we have verified the regioselectivity of the ROP of **(*R*)-5** into **PCBT**, and validated our hypothesis with model reactions to establish the steric hindrance-based origin of the selectivity. From syntheses of model compounds **11**–**13** with 3′,3′-, 5′,5′-, and 3′,5′-linkages, we concluded that signals resonating in the ^{31}P NMR spectra of **PCBT** from –2.7 to –2.9 ppm, from –0.9 to –1.1 ppm, and from –1.7 to –1.9 ppm arose from 3′,3′-, 5′,5′-, and 3′,5′-linkages, respectively. Further model reactions employing different alcohols, including 4-methoxybenzyl alcohol, ethanol, isopropyl alcohol, *tert*-butyl alcohol, and **10a**, revealed that the preference of P-O3′ and P–O5′ cleavages was dictated by steric hindrance. DFT calculations on the reaction coordinates of the ethanol and isopropyl alcohol model reactions demonstrated that, the

transition state energy difference between the two routes was the major reason for changes in product distribution. Overall, this work provides fundamental understanding of the polymerization behavior of six-membered 3′,5′-bicyclic phosphoesters, and broadens the scope of designing different DNA analogues. The ring-opening preference of the six-membered cyclic phosphotriester thymidine analogues presented here affords polymerization primarily in the 3′-to-5′ direction, opposite relative to the 5′-to-3′ polymerization of DNA in Nature. Notably, both systems yield head-to-tail linkages as the major connectivity. We anticipate the exploration of reasons behind the varying ring opening preferences in our ROP system will further the development of a next generation of 3′,5′-bicyclic monomers that mimics natural DNA.

CHAPTER IV

TOWARD WATER SOLUBLE, DNA-MIMICKING POLYPHOSPHOESTERS

4.1 Introduction

Polymers with repeating phosphoester bonds in the backbone are structurally versatile and biodegradable through hydrolysis and possibly through enzymatic digestion (*e.g.*, phosphodiesterase I and alkaline phosphatase) of phosphate linkages under physiological conditions.[11,129,130] With the aims of studying the enzymatic degradability and future biomedical applications, the water solubility of our current polyphosphoesters needs to be improved since all polymers currently discussed are only organic soluble.

To increase the hydrophilicity of hydrophobic polymers, poly(ethylene glycol) is commonly used as a nucleophilic initiator in ROP, also known as PEGylation, due to its water solubility and low intrinsic toxicity.[131-133] However, a review paper published in 2010 by the Schubert group[134] detailing the pros and cons of using poly(ethylene glycol) in drug delivery suggested that poly(ethylene glycol) alternatives that impart water solubility will be attractive, due to some potentially unfavorable effects — including adverse immunological responses, unexpected changes in the pharmacokinetic behavior, and toxicity of oligomers with a molar mass below 400 Da. One potential new class of polymers that might replace poly(ethylene glycol) would be hydrophilic analogues of the polyphosphoesters discussed in this work. Therefore, we have recently focused our

attention on the synthesis of phosphodiester **19** and natural thymidine-based polyphosphoester **20**, to improve water solubility (Figure 4.1).

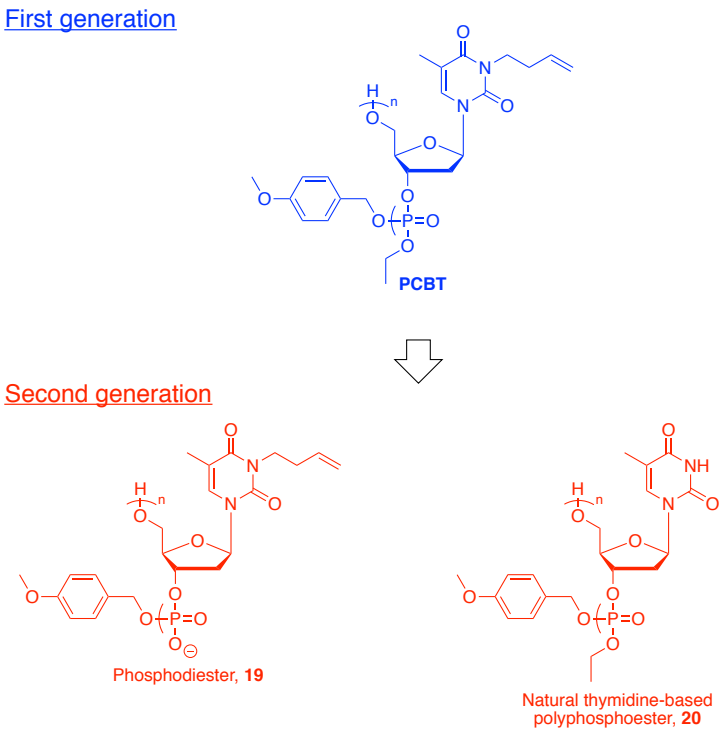

Figure 4.1. Recent efforts on the synthesis of **19** and **20** to improve water solubility of the polymers.

4.2 Results and Discussions

Functional group transformation to give phosphodiester and/or introduction of a natural thymidine, to enable the hydrogen bond interaction of polymers with water, are expected to increase the water solubility. We approached the synthesis of phosphodiester **19** using the previously-reported acid-labile phosphoramidate chemistry

that allows for hydrolytic degradation under acidic conditions to give phosphodiester (Figure 4.2).[135] The 3′,5′-bicyclic phosphoramidate **(*R*)-21** was synthesized from **6** using DMAP under kinetically-controlled conditions at –78 °C. However, TBD-catalyzed ROP of **(*R*)-21** did not yield polymer. The optimized conformation of **(*R*)-21** by DFT calculation at the B3LYP/6-31+G* level of theory (Figure 4.3) suggested the ROP may be difficult due to extra steric hindrance provided by the sterically-bulky *N*,*N*-dimethyl substituent on the phosphorus. Unfortunately, no successful cyclization was observed when the less steric hindered *N*-methylphosphoramic dichloride **23** was used to reduce the steric hindrance of the 3′,5′-bicyclic monomer (Figure 4.4). Therefore, we pursued the development of water-soluble DNA-mimicking phosphoester by the incorporation of natural thymidine.

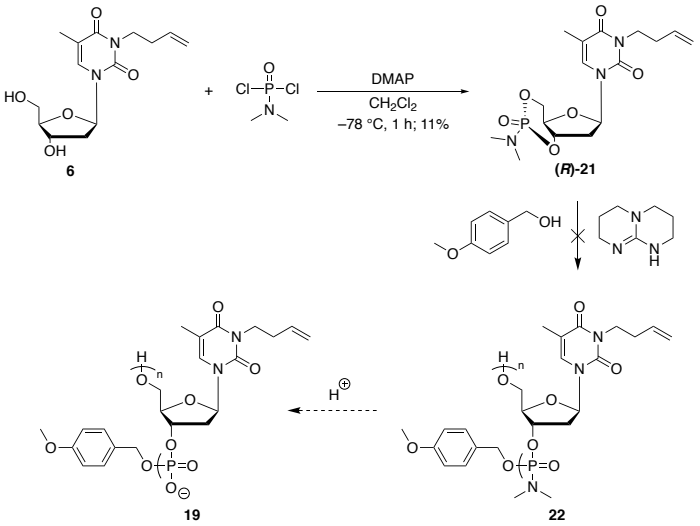

Figure 4.2. Synthetic approach to phosphodiester **19** by acid-labile phosphoramidate approach. No polymerization catalyzed by TBD was observed from **(*R*)-21**.

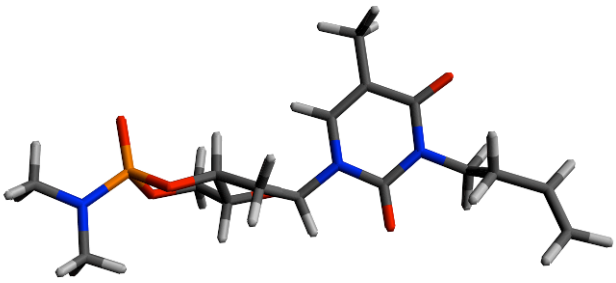

Figure 4.3. DFT calculated structure of **(*R*)-21** at the B3LYP/6-31+G* level of theory.

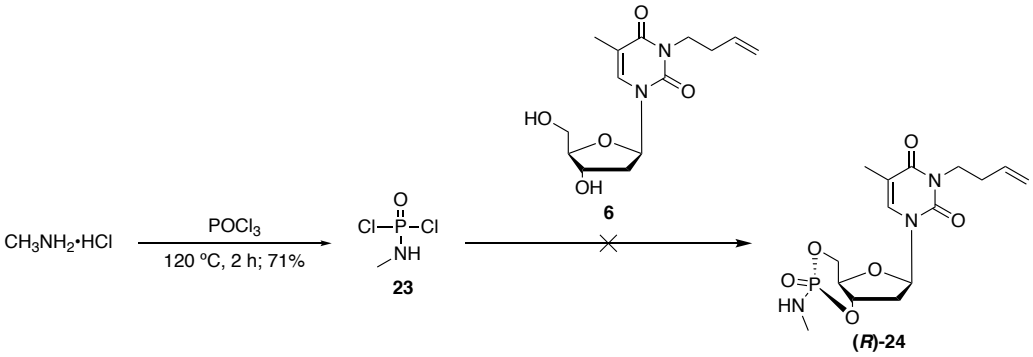

Figure 4.4. Attempted cyclization of **6** with the less steric hindered *N*-methylphosphoramic dichloride **23**.

Synthesis of natural thymidine-based polyphosphoester **20** requires a selective protection–deprotection scheme, to allow for the selective N^3-protection and selective deprotection under conditions that do not degrade the polymer backbone. Initial attempts to selectively install *tert*-butyloxycarbonyl (Boc) protecting group at the N^3-position of thymidine were unsuccessful. Despite the large pK_a difference between 3′-OH, 5′-OH and N^3-positions, installation of Boc protecting group was observed at all three positions, presumably due to the high reactivity of the reagent, Boc_2O.

The condition screening to achieve 3′,5′-bicyclic thymidine **(*R*)-25** in one step without any N^3-protection was then conducted (Figure 4.5). Our previous attempts to cyclize **6** with ethyl dichlorophosphate (Table 2.2) concluded that a polar solvent like DMF preferred oligomerization over cyclization. Therefore, in order to cyclize thymidine and meanwhile provide optimal solubility, a combination of polar and non-polar solvents is necessary. The screening of the solvent system, including the use of DMF, THF, acetone, ethyl acetate, dichloromethane, and hexanes, suggested that we were able to obtain 3′,5′-bicyclic thymidine **(*R*)-25** by using a combination of dichloromethane and DMF. Direct polymerization from **(*R*)-25** to **20** was not observed, presumably due to deactivation of the basic organocatalyst (TBD) by the acidic N–H. Boc was successfully installed on **(*R*)-25** without the presence of free hydroxyl functionality, to prepare the 3′,5′-bicyclic monomer **(*R*)-26**. ROP and acidic deprotection were attempted in one-pot to give natural thymidine-based polyphosphoester **20** (Figure 4.6). Compared to the butenylated **PCBT**, **20** was found to be water-soluble (10.61 ± 0.91 mg/mL). This initial effort to obtain a water-soluble polyphosphoester allows us to further expand the scope of our thymidine-derived polyphosphoesters into biomedical applications without the involvement of poly(ethylene glycol).

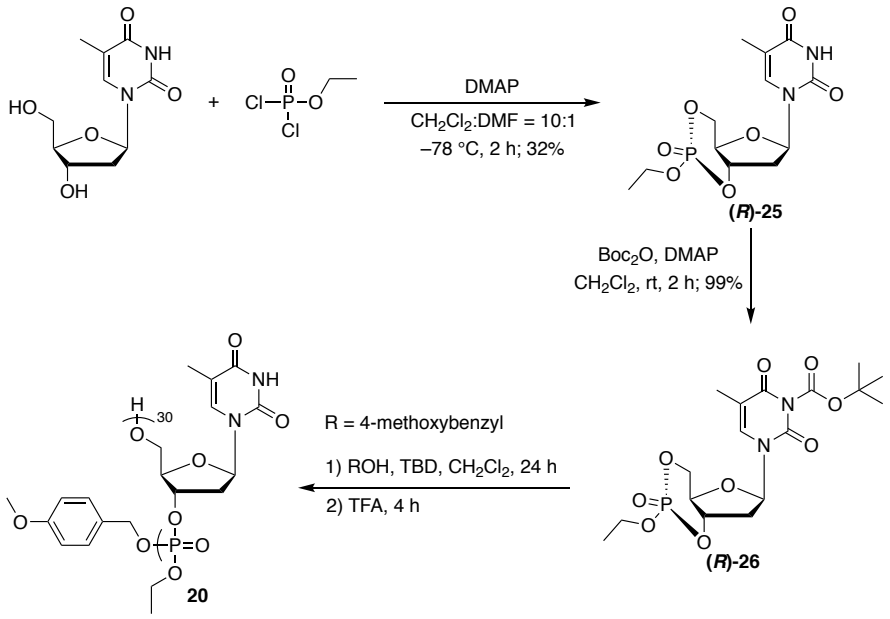

Figure 4.5. Synthetic approach to natural thymidine-based polyphosphoester **20**.

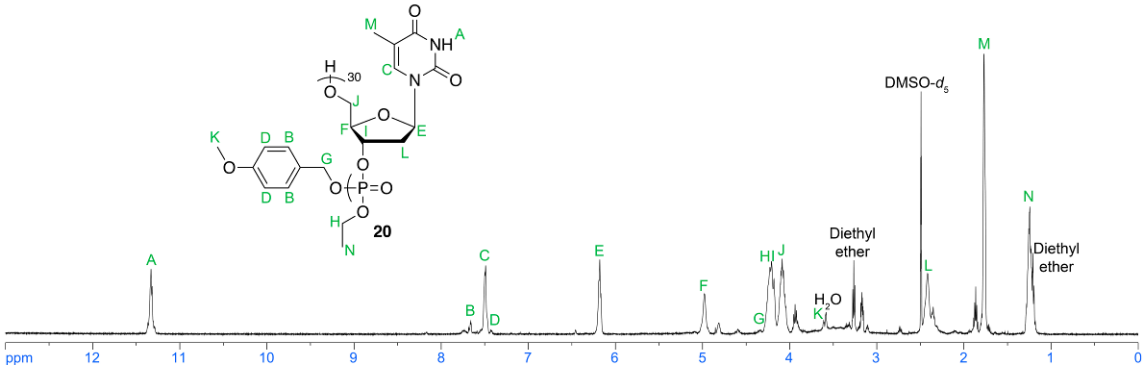

Figure 4.6. ^{1}H NMR (500 MHz; DMSO-d_6) spectrum of **20**.

4.3 Experimental Section

4.3.1 Materials

Thymidine and 4-dimethylaminopyridine (DMAP) were used as received from Chem-Impex International, Inc. (Wood Dale, IL). TBD was used as received from TCI America (Portland, OR). *N*,*N*-Dimethylphosphoramidodichloridate was used as received from Alfa Aesar (Ward Hill, MA). *N*,*N*-Dimethylformamide (DMF, ACS grade), hexanes (ACS grade), ethyl acetate (ACS grade), dichloromethane (ACS grade), and acetone (ACS grade) were used as received from VWR International. Anhydrous solvents were obtained after passage through a drying column of a solvent purification system from JC Meyer Solvent Systems (Laguna Beach, CA). All other chemicals were purchased from Sigma-Aldrich (St. Louis, MO) and used without further purification unless otherwise noted.

4.3.2 Instrumentation

^{1}H, ^{13}C, and ^{31}P NMR spectra were recorded on a Varian 500 spectrometer interfaced to a Linux computer using VNMR-J software. ^{1}H–^{31}P HMBC experiments were performed on a Varian 500 spectrometer interfaced to a Linux computer using VNMR-J software with $^{n}J_{HP}$ = 8 Hz. All NMR experiments were performed at ambient

temperature. Chemical shifts were referenced to the solvent residual signals. All ^{1}H NMR spectra are reported in parts per million (ppm) downfield of tetramethylsilane and were measured relative to the signals for residual $CHCl_3$ (7.26 ppm) or DMSO-d_5 (2.50 ppm). All ^{13}C NMR spectra are reported in ppm relative to $CDCl_3$ (77.0 ppm) or DMSO-d_6 (39.52 ppm), and were obtained with ^{1}H decoupling. For ^{31}P NMR spectroscopy, phosphoric acid (85 wt% in H_2O) at 0 ppm was used as an external standard. The splitting patterns are reported as s (singlet), d (doublet), t (triplet), q (quartet), quin (quintet), m (multiplet), and br (broad). Fourier transform infrared (FTIR) spectra were recorded on an IR Prestige 21 system using a diamond attenuated total reflectance (ATR) lens (Shimadzu Corp., Japan) and analyzed using IRsolution v.1.40 software.

4.3.3 Synthesis

Synthesis of 3′,5′-bicyclic 3-(3-butenyl) thymidine *N*,*N*-dimethylphosphoramidate (**(*R*)-21**). In a 50-mL two-neck round-bottom flask equipped with a magnetic stir bar were placed 4-dimethylaminopyridine (1145.4 mg, 9.375 mmol, 2.221 equiv) and **6** (1250.9 mg, 4.221 mmol, 1 equiv) in 20.0 mL of dichloromethane at –78 °C. A solution of *N*,*N*-dimethylphosphoramidodichloridate (758.2 mg, 4.681 mmol, 1.109 equiv) in 5.0 mL of dichloromethane was injected *via* syringe in one portion. The reaction mixture was allowed to stir for 1 h while gradually warming up to ambient

temperature before it was washed with 5.0 mL of water, dried over magnesium sulfate, filtered, concentrated, and purified by silica gel column chromatography hexanes/acetone = 75:25 as eluent as eluent to give **(*R*)-21** with a yield of 11% (179.6 mg) as a white solid. ^{1}H NMR (500 MHz; $CDCl_3$) δ 6.97 (d, J = 1.2 Hz, 1H, H^A), 6.41 (dd, J = 8.8, 2.4 Hz, 1H, H^B), 5.80 (ddt, J = 17.1, 10.1, 7.0 Hz, 1H, H^C), 5.05 (dd, J = 17.1, 1.6 Hz, 1H, H^D), 5.01 (dd, J = 10.2, 1.7 Hz, 1H, H^E), 4.79–4.73 (m, 1H, H^F), 4.57–4.52 (m, 1H, H^G), 4.53–4.46 (m, 1H, H^H), 4.00 (td, J = 7.4, 3.9 Hz, 2H, H^I), 3.80–3.75 (m, 1H, H^J), 2.74 (d, J = 10.3 Hz, 6H, H^K), 2.56 (ddd, J = 13.5, 10.7, 8.9 Hz, 1H, H^L), 2.40–2.33 (m, 3H, H^M and H^N), 1.96 (d, J = 1.2 Hz, 3H, H^O); ^{13}C NMR (126 MHz; $CDCl_3$) δ 162.8, 150.6, 134.7, 132.4, 117.0, 111.6, 84.7, 76.1 (d, J = 4.3 Hz), 74.5 (d, J = 4.3 Hz), 68.3 (d, J = 7.4 Hz), 40.7, 36.2 (d, J = 5.0 Hz), 35.8 (d, J = 8.3 Hz), 31.9, 13.3; ^{31}P NMR (202 MHz; $CDCl_3$) δ 8.7. FTIR (cm^{-1}): 3113–2770, 1704, 1668, 1639, 1464, 1448, 1398, 1360, 1321, 1277, 1246, 1222, 1181, 1155, 1109, 1095, 1062, 998, 923, 869, 836, 790, 767, 716.

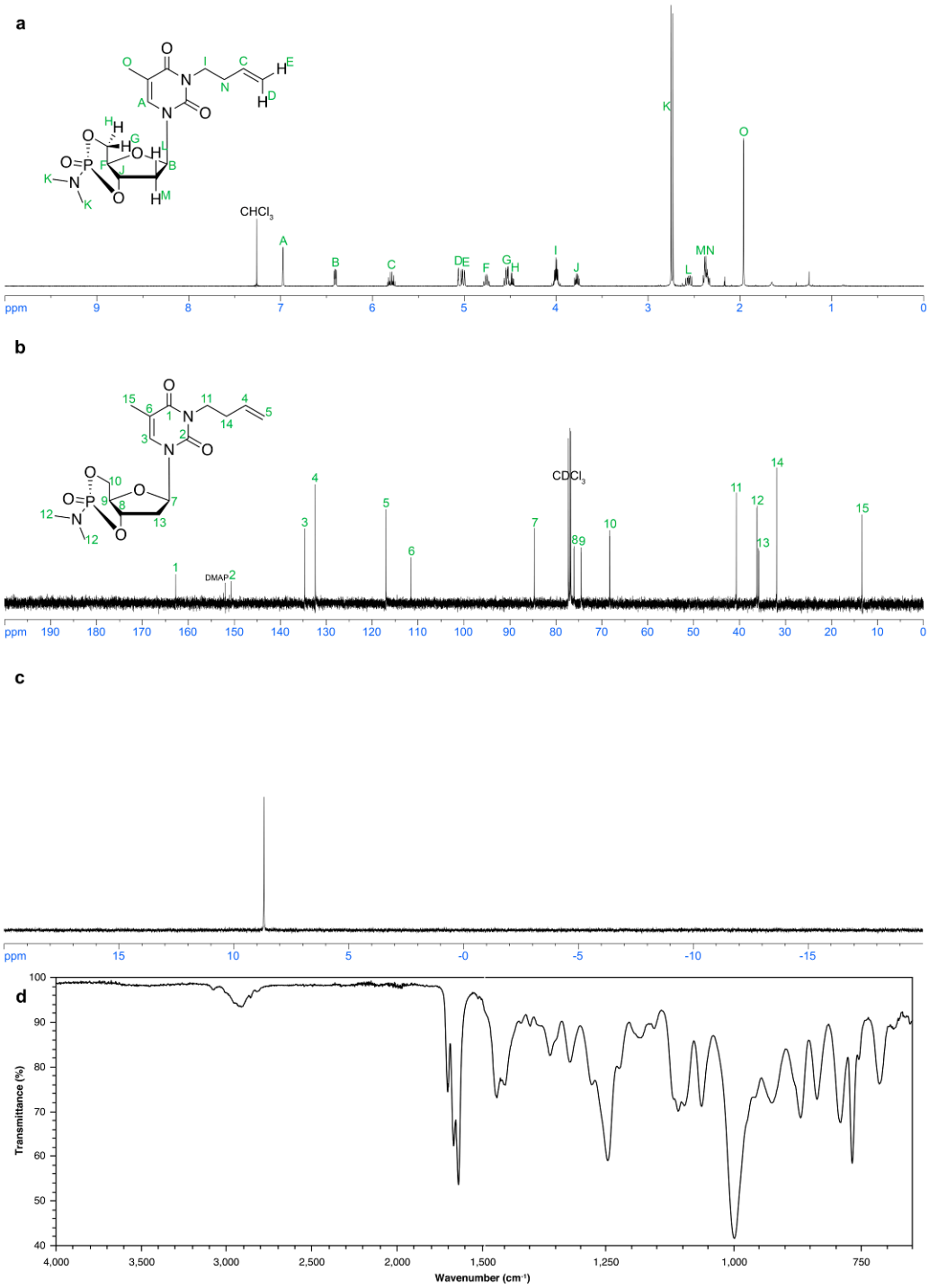

Figure 4.7. Spectroscopic characterization of ***(R)*-21**. (a) ^{1}H NMR (500 MHz; $CDCl_3$). (b) ^{13}C NMR (125 MHz; $CDCl_3$). (c) ^{31}P NMR (202 MHz; $CDCl_3$). (d) IR spectrum.

Synthesis of methylphosphoramidic dichloride (**23**). To a 25-mL round-bottom flask equipped with a magnetic stir bar were placed methylamine hydrochloride (6.2523 g, 92.60 mmol) in 15.0 mL of phosphoryl chloride. The reaction mixture was allowed to reflux at 120 °C for 2 days until the solid disappeared. Excess of phosphoryl chloride was removed under reduced pressure without heating, and **23** was collected by distillation (boiling point 65.0–68.0 °C at 500 mTorr) with a yield of 71% (9.7278 g) as a colorless oil. ^{1}H NMR (500 MHz; $CDCl_3$) δ 4.86–4.67 (br, 1H, H^A), 2.78 (dd, J = 19.3, 5.4 Hz, 3H, H^B); ^{13}C NMR (126 MHz; $CDCl_3$) δ 28.3 (d, J = 1.4 Hz), 31.9, 13.3; ^{31}P NMR (202 MHz; $CDCl_3$) δ 18.7.

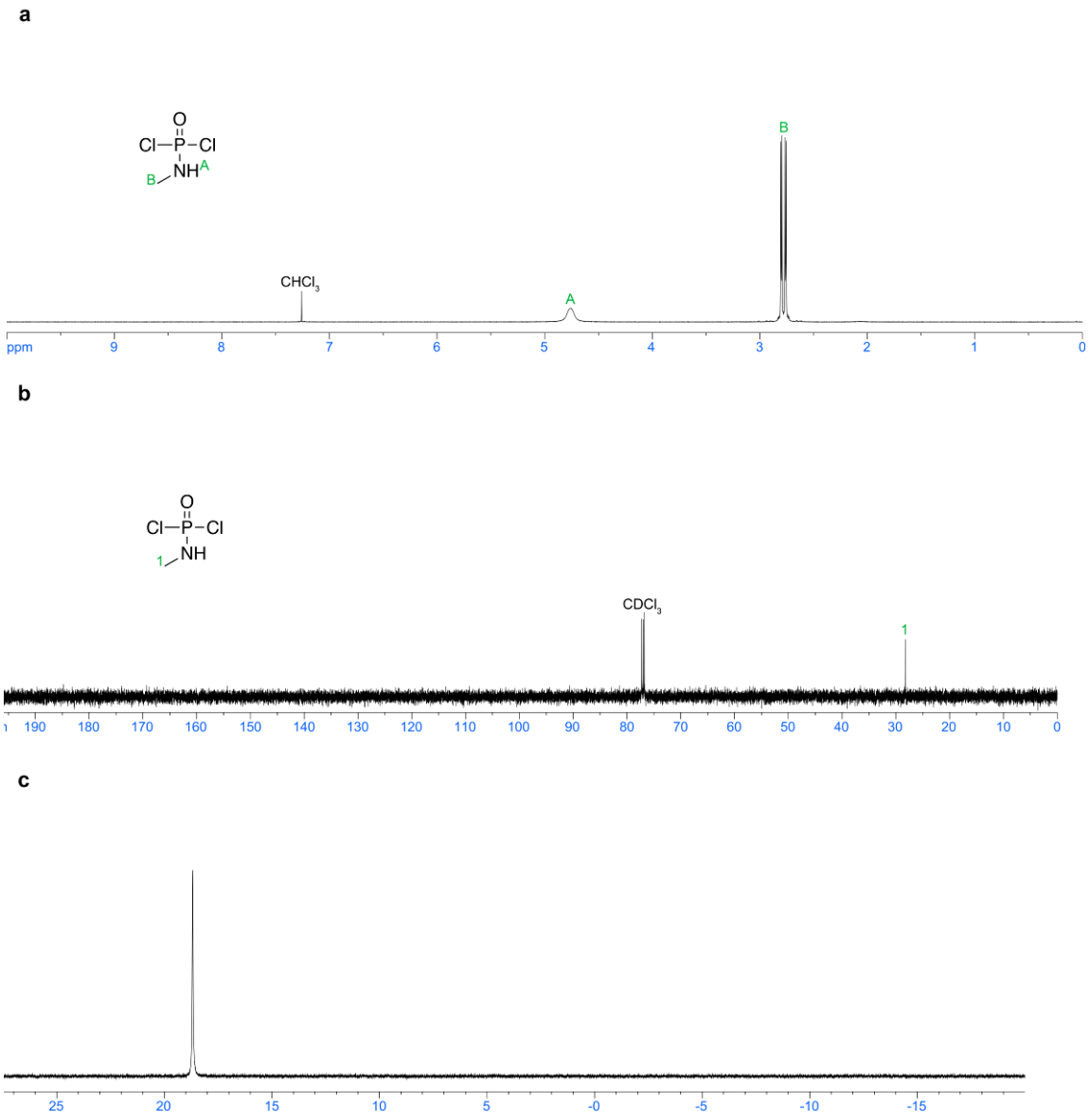

Figure 4.8. Spectroscopic characterization of **23**. (a) ^{1}H NMR (500 MHz; $CDCl_3$). (b) ^{13}C NMR (125 MHz; $CDCl_3$). (c) ^{31}P NMR (202 MHz; $CDCl_3$).

Synthesis of 3′,5′-bicyclic thymidine ethylphosphate (**(*R*)-25**). To a 250-mL two-neck round-bottom flask equipped with a magnetic stir bar were placed 4-dimethylaminopyridine (1929.0 mg, 15.79 mmol, 3.001 equiv) and thymidine (1274.3

mg, 5.261 mmol, 1 equiv) in a mixture of dichloromethane/DMF = 90 mL/9 mL at –78 °C. Ethyl dichlorophosphate (957.4 mg, 5.876 mmol, 1.117 equiv) was injected *via* syringe in one portion. The reaction mixture was allowed to stir for 1 h while gradually warming up to ambient temperature before it was washed with 5.0 mL of 1 N HCl, dried over magnesium sulfate, filtered, concentrated, and purified by silica gel column chromatography hexanes/acetone = 65:35 as eluent as eluent to give **(*R*)-25** with a yield of 31% (544.4 mg) as a white solid. ^{1}H NMR (500 MHz; $CDCl_3$) δ 8.87 (br, 1H, H^A), 7.01 (d, J = 1.3 Hz, 1H, H^B), 6.35 (dd, J = 8.9, 2.6 Hz, 1H, H^C), 4.89–4.84 (m, 1H, H^D), 4.62–4.49 (m, 2H, H^E), 4.25 (dq, J = 8.9, 7.1 Hz, 2H, H^F), 3.95–3.90 (m, 1H, H^G), 2.58 (ddd, J = 13.6, 10.4, 9.0 Hz, 1H, H^H), 2.45 (ddd, J = 13.6, 8.3, 2.6 Hz, 1H, H^I), 1.96 (d, J = 1.2 Hz, 3H, H^J), 1.38 (td, J = 7.1, 1.0 Hz, 3H, H^K); ^{13}C NMR (126 MHz; $CDCl_3$) δ 163.1, 149.9, 134.8, 112.5, 84.6, 76.8 (d, J = 3.7 Hz), 74.0 (d, J = 6.2 Hz), 68.9 (d, J = 7.4 Hz), 65.9 (d, J = 6.3 Hz), 35.4 (d, J = 8.5 Hz), 16.1 (d, J = 6.6 Hz), 12.6; ^{31}P NMR (202 MHz; $CDCl_3$) δ –3.5. FTIR (cm^{-1}): 3186, 3116–2769, 1674, 1466, 1373, 1273, 1265, 1165, 1095, 1010, 941, 887, 817, 756, 702, 655.

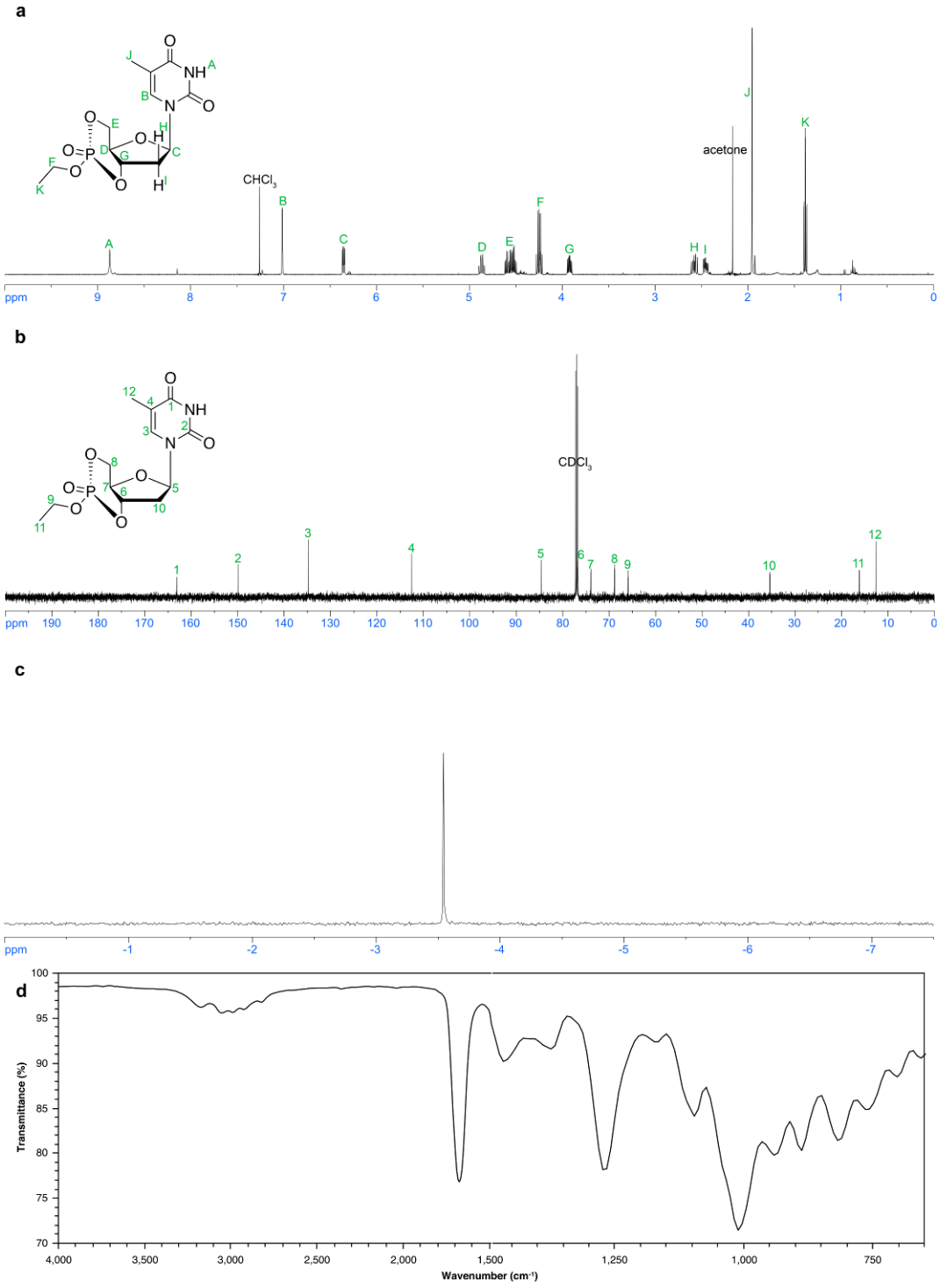

Figure 4.9. Spectroscopic characterization of **(*R*)-25**. (a) ^{1}H NMR (500 MHz; $CDCl_3$). (b) ^{13}C NMR (125 MHz; $CDCl_3$). (c) ^{31}P NMR (202 MHz; $CDCl_3$). (d) IR spectrum.

Synthesis of 3′,5′-bicyclic 3-(*tert*-butyloxycarbonyl) thymidine ethylphosphate (**(*R*)-26**). To a 25-mL round-bottom flask equipped with a magnetic stir bar were placed **(*R*)-25** (415.0 mg, 1.249 mmol, 1 equiv) and 4-dimethylaminopyridine (158.5 mg, 1.413 mmol, 1.131 equiv) in 10 mL of dichloromethane. Di-*tert*-butyl dicarbonate (568.6 mg, 2.605 mmol, 2.086 equiv) was added in one portion. The reaction mixture was allowed to stir for 2 h before it was washed with 5.0 mL of water, dried over magnesium sulfate, filtered, concentrated, and purified by silica gel column chromatography hexanes/acetone = 80:20 as eluent as eluent to give **(*R*)-26** with a yield of 99% (535.7 mg) as a white solid. ^{1}H NMR (500 MHz; $CDCl_3$) δ 6.96 (d, J = 1.3 Hz, 1H, H^A), 6.28 (dd, J = 8.7, 2.6 Hz, 1H, H^B), 4.83 (dd, J = 9.3, 0.9 Hz, 1H, H^C), 4.59 (ddd, J = 16.9, 9.8, 5.4 Hz, 1H, H^D), 4.51 (td, J = 10.1, 5.7 Hz, 1H, H^E), 4.25 (dq, J = 9.0, 7.1 Hz, 2H, H^F), 3.93 (ddd, J = 10.2, 9.5, 5.4 Hz, 1H, H^G), 2.58 (ddd, J = 13.6, 10.4, 8.8 Hz, 1H, H^H), 2.49 (ddd, J = 13.7, 8.2, 2.6 Hz, 1H, H^I), 1.97 (d, J = 1.2 Hz, 3H, H^J), 1.60 (s, 9H, H^K), 1.39 (td, J = 7.1, 1.0 Hz, 3H, H^L); ^{13}C NMR (126 MHz; $CDCl_3$) δ 160.8, 148.1, 147.4, 134.6, 111.9, 87.0, 85.0, 76.6 (d, J = 3.7 Hz), 73.9 (d, J = 6.6 Hz), 68.8 (d, J = 7.4 Hz), 65.7 (d, J = 6.2 Hz), 35.3 (d, J = 8.4 Hz), 27.3, 16.0 (d, J = 6.4 Hz), 12.4; ^{31}P NMR (202 MHz; $CDCl_3$) δ –4.0. FTIR (cm^{-1}): 3101–2816, 1782, 1712, 1666, 1442, 1373, 1365, 1273, 1265, 1141, 1103, 1010, 956, 879, 833, 771, 694.

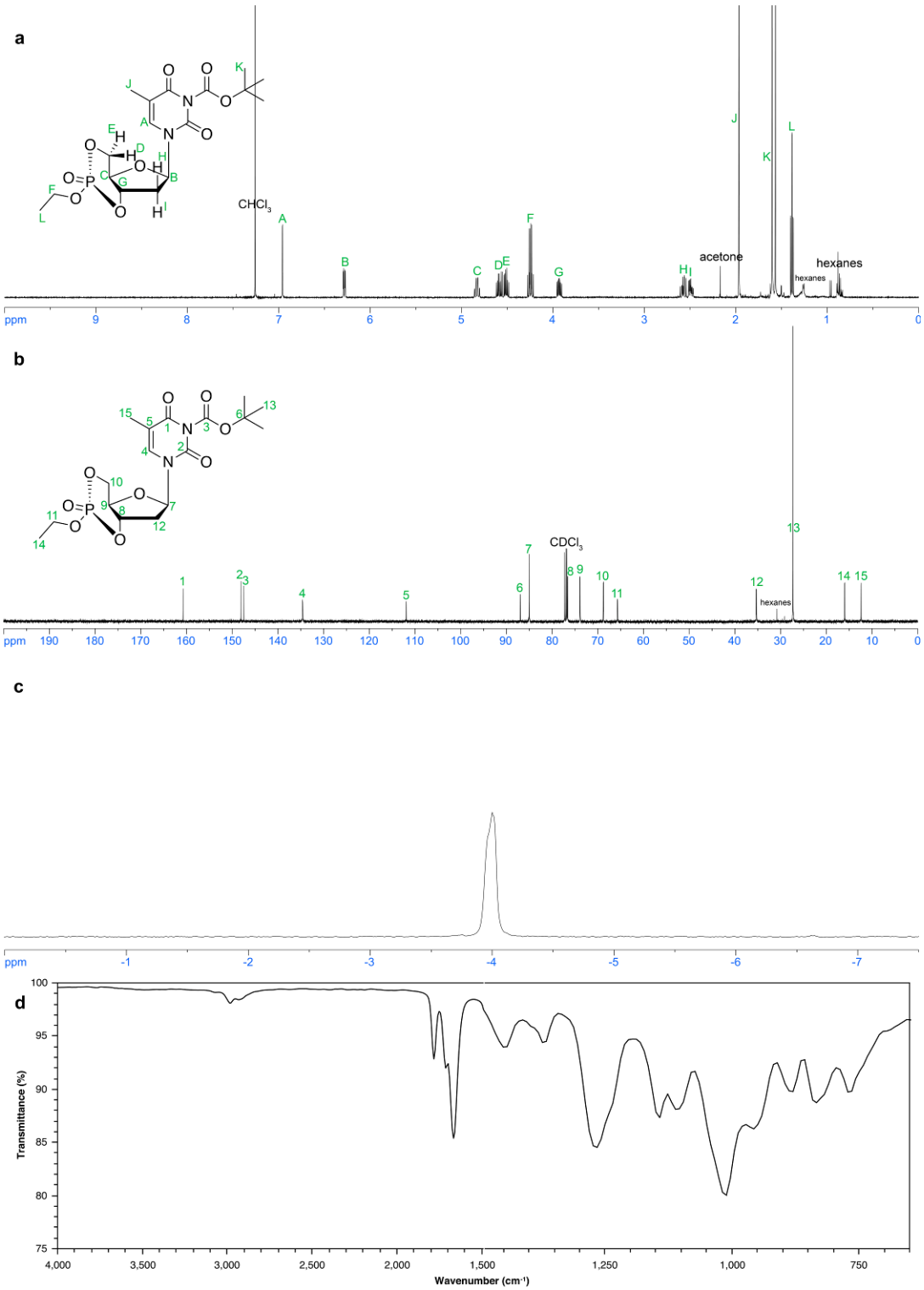

Figure 4.10. Spectroscopic characterization of **(*R*)-26**. (a) ^{1}H NMR (500 MHz; $CDCl_3$). (b) ^{13}C NMR (125 MHz; $CDCl_3$). (c) ^{31}P NMR (202 MHz; $CDCl_3$). (d) IR spectrum.

Synthesis of poly(3′,5′-bicyclic thymidine ethylphosphate) (**20**). A solution of **(*R*)-26** (65.2 mg, 0.151 mmol, 30.0 equiv) and 4-methoxybenzyl alcohol (0.6944 mg, 0.005026 mmol, 1 equiv) in anhydrous dichloromethane (0.90 mL) was transferred into a flame-dried 10-mL Schlenk flask equipped with a magnetic stir bar and a rubber septum on a dual-manifold Schlenk line. A solution of TBD (1.7 mg, 0.012 mmol, 2.4 equiv) in anhydrous dichloromethane (0.10 mL) was injected into the Schlenk flask *via* syringe to initiate the polymerization, while being maintained under a nitrogen gas atmosphere at ambient temperature. After stirring for 24 h, the reaction was quenched by addition of 0.5 mL of trifluoroacetic acid, and the reaction mixture was stirred for another 4 h. The poly(3′,5′-bicyclic thymidine ethylphosphate) (**20**) was purified by precipitation from dichloromethane into 30 mL of diethyl ether, and dried *in vacuo* to give a yield of 96% (48.2 mg). δ ^{1}H NMR (500 MHz; DMSO-d_6) δ 11.40–11.30 (br), 7.68–7.66 (br), 7.52–7.48 (br), 7.46–7.42 (br), 6.22–6.16 (br), 5.02–4.96 (br), 4.36–4.32 (br), 4.30–4.15 (br), 4.15–4.00 (br), 3.60–3.58 (br), 2.46–2.40 (br), 1.80–1.75 (br), 1.30–1.20 (br); ^{13}C NMR (126 MHz; DMSO-d_6) δ 163.6, 150.4, 135.9, 110.1, 84.1, 66.4, 64.3, 46.3, 37.6, 20.3, 15.9, 12.0; ^{31}P NMR (202 MHz; DMSO-d_6) δ –0.6, –1.4, –1.5, –1.6, –2.6. FTIR (cm^{-1}): 3657–2708, 1689, 1465, 1373, 1265, 1195, 1110, 1010, 894, 833, 763, 717.

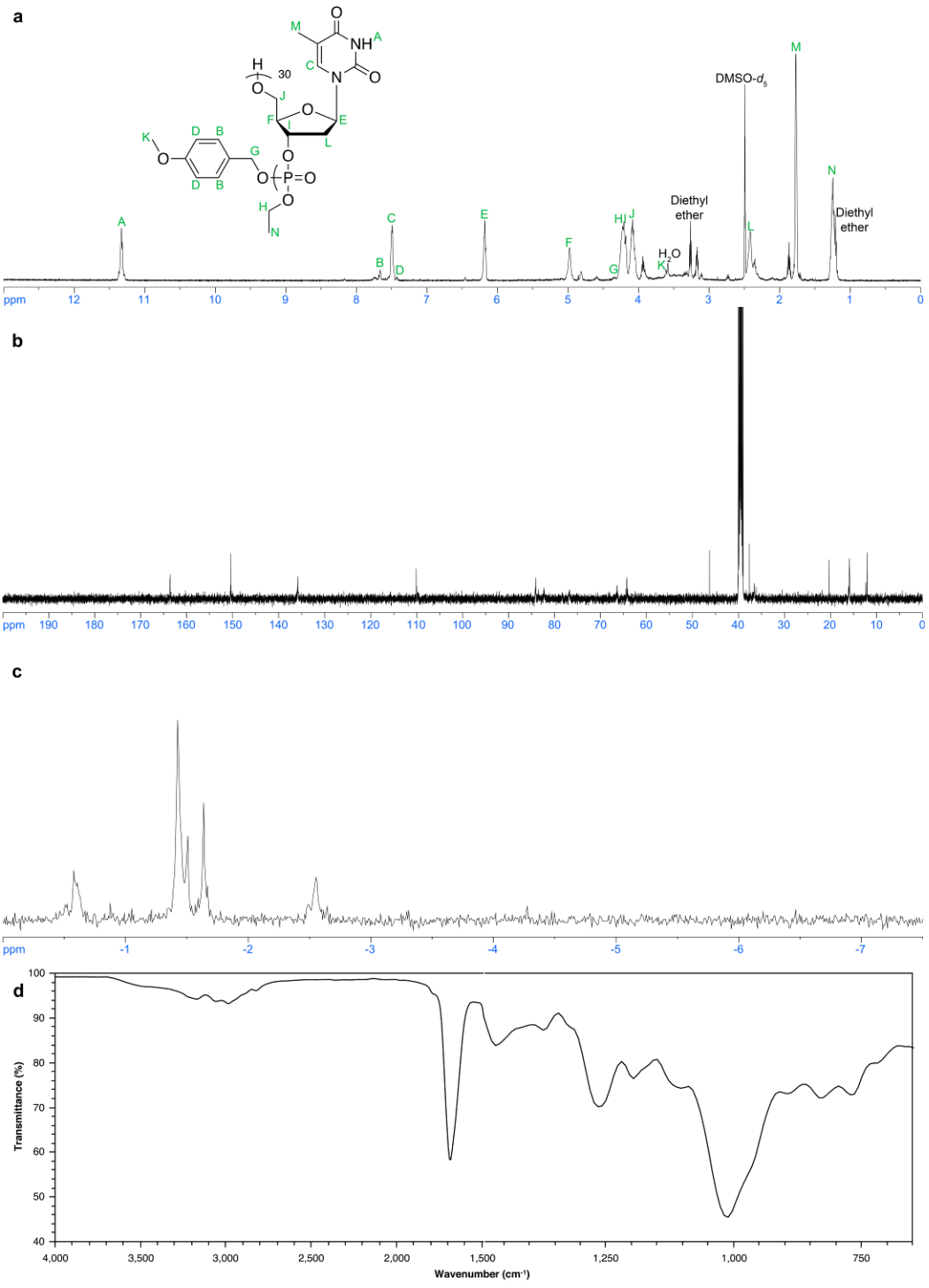

Figure 4.11. Spectroscopic characterization of **20**. (a) ^{1}H NMR (500 MHz; DMSO-d_6). (b) ^{13}C NMR (125 MHz; DMSO-d_6). (c) ^{31}P NMR (202 MHz; DMSO-d_6). (d) IR spectrum.

4.4 Conclusions

In summary, we have established the synthesis of water-soluble, natural thymidine-based polyphosphoester **20**. The monomer synthesis was achieved by the direct cyclization of thymidine with ethyl dichlorophosphate, followed by the N^3-Boc protection. The ROP of **(*R*)-26** and acidic deprotection were attempted in one-pot to give the natural thymidine-based polyphosphoester **20**, which was found to be water-soluble (10.61 ± 0.91 mg/mL).

The future outlook in the water-soluble, natural thymidine-based polyphosphoester should include the hybridization with poly(deoxy)adenosine. We will be able to use agarose gel electrophoresis to analyze the base paring behavior between **20** and poly(deoxy)adenosine. It is known that the polyadenosine tail is added to a messenger RNA to increase the stability of the molecule in eukaryotes.[136] The strong A–T base pair from **20** would destabilize RNA by interfering with the polyadenosine tail. We anticipate to see differences in cytotoxicity from **20** and **PCBT** based on their capability differences in hydrogen bonding and RNA destabilizing.

CHAPTER V

CONCLUSIONS AND FUTURE WORK

5.1 Conclusions

This dissertation has presented the design, synthesis and characterization of novel thymidine-derived polyphosphoesters toward biomedical applications. The nucleobase thymidine was selected as the starting material in this work, from which the corresponding six-membered 3′,5′-bicyclic monomer was prepared with an alkene functionality amenable to post-polymerization modification *via* click chemistry. This work has laid a foundation for synthetic non-natural DNA-mimicking polymers *via* ROP of six-membered 3′,5′-bicyclic phosphoesters with tunable properties.

In Chapter II, we described the development and successful implementation of a synthetic strategy to achieve thymidine-derived polyphosphoester by the ROP of a fused six-membered 3′,5′-bicyclic monomer. Theoretical DFT calculations corroborated our hypothesis that the higher ring strain energy (6–7 kcal/mol) of the six-membered 3′,5′-bicyclic phosphotriester, relative to the unsubstituted, non-strained six-membered cyclic phosphoester, would promote ROP. Experimentally, thymidine was functionalized at the N^3-position, and cyclized through the 3′- and 5′-positions *via* kinetically controlled cyclization at –78 °C to provide the thermodynamically unstable, strained six-membered cyclic phosphotriester (*R*)-monomers as major product, for which the TBD-catalyzed polymerization kinetics were explored with 4-methoxybenzyl alcohol as the initiator.

Selective ROP of the more strained (*R*)-monomer over (*S*)-monomer was successfully demonstrated. All the ROPs proceeded in a controlled manner ($Đ < 1.10$) with different monomer-to-initiator ratios to yield polyphosphoester DNA analogues with molar masses ranging from 3.9–12.4 kDa from end-group analysis by NMR. These results present a novel and reliable synthetic methodology to obtain functional DNA analogues with unique properties.

Chapter III focused on investigation of regioisomeric preference in ROP of 3′,5′-bicyclic phosphoesters derived from thymidine, to gain a deeper understanding of the polymerization behavior. From the synthesis of model compounds, we concluded that the three ^{31}P NMR resonance signals of **PCBT** can be attributed to 3′,3′-, 5′,5′- and 3′,5′-linkages, which enabled us to determine the relative amount of each of these linkages in the polymers. Further model initiation reactions revealed that the preferential cleavage of P–O3′ *vs.* P–O5′ can be tuned by the steric hindrance of the alcohol initiators. DFT calculations successfully demonstrated the energy differences of the transition states between the P–O3′ and P–O5′ cleavages decreased, when a more steric hindered initiator was used, and therefore the product distribution changed to favor P–O5′ cleavages with decreasing initiator steric effect. The ring opening of the six-membered 3′,5′-bicyclic phosphotriester thymidine analogues presented in this dissertation, although meant to mimic DNA, preferably polymerized in the 3′-to-5′ direction, as opposed to the 5′-to-3′ polymerization of DNA in Nature. It is worth noting that both systems generate polymers with a majority of 3′,5′-linkages (head-to-tail configurations). These studies provide a fundamental understanding of the ROP of six-membered 3′,5′-bicyclic

phosphoesters, and broaden the scope of designing different DNA analogues, which is anticipated to guide the synthesis of future DNA analogues, functional polyphosphoesters, and degradable polymers synthesized by ROP.

Chapter IV described the development of water-soluble, natural thymidine-based polyphosphoesters. With the direct cyclization of thymidine, the installation of the Boc protecting group was realized without the side reaction at 3′- and 5′-OH. The protection of the acidic N–H allows for the TBD-catalyzed ROP, to prepare the natural thymidine-based polyphosphoesters that are soluble in water. These results provide an outlook to the synthetic DNA-mimicking polymers that preserve natural nucleobases, and therefore introduce the possibility of future investigation utilizing the base-pairing behavior.

5.2 Future Work

Given the novel thymidine-derived polyphosphoesters toward biomedical applications presented in this dissertation, future work should also include the development of polymers based on deoxyadenosine, deoxycytidine, and deoxyguanosine. The incorporation of nucleosides besides thymidine will allow for the investigation of hybridization-driven supramolecular assemblies, as well as hydrogels that are biologically responsive. Synthetic challenges including the solubility of these nucleosides in organic solvent, in order to achieve 3′,5′-bicyclic monomers with or without protection of the nucleobases, will need to be overcome by thorough condition

screenings. Natural systems may be able to recognize these synthetic, non-natural DNA-mimicking polymers, but with synthetic chemistry, the incorporation of other functionalities to gain control over geometry, morphology, degradation, *etc.*, will allow scientists to create synthetic DNA polymers that have known degradation kinetics different from natural DNA while also carrying other functional features or capabilities that could be beneficial in terms of drug delivery, sensing, or other applications.

Chapter IV described the development of water-soluble, thymidine-based polyphosphoesters *via* deprotection at the N^3-position, to generate polyphosphoesters with hydrogen bond-capable, natural thymidine units. However, our initial attempt to achieve phosphodiester **19** did not yield the expected product. Therefore, it is necessary to screen conditions to enable the cyclization of N^3-butenyl thymidine **6** with *N*-methylphosphoramic dichloride **23**. This cyclization product is expected to undergo hydrolytic degradation *via* cleavage of the acid-labile phosphoramidate to give the desired phosphodiester **20**. If the cyclization remains unsuccessful, an alternative route of cyclization involving a phosphorus(III) species[48] is suggested (Figure 5.1).

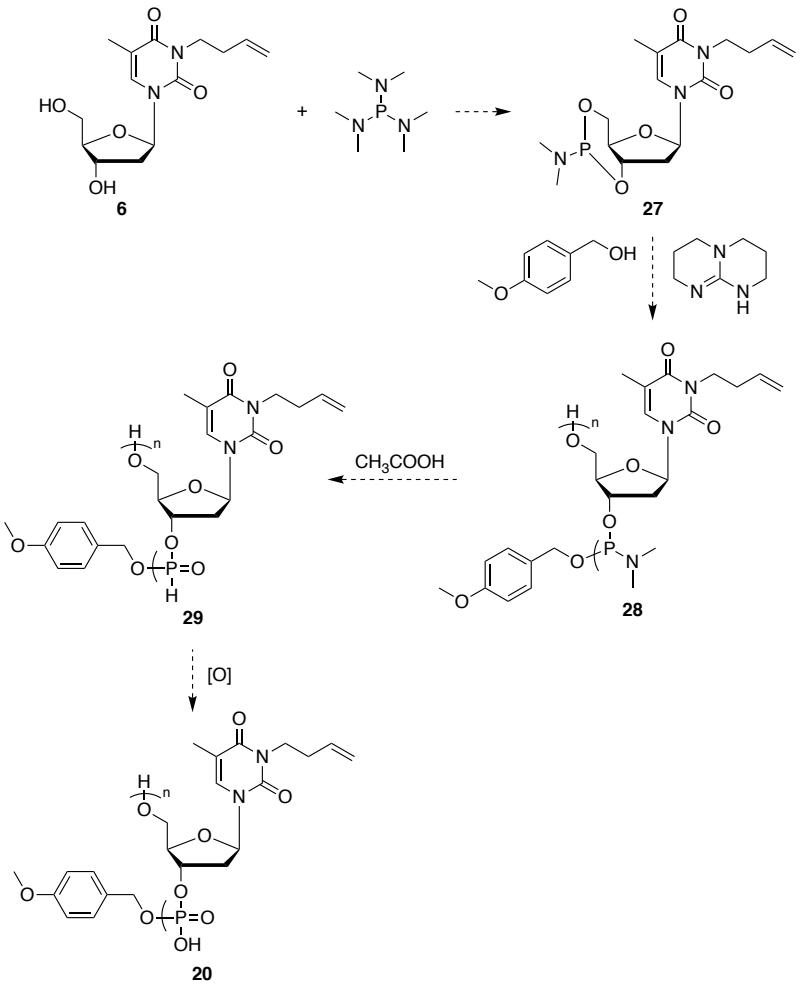

Figure 5.1. An alternative route to synthesize thymidine-based phosphodiester **20** involving a phosphorus(III) species.

Enzymatic degradation of the thymidine-based polyphosphoesters **PCBT** and **20** are of interest due to the structural similarity to DNA. It is known that polymers with repeating phosphoester bonds in the backbone are biodegradable through hydrolysis and possibly through enzymatic digestion (*e.g.*, by nucleases such as phosphodiesterase I and alkaline phosphatase) under physiological conditions.[11,129,130] Therefore, with our development of water-soluble polymer **20** discussed in Chapter IV, it is expected that

future work will include a study on hydrolytic and enzymatic degradation. This study will be useful in developing a better understanding of the degradation kinetics and the structural requirements for polyphosphoester substrates to bind various enzymes.

Amphiphilic block polymers, which contain both hydrophilic and hydrophobic parts, are capable of self-assembly in water to form a variety of well-defined nanostructures, such as spherical and cylindrical/worm-like micelles, vesicles, disks, and toroids.[137-145] The development of new building blocks and creation of diversified supramolecular nanostructures has always been one of the most important efforts in the area of self-assembly.[143] With the extension from thymidine to other nucleosides, our DNA-based polyphosphoesters are expected to be amenable to synthesis and post-polymerization modification to afford hydrophobic or hydrophilic segments. While hydrogen bond interactions provide additional stabilization to the self-assembly structures as supra-amphiphiles, incorporation of nucleoside-containing polyphosphoesters has not yet been explored in this context, and is expected to enrich the family of conventional covalent amphiphiles by bridging the gap between material sciences and life sciences.

Studies presented in Chapters II and III provided fundamental understanding of the synthesis of monomer **(*R*)-5** and its polymerization behavior to obtain **PCBT**. From this point, there is potential for **PCBT** to be used in a variety of applications by functionalizing the N^3-butenyl group using thiol–ene click chemistry.[146,147] For example, **PCBT** can be funcationalized thiol–ene chemistry with cysteamine hydrochloride, 3-mercaptopropionic acid, and L-cysteine hydrochloride to generate cationic, anionic, and

zwitterionic side chains, respectively. These polymers are expected to exhibit different self-assembly behaviors compared to **PCBT**, and detailed physicochemical and biological studies of the polymeric micelles with different surface properties will be conducted to understand the effect of surface chemistry on their behavior. The Wooley group has performed extensive studies involving the click chemistry to install drugs and other funcational molecules onto polyphosphoesters for use of these constructs as drug-delivery vehicles.[24-26,148] With our thymidine-based polyphosphoesters, we anticipate that a similar approach can be applied, while eliminating the potential cytotoxicity from ethylene glycol as a degradation product.

Ribonucleosides are also of interest for the development of degradable polyphosphoesters, as the 2′-OH provides an extra hydrolytic degradation pathway in RNA. There are some advantages of RNA-mimicking materials over DNA, including single-stranded enzymatic stability,[149] capability of forming hyperbranched polymers, and more choices of functionalization position. Similar cyclization strategy can be applied to acquire 3′,5′-bicyclic monomer **31** and 2′,3′-bicyclic monomer **32**, for which the branched networks are possible (Figure 5.2). It is well-known that Flory first hypothesized the concept of highly branched polymers in 1952,[150] but no attention had been paid to hyperbranched polyphosphoesters until Liu *et al.* reported the first synthesis in 2009[151] with the approach of self-condensing ROP.[152,153] Hyperbranched polymer provides not only simple preparation over dendrimers, but also a unique opportunity for further functionalization due to a great number of terminal hydroxyl groups in this biocompatible and biodegradable hyperbranched polyphosphoester. This advance

including RNA into the synthetic polyphosphoester by ROP will be considered foundational work in the development and characterization of a new type of biocompatible and functional polymer.

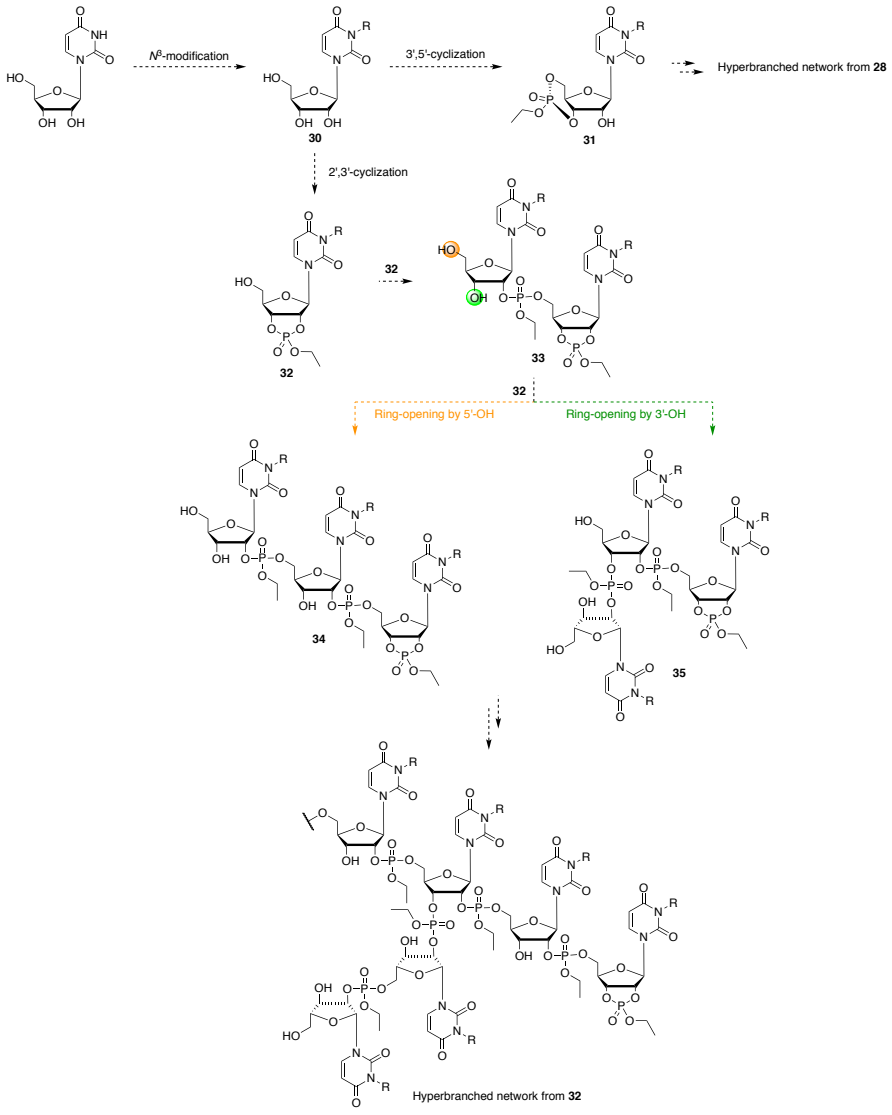

Figure 5.2. Formation of hyperbranched networks from the 3′,5′- and 2′,3′-bicyclic N^3-functionalized deoxyuridine. Illustration here only shows the complete reaction route to hyperbranched polymers from **32**.

Although many nucleobase-containing polymers have been synthesized and applied in polymer science, the number of known nucleobase-containing polymers remains limited. The importance of applying synthetic DNA/RNA at will is touted, but to enable the broader implementation of nucleobases in polymer science, three future directions for nucleobase-containing polymers are suggested. Firstly, there is still a monumental need to develop new nucleobase-containing polymers. Secondly, the development of novel synthetic approaches for nucleobase-containing polymers remains another critical need. Gaining control of the sequence of these polymers would enable synthetic materials that emulate the sequence-dependent behaviors observed in Nature. Finally, with further advances in polymer chemistry, innovative materials will be designed from nucleobase-containing polymers, which could provide the sequence-controlled features for these "smart" materials in wide ranges of applications.

REFERENCES

(1) Nair, L. S.; Laurencin, C. T. *Prog. Polym. Sci.* **2007**, *32*, 762–798.

(2) Ulery, B. D.; Nair, L. S.; Laurencin, C. T. *J Polym Sci B Polym Phys* **2011**, *49*, 832–864.

(3) Manavitehrani, I.; Fathi, A.; Badr, H.; Daly, S.; Negahi Shirazi, A.; Dehghani, F. *Polymers* **2016**, *8*, 20.

(4) Xu, J.; Feng, E.; Song, J. *J. Appl. Polym. Sci.* **2014**, *131*, 39822.

(5) Wen, J.; Kim, G. J. A.; Leong, K. W. *J. Control. Release* **2003**, *92*, 39–48.

(6) Zhao, Z.; Wang, J.; Mao, H. Q.; Leong, K. W. *Adv. Drug Deliv. Rev.* **2003**, *55*, 483–499.

(7) Huang, S.-W.; Wang, J.; Zhang, P.-C.; Mao, H.-Q.; Zhuo, R.-X.; Leong, K. W. *Biomacromolecules* **2004**, *5*, 306–311.

(8) Wen, J.; Mao, H.-Q.; Li, W.; Lin, K. Y.; Leong, K. W. *J. Pharm. Sci.* **2004**, *93*, 2142–2157.

(9) Song, W.-J.; Du, J.-Z.; Liu, N.-J.; Dou, S.; Cheng, J.; Wang, J. *Macromolecules* **2008**, *41*, 6935–6941.

(10) Wang, Y.-C.; Tang, L.-Y.; Li, Y.; Wang, J. *Biomacromolecules* **2009**, *10*, 66–73.

(11) Xiong, M.-H.; Wu, J.; Wang, Y.-C.; Li, L.-S.; Liu, X.-B.; Zhang, G.-Z.; Yan, L.-F.; Wang, J. *Macromolecules* **2009**, *42*, 893–896.

(12) Yang, X.-Z.; Sun, T.-M.; Dou, S.; Wu, J.; Wang, Y.-C.; Wang, J. *Biomacromolecules* **2009**, *10*, 2213–2220.

(13) Wang, Y.-C.; Yuan, Y.-Y.; Du, J.-Z.; Yang, X.-Z.; Wang, J. *Macromol. Biosci.* **2009**, *9*, 1154–1164.

(14) Iwasaki, Y.; Yamaguchi, E. *Macromolecules* **2010**, *43*, 2664–2666.

(15) Troev, K. D. *Polyphosphoesters*; Elsevier, 2012.

(16) Zhang, S.; Li, A.; Zou, J.; Lin, L. Y.; Wooley, K. L. *ACS Macro Lett.* **2012**, *1*, 328–333.

(17) Clément, B.; Grignard, B.; Koole, L.; Jérôme, C.; Lecomte, P. *Macromolecules* **2012**, *45*, 4476–4486.

(18) Zhang, S.; Zou, J.; Zhang, F.; Elsabahy, M.; Felder, S. E.; Zhu, J.; Pochan, D. J.; Wooley, K. L. *J. Am. Chem. Soc.* **2012**, *134*, 18467–18474.

(19) Elsabahy, M.; Zhang, S.; Zhang, F.; Deng, Z. J.; Lim, Y. H.; Wang, H.; Parsamian, P.; Hammond, P. T.; Wooley, K. L. *Sci. Rep.* **2013**, *3*, 3313–3313.

(20) Zhang, S.; Wang, H.; Shen, Y.; Zhang, F.; Seetho, K.; Zou, J.; Taylor, J.-S. A.; Dove, A. P.; Wooley, K. L. *Macromolecules* **2013**, *46*, 5141–5149.

(21) Lim, Y. H.; Heo, G. S.; Cho, S.; Wooley, K. L. *ACS Macro Lett.* **2013**, *2*, 785–789.

(22) Shen, Y.; Zhang, S.; Zhang, F.; Loftis, A.; Pavía-Sanders, A.; Zou, J.; Fan, J.; Taylor, J.-S. A.; Wooley, K. L. *Adv. Mater.* **2013**, *25*, 5609–5614.

(23) Sun, C.-Y.; Dou, S.; Du, J.-Z.; Yang, X.-Z.; Li, Y.-P.; Wang, J. *Adv. Healthc. Mater.* **2014**, *3*, 261–272.

(24) Zou, J.; Zhang, F.; Zhang, S.; Pollack, S. F.; Elsabahy, M.; Fan, J.; Wooley, K. L. *Adv. Healthc. Mater.* **2014**, *3*, 441–448.

(25) Zhang, F.; Smolen, J. A.; Zhang, S.; Li, R.; Shah, P. N.; Cho, S.; Wang, H.; Raymond, J. E.; Cannon, C. L.; Wooley, K. L. *Nanoscale* **2015**, *7*, 2265–2270.

(26) Zhang, F.; Zhang, S.; Pollack, S. F.; Li, R.; Gonzalez, A. M.; Fan, J.; Zou, J.; Leininger, S. E.; Pavía-Sanders, A.; Johnson, R.; Nelson, L. D.; Raymond, J. E.; Elsabahy, M.; Hughes, D. M. P.; Lenox, M. W.; Gustafson, T. P.; Wooley, K. L. *J. Am. Chem. Soc.* **2015**, *137*, 2056–2066.

(27) Lim, Y. H.; Tiemann, K. M.; Heo, G. S.; Wagers, P. O.; Rezenom, Y. H.; Zhang, S.; Zhang, F.; Youngs, W. J.; Hunstad, D. A.; Wooley, K. L. *ACS Nano* **2015**, *9*, 1995–2008.

(28) Aweda, T. A.; Zhang, S.; Mupanomunda, C.; Burkemper, J.; Heo, G. S.; Bandara, N.; Lin, M.; Cutler, C. S.; Cannon, C. L.; Youngs, W. J.; Wooley, K. L.; Lapi, S. E. *J. Labelled Comp. Radiopharm.* **2015**, *58*, 234–241.

(29) Kootala, S.; Tokunaga, M.; Hilborn, J.; Iwasaki, Y. *Macromol. Biosci.* **2015**, *15*, 1634–1640.

(30) Ma, Y.-C.; Wang, J.-X.; Tao, W.; Sun, C.-Y.; Wang, Y.-C.; Li, D.-D.; Fan, F.; Qian, H.-S.; Yang, X.-Z. *ACS Appl. Mater. Interfaces* **2015**, *7*, 26315–26325.

(31) Yilmaz, Z. E.; Jérôme, C. *Macromol. Biosci.* **2016**, *16*, 1745–1761.

(32) Henke, H.; Brüggemann, O.; Teasdale, I. *Macromol. Rapid Commun.* **2017**, *38*, 1600644.

(33) Busch, H.; Majumder, S.; Reiter, G.; Mecking, S. *Macromolecules* **2017**, *50*, 2706–2713.

(34) Tsao, Y.-Y. T.; Wooley, K. L. *J. Am. Chem. Soc.* **2017**, *139*, 5467–5473.

(35) Appukutti, N.; Serpell, C. J. *Polym. Chem.* **2018**, *9*, 2210–2226.

(36) Zhang, Y.; Ma, C.; Zhang, S.; Wei, C.; Xu, Y.; Lu, W. *Materials Today Chemistry* **2018**, *9*, 34–42.

(37) Richards, M.; Dahiyat, B. I.; Arm, D. M.; Lin, S.; Leong, K. W. *J. Polym. Sci. A Polym. Chem.* **1991**, *29*, 1157–1165.

(38) Branham, K. E.; Mays, J. W.; Gray, G. M.; Bharara, P. C.; Byrd, H.; Bittinger, R.; Farmer, B. *Polymer* **2000**, *41*, 3371–3379.

(39) Pretula, J.; Kaluzynski, K.; Szymanski, R.; Penczek, S. *J. Polym. Sci. A Polym. Chem.* **1999**, *37*, 1365–1381.

(40) Dustan Myrex, R.; Farmer, B.; Gray, G. M.; Wright, Y.-J.; Dees, J.; Bharara, P. C.; Byrd, H.; Branham, K. E. *Eur. Polym. J.* **2003**, *39*, 1105–1115.

(41) Wen, J.; Zhuo, R. X. *Macromol. Rapid Commun.* **1998**, *19*, 641–642.

(42) Libiszowski, J.; Kałużynski, K.; Penczek, S. *J. Polym. Sci. Polym. Chem. Ed.* **1978**, *16*, 1275–1283.

(43) Nykypanchuk, D.; Maye, M. M.; van der Lelie, D.; Gang, O. *Nature* **2008**, *451*, 549–552.

(44) Leunissen, M. E.; Dreyfus, R.; Sha, R.; Wang, T.; Seeman, N. C.; Pine, D. J.; Chaikin, P. M. *Soft Matter* **2009**, *5*, 2422–2430.

(45) Yang, H.; Xi, W. *Polymers* **2017**, *9*, 666.

(46) Kaluzynski, K.; Libisowski, J.; Penczek, S. *Macromolecules* **1976**, *9*, 365–367.

(47) Kaluzynski, K.; Penczek, S. *Makromol. Chem.* **1979**, *180*, 2289–2293.

(48) Lapienis, G.; Pretula, J.; Penczek, S. *Macromolecules* **1983**, *16*, 153–158.

(49) Kałużynski, K.; Libiszowski, J.; Penczek, S. *Makromol. Chem.* **1977**, *178*, 2943–2947.

(50) Łapienis, G.; Penczek, S. *J. Polym. Sci. Polym. Chem. Ed.* **1977**, *15*, 371–382.

(51) Vandenberg, E. J. *J. Polym. Sci. A Polym. Chem.* **1971**, *9*, 2451–2468.

(52) Biela, T.; Klosinski, P.; Penczek, S. *J. Polym. Sci. A Polym. Chem.* **1989**, *27*, 763–774.

(53) Steinbach, T.; Schröder, R.; Ritz, S.; Wurm, F. R. *Polym. Chem.* **2013**, *4*, 4469–4479.

(54) Watson, J. D.; Crick, F. H. C. *Nature* **1953**, *171*, 737–738.

(55) Zuckermann, R.; Corey, D.; Schultz, P. *Nucleic Acids Res.* **1987**, *15*, 5305–5321.

(56) Karkare, S.; Bhatnagar, D. *Appl. Microbiol. Biotechnol.* **2006**, *71*, 575–586.

(57) Matsuda, S.; Fillo, J. D.; Henry, A. A.; Rai, P.; Wilkens, S. J.; Dwyer, T. J.; Geierstanger, B. H.; Wemmer, D. E.; Schultz, P. G.; Spraggon, G.; Romesberg, F. E. *J. Am. Chem. Soc.* **2007**, *129*, 10466–10473.

(58) Maruyama, H.; Furukawa, K.; Kamiya, H.; Minakawa, N.; Matsuda, A. *Chem. Commun.* **2015**, *51*, 7887–7890.

(59) Malyshev, D. A.; Romesberg, F. E. *Angew. Chem. Int. Ed.* **2015**, *54*, 11930–11944.

(60) Taylor, A. I.; Pinheiro, V. B.; Smola, M. J.; Morgunov, A. S.; Peak-Chew, S.; Cozens, C.; Weeks, K. M.; Herdewijn, P.; Holliger, P. *Nature* **2015**, *518*, 427–430.

(61) Anosova, I.; Kowal, E. A.; Dunn, M. R.; Chaput, J. C.; Van Horn, W. D.; Egli, M. *Nucleic Acids Res.* **2016**, *44*, 1007–1021.

(62) Horiya, S.; MacPherson, I. S.; Krauss, I. J. *Nat. Chem. Biol.* **2014**, *10*, 990–999.

(63) Friedman, A. D.; Kim, D.; Liu, R. *Biomaterials* **2015**, *36*, 110–123.

(64) Diafa, S.; Hollenstein, M. *Molecules* **2015**, *20*, 16643–16671.

(65) Ibach, J.; Dietrich, L.; Koopmans, K. R. M.; Nöbel, N.; Skoupi, M.; Brakmann, S. *J. Biotechnol.* **2013**, *167*, 287–295.

(66) Meyer, A. J.; Garry, D. J.; Hall, B.; Byrom, M. M.; McDonald, H. G.; Yang, X.; Yin, Y. W.; Ellington, A. D. *Nucleic Acids Res.* **2015**, *43*, 7480–7488.

(67) Hottin, A.; Marx, A. *Acc. Chem. Res.* **2016**, *49*, 418–427.

(68) Chen, T.; Hongdilokkul, N.; Liu, Z.; Adhikary, R.; Tsuen, S. S.; Romesberg, F. E. *Nat. Chem.* **2016**, *8*, 556–562.

(69) Michelson, A. M.; Todd, A. R. *J. Chem. Soc.* **1955**, 2632–2638.

(70) Devine, K. G.; Reese, C. B. *Tetrahedron Lett.* **1986**, *27*, 5529–5532.

(71) Letsinger, R. L.; Ogilvie, K. K.; Miller, P. S. *J. Am. Chem. Soc.* **1969**, *91*, 3360–3365.

(72) Beaucage, S. L.; Caruthers, M. H. *Tetrahedron Lett.* **1981**, *22*, 1859–1862.

(73) Roy, B.; Depaix, A.; Périgaud, C.; Peyrottes, S. *Chem. Rev.* **2016**, *116*, 7854–7897.

(74) Kondo, K.; Iwasaki, H.; Ueda, N.; Takemoto, K.; Imoto, M. *Makromol. Chem.* **1968**, *120*, 21–26.

(75) Akashi, M.; Kita, Y.; Inaki, Y.; Takemoto, K. *J. Polym. Sci. Polym. Chem. Ed.* **1979**, *17*, 301–312.

(76) Khan, A.; Haddleton, D. M.; Hannon, M. J.; Kukulj, D.; Marsh, A. *Macromolecules* **1999**, *32*, 6560–6564.

(77) Marsh, A.; Khan, A.; Haddleton, D. M.; Hannon, M. J. *Macromolecules* **1999**, *32*, 8725–8731.

(78) Spijker, H. J.; van Delft, F. L.; van Hest, J. C. M. *Macromolecules* **2007**, *40*, 12–18.

(79) McHale, R.; O'Reilly, R. K. *Macromolecules* **2012**, *45*, 7665–7675.

(80) Pradere, U.; Garnier-Amblard, E. C.; Coats, S. J.; Amblard, F.; Schinazi, R. F. *Chem. Rev.* **2014**, *114*, 9154–9218.

(81) Zhang, X.; Jones, G. O.; Hedrick, J. L.; Waymouth, R. M. *Nat. Chem.* **2016**, *8*, 1047–1053.

(82) Hong, M.; Chen, E. Y.-X. *Nat. Chem.* **2016**, *8*, 42–49.

(83) Kadota, J.; Pavlović, D.; Desvergne, J.-P.; Bibal, B.; Peruch, F.; Deffieux, A.

Macromolecules **2010**, *43*, 8874–8879.

(84) Dove, A. P. *ACS Macro Lett.* **2012**, *1*, 1409–1412.

(85) Steinbach, T.; Ritz, S.; Wurm, F. R. *ACS Macro Lett.* **2014**, *3*, 244–248.

(86) Kluger, R.; Taylor, S. D. *J. Am. Chem. Soc.* **1990**, *112*, 6669–6671.

(87) Aksnes, G.; Bergesen, K. *Acta Chem. Scand.* **1966**, *20*, 2508–2514.

(88) Dudev, T.; Lim, C. *J. Am. Chem. Soc.* **1998**, *120*, 4450–4458.

(89) Taylor, S. D.; Kluger, R. *J. Am. Chem. Soc.* **1992**, *114*, 3067–3071.

(90) Gerlt, J. A.; Westheimer, F. H.; Sturtevant, J. M. *J. Biol. Chem.* **1975**, *250*, 5059–5067.

(91) Geise, H. J. *Recl. Trav. Chim., Pays-Bas* **1967**, *86*, 362–370.

(92) Bodkin, C.; Simpson, P. *J. Chem. Soc. D* **1969**, 829–830.

(93) Bentrude, W. G.; Hargis, J. H. *J. Am. Chem. Soc.* **1970**, *92*, 7136–7144.

(94) Hall, L. D.; Malcolm, R. B. *Can. J. Chem.* **1972**, *50*, 2092–2101.

(95) Mosbo, J. A.; Verkade, J. G. *J. Org. Chem.* **1977**, *42*, 1549–1555.

(96) Gregory, G. L.; Hierons, E. M.; Kociok-Köhn, G.; Sharma, R. I.; Buchard, A. *Polym. Chem.* **2017**, *8*, 1714–1721.

(97) Gregory, G. L.; Kociok-Köhn, G.; Buchard, A. *Polym. Chem.* **2017**, *8*, 2093–2104.

(98) Pereira, M. S.; Murta, B.; Oliveira, T. C. F.; Manfredi, A. M.; Nome, F.; Hengge, A. C.; Brandao, T. A. S. *J. Org. Chem.* **2016**, *81*, 8663–8672.

(99) Jain, H. V.; Kalman, T. I. *Bioorg. Med. Chem. Lett.* **2012**, *22*, 4497–4501.

(100) Pratt, R. C.; Lohmeijer, B. G. G.; Long, D. A.; Waymouth, R. M.; Hedrick, J. L. *J. Am. Chem. Soc.* **2006**, *128*, 4556–4557.

(101) Jin, J.; Grote, J. *Materials Science of DNA*; CRC Press, Boca Raton, 2011.

(102) Greve, J.; Maestre, M. F.; Levin, A. *Biopolymers* **1977**, *16*, 1489–1504.

(103) Yao, K.; Tang, C. *Macromolecules* **2013**, *46*, 1689–1712.

(104) Holmberg, A. L.; Reno, K. H.; Wool, R. P.; Iii, T. H. E. *Soft Matter* **2014**, *10*, 7405–7424.

(105) Gandini, A.; Lacerda, T. M.; Carvalho, A. J. F.; Trovatti, E. *Chem. Rev.* **2016**, *116*, 1637–1669.

(106) Kristufek, S. L.; Wacker, K. T.; Tsao, Y.-Y. T.; Su, L.; Wooley, K. L. *Nat. Prod. Rep.* **2017**, *34*, 433–459.

(107) Zhang, K.; Nelson, A. M.; Talley, S. J.; Chen, M.; Margaretta, E.; Hudson, A. G.; Moore, R. B.; Long, T. E. *Green Chem.* **2016**, *18*, 4667–4681.

(108) Lamarzelle, O.; Durand, P.-L.; Wirotius, A.-L.; Chollet, G.; Grau, E.; Cramail, H. *Polym. Chem.* **2016**, *7*, 1439–1451.

(109) Bähr, M.; Bitto, A.; Mülhaupt, R. *Green Chem.* **2012**, *14*, 1447–1454.

(110) Shin, J.; Lee, Y.; Tolman, W. B.; Hillmyer, M. A. *Biomacromolecules* **2012**, *13*, 3833–3840.

(111) Yang, J.; Lee, S.; Choi, W. J.; Seo, H.; Kim, P.; Kim, G.-J.; Kim, Y.-W.; Shin, J. *Biomacromolecules* **2015**, *16*, 246–256.

(112) Ding, K.; John, A.; Shin, J.; Lee, Y.; Quinn, T.; Tolman, W. B.; Hillmyer, M. A. *Biomacromolecules* **2015**, *16*, 2537–2539.

(113) Shen, Y.; Chen, X.; Gross, R. A. *Macromolecules* **1999**, *32*, 2799–2802.

(114) Dane, E. L.; Chin, S. L.; Grinstaff, M. W. *ACS Macro Lett.* **2013**, *2*, 887–890.

(115) Lonnecker, A. T.; Lim, Y. H.; Felder, S. E.; Besset, C. J.; Wooley, K. L. *Macromolecules* **2016**, *49*, 7857–7867.

(116) Gregory, G. L.; Jenisch, L. M.; Charles, B.; Kociok-Köhn, G.; Buchard, A. *Macromolecules* **2016**, *49*, 7165–7169.

(117) Lonnecker, A. T.; Lim, Y. H.; Wooley, K. L. *ACS Macro Lett.* **2017**, *6*, 748–753.

(118) Su, L.; Khan, S.; Fan, J.; Lin, Y.-N.; Wang, H.; Gustafson, T. P.; Zhang, F.; Wooley, K. L. *Polym. Chem.* **2017**, *8*, 1699–1707.

(119) Xiao, R.; Dane, E. L.; Zeng, J.; McKnight, C. J.; Grinstaff, M. W. *J. Am. Chem. Soc.* **2017**, *139*, 14217–14223.

(120) Coull, J. M.; Carlson, D. V.; Weith, H. L. *Tetrahedron Lett.* **1987**, *28*, 745–748.

(121) Isobe, H.; Fujino, T.; Yamazaki, N.; Guillot-Nieckowski, M.; Nakamura, E. *Org. Lett.* **2008**, *10*, 3729–3732.

(122) Sengupta, J.; Bhattacharjya, A. *J. Org. Chem.* **2008**, *73*, 6860–6863.

(123) Suzuki, M.; Sekido, T.; Matsuoka, S.-I.; Takagi, K. *Biomacromolecules* **2011**, *12*, 1449–1459.

(124) Bauer, K. N.; Tee, H. T.; Velencoso, M. M.; Wurm, F. R. *Prog. Polym. Sci.* **2017**, *73*, 61–122.

(125) Mikami, K.; Lonnecker, A. T.; Gustafson, T. P.; Zinnel, N. F.; Pai, P.-J.; Russell, D. H.; Wooley, K. L. *J. Am. Chem. Soc.* **2013**, *135*, 6826–6829.

(126) Hajipour, A. R.; Mallakpour, S. E.; Najafi, A. R. *Phosphorus Sulfur Silicon Relat. Elem.* **2000**, *165*, 165–170.

(127) van Deemter, J. J.; Zuiderweg, F. J.; Klinkenberg, A. *Chem. Eng. Sci.* **1956**, *5*, 271–289.

(128) Simón, L.; Goodman, J. M. *J. Org. Chem.* **2007**, *72*, 9656–9662.

(129) Baran, J.; Penczek, S. *Macromolecules* **1995**, *28*, 5167–5176.

(130) Wang, Y.-C.; Wu, J.; Li, Y.; Du, J.-Z.; Yuan, Y.-Y.; Wang, J. *Chem. Commun.* **2010**, *46*, 3520–3522.

(131) Veronese, F. M.; Mero, A. *BioDrugs* **2008**, *22*, 315–329.

(132) Joralemon, M. J.; McRae, S.; Emrick, T. *Chem. Commun.* **2010**, *46*, 1377–1393.

(133) Jokerst, J. V.; Lobovkina, T.; Zare, R. N.; Gambhir, S. S. *Nanomedicine* **2011**, *6*, 715–728.

(134) Knop, K.; Hoogenboom, R.; Fischer, D.; Schubert, U. S. *Angew. Chem. Int. Ed.* **2010**, *49*, 6288–6308.

(135) Wang, H.; Su, L.; Li, R.; Zhang, S.; Fan, J.; Zhang, F.; Nguyen, T. P.; Wooley, K. L. *ACS Macro Lett.* **2017**, *6*, 219–223.

(136) Richter, J. D. *Microbiol. Mol. Biol. Rev.* **1999**, *63*, 446–456.

(137) Bates, F. S.; Fredrickson, G. H. *Physics Today* **1999**, *52*, 32–38.

(138) Jain, S.; Bates, F. S. *Science* **2003**, *300*, 460–464.

(139) Blanazs, A.; Armes, S. P.; Ryan, A. J. *Macromol. Rapid Commun.* **2009**, *30*, 267–277.

(140) Blanazs, A.; Madsen, J.; Battaglia, G.; Ryan, A. J.; Armes, S. P. *J. Am. Chem. Soc.* **2011**, *133*, 16581–16587.

(141) Holder, S. J.; Sommerdijk, N. A. J. M. *Polym. Chem.* **2011**, *2*, 1018–1028.

(142) Mai, Y.; Eisenberg, A. *Chem. Soc. Rev.* **2012**, *41*, 5969–5985.

(143) Wang, C.; Wang, Z.; Zhang, X. *Acc. Chem. Res.* **2012**, *45*, 608–618.

(144) Qiu, H.; Hudson, Z. M.; Winnik, M. A.; Manners, I. *Science* **2015**, *347*, 1329–1332.

(145) Fetsch, C.; Gaitzsch, J.; Messager, L.; Battaglia, G.; Luxenhofer, R. *Sci. Rep.* **2016**, *6*, 33491.

(146) Hoyle, C. E.; Lowe, A. B.; Bowman, C. N. *Chem. Soc. Rev.* **2010**, *39*, 1355–1387.

(147) Hoyle, C. E.; Bowman, C. N. *Angew. Chem. Int. Ed.* **2010**, *49*, 1540–1573.

(148) Zhang, S.; Zou, J.; Elsabahy, M.; Karwa, A.; Li, A.; Moore, D. A.; Dorshow, R. B.; Wooley, K. L. *Chem. Sci.* **2013**, *4*, 2122–2126.

(149) Desai, N. A.; Shankar, V. *FEMS Microbiol. Rev.* **2003**, *26*, 457–491.

(150) Flory, P. J. *J. Am. Chem. Soc.* **1952**, *74*, 2718–2723.

(151) Liu, J.; Huang, W.; Zhou, Y.; Yan, D. *Macromolecules* **2009**, *42*, 4394–4399.

(152) Trollsås, M.; Löwenhielm, P.; Lee, V. Y.; Moller, M.; Miller, R. D.; Hedrick, J. L. *Macromolecules* **1999**, *32*, 9062–9066.

(153) Liu, M.; Vladimirov, N.; Fréchet, J. M. J. *Macromolecules* **1999**, *32*, 6881–6884.